MULTIUSER RECEIVER STRUCTURES FOR CDMA

by

Wei Zha

A thesis submitted to the
Department of Electrical and Computer Engineering
in conformity with the requirements
for the degree of Doctor of Philosophy

Queen's University
Kingston, Ontario, Canada
August 2002

Abstract

CDMA (Code Division Multiple Access) with multiuser detection at the basestation is an effective way to increase the system capacity. Multiuser detectors are extremely sensitive to time delay estimation errors (delay mismatch) in near-far environments. The required accuracy of time delay estimation is beyond that of current single-user or multi-user delay estimation algorithms, so it is very important to investigate delay-robust CDMA multiuser detection methods operating under delay mismatch.

In the first part of this thesis, a delay-robust multistage successive interference cancellation (SIC) multiuser detector that is near-far resistant under delay mismatch is proposed. The detector is based on a linear SIC implementation of the decorrelating detector, which can be shown to be equivalent to the space alternating generalized expectation-maximization (SAGE) algorithm, which has guaranteed local convergence. While other multiuser detectors that are robust to delay mismatch have a capacity limit of 50% of the spreading factor, and can only be applied to rectangular chip pulse shapes, our proposed delay-robust SIC has a capacity close to 100% of the spreading factor, and can be applied to general band-limited chip pulse shapes, e.g., the square-root raised cosine pulse. The delay-robust SIC's asymptotic multiuser efficiency (AME) and bit error rate (BER) are both analyzed and confirmed by computer simulation. For larger delay errors, a local decorrelation operation is inserted into the delay-robust SIC iterations to improve its performance. This delay-robust SIC can also be used for delay error estimation, whose root mean square error (RMSE) performance is compared to the Cramér-Rao lower bound (CRLB).

In the second part of this thesis, we propose a new soft-decision function to be

used in multistage SIC detectors. The soft-decision function combines the desirable convergence properties of the linear-soft decision function with the noise reduction of the hard-limiter decision function. The result is a SIC detector with both good noise performance and convergence. This soft-decision function has been combined with amplitude time-averaging. The steady-state performance is analyzed and confirmed by PN (pseudo-noise) chip level simulation. We then incorporate this new soft-decision function and amplitude averaging in the delay-robust SIC. For the case of a highly loaded system, the superiority of soft-decision and amplitude averaging is shown by simulation. Since a delay-robust SIC with soft-decision and amplitude averaging can also be used as a delay error estimator, we further propose applying these techniques to a multi-user delay tracking receiver. Since the time delay error detector in the delay-robust SIC is similar to a single-branch realization of an early-late delay tracking loop in a conventional single-user receiver, we have combined the delay tracking loop into a multiuser detector. Tracking performance is demonstrated for both rectangular and square-root raised cosine PN chip pulse shapes. The multiuser detection and delay tracking for time-varying multi-path fading channel is considered and the tracking performance of the delay-robust SIC is evaluated by computer simulation.

The third part of the thesis considers the application of CDMA multiuser detection methods to multi-antenna systems known as MIMO (multiple input multiple output) systems, e.g., the BLAST (Bell Labs Layered Space-Time) system, by observing the similarity between a linear MIMO system and a synchronous CDMA multiuser system. An ordered SIC method was proposed by other researchers for bit detection in BLAST systems. However, its complexity is too high for high-rate applications. We apply a decorrelating decision-feedback CDMA multiuser detection method to BLAST systems. Since only one matrix decomposition is performed at the beginning of the algorithm, the computational complexity is greatly reduced. However, BLAST's decision-feedback ordering is according to decreasing signal power, not in

the optimum decreasing signal-to-noise ratio (SNR) ordering. We further propose using a series of numerically stable unitary transformations to reorder the decomposed matrices. We show that complexity is an order lower than that of the ordered SIC while its stability is improved as well.

Acknowledgements

It is my great pleasure to thank my supervisor, Dr. Steven D. Blostein, for his excellent guidance and support throughout this thesis research.

I would like to thank my thesis defense committee members, Dr. M. Ibnkahla, Dr. T. J. Lim (University of Toronto), Dr. P. J. McLane and Dr. G. Takahara (Mathematics and Statistics) for their taking time to review my thesis and for their helpful suggestions to improve this thesis.

To my colleagues and friends at IPCL and Queen's, whose help and friendship make Queen's a wonderful place to spend four years.

Finally, I would like to thank my wife, Feng, for her encouragement and patience throughout my Ph.D. study and research at Queen's.

This work was supported financially by the Canadian Institute for Telecommunications Research (CITR), the School of Graduate Studies and Research at Queen's University and the Ontario Graduate Scholarship in Science and Technology.

Contents

List of Figures

List of Important Symbols

$\alpha_{k,l}$	complex channel attenuation for user k through lth path
η_k	asymptotic efficiency of multiuser detector for user k
σ^2	variance of additive white Gaussian noise
θ_k	phase shift of user k
τ_k	relative time delay of user k
$\tau_{k,l}$	relative time delay of user k through lth path
$a_k(i)$	amplitude of the ith bit of kth user
$b_k(i)$	ith data bit of kth user
$\mathbf{b}(i)$	bit vector for the ith data bit of all the users
$\mathbf{b}$	bit vector over a block of M bits
$s_k(t)$	normalized spreading waveform of kth user
$c_k(j)$	jth chip of kth user
$\mathbf{c}_k$	spreading code vector of kth user
$\mathbf{c}_k(p_k, i)$	$\mathbf{c}_k$ right-shifted by $(i-1)N + p_k$ chips
$\mathbf{d}_k(i)$	signature vector of user k for the ith data bit
$\mathbf{D}$	signature matrix of all users over a block of M bits
$\Delta\mathbf{d}_k(i)$	the error vector, first derivative of signature vector of user k for the ith data bit
$\mathbf{e}_k$	combined error vector of user k using bit decision-feedback over a block of M bits

$\mathbf{h}_m$	spatial-temporal channel vector for the mth receive antenna in BLAST
H	spatial-temporal channel matrix for flat fading channels in BLAST
i	bit index
k	user index
K	number of users in the system
l	path index
L	number of paths
N	processing gain for CDMA
M	block length in asynchronous CDMA
M_T	number of transmit antenna elements in BLAST
M_R	number of receive antenna elements in BLAST
$\mathbf{n}(.)$	additive white Gaussian noise vector
$h(t)$	spreading chip pulse shape
R	cross-correlation matrix for synchronous single-path channels
R_{kj}	kjth component in R
$\mathcal{R}$	cross-correlation matrix for asynchronous multipath channels
$\mathcal{R}_{kj}$	kjth sub-matrix in $\mathcal{R}$, denoting cross-correlation between users k and j
$r(t)$	received continuous signal
$\mathbf{r}(.)$	received signal vector after chip-matched filtering and chip-rate sampling
$\mathbf{y}(.)$	received signal vector after bit-matched filtering and bit-rate sampling

Chapter 1

Introduction

1.1 Motivation

Wireless communications has been undergoing rapid development for the past two decades. With the high demand of high speed wireless access to information and a growing number of users, current wireless communication technologies and standards need further improvement to satisfy the ever increasing demand.

Code division multiple access (CDMA) cellular systems are effective in making the most use of existing spectrum. The cellular concept enables reusing the same frequency bands at different physical locations. CDMA provides the largest cell capacity for a specified frequency band in a multicell environment, since its frequency reuse factor is one, i.e., the same frequency band can be reused in the adjacent cells and thus frequency planning is not required. One of the second generation wireless standards, IS-95, uses narrow-band CDMA, whose voice capacity is 4-6 times that of digital TDMA (time division multiple access) or FDMA (frequency division multiple access) systems [30]. This capacity improvement is due to voice activity, spatial isolation and the reuse of the same spectrum over all the cells. The third generation (3G) wireless communication system, with standards IMT-2000 (cdma2000 and UMTS), is based almost exclusively on wide-band CDMA to support both voice and data services [1] [17]. The 3G wireless also includes features that support capacity increasing technologies such as multiuser detection and adaptive antenna arrays. Optional short

spreading codes can be used in the uplink direction to facilitate multiuser detection at the basestation. Dedicated pilot symbols in the uplink for each user can be used for the adaptive antenna array [17].

The conventional CDMA receiver is a filter matched to the signature waveform of the desired user, which is optimum under white Gaussian noise conditions. Due to the multiple-access interference (MAI) from other users in the same cell (intracell interference), and the MAI from adjacent cells (intercell interference), the conventional matched filter receiver is near-far limited. Its performance degrades greatly when the interfering users have much stronger received powers than that of the desired user. The IS-95 system must therefore use precise power control to make the received power levels of all users at the base station to be about the same, which is difficult to do in practice.

Verdú's novel work [120] showed that the near-far problem is not inherent to CDMA, but can be solved by using an optimum maximum likelihood (ML) multiuser detector. The outputs of matched filters at the base station provide sufficient statistics to detect all users' signals. The matched filters followed by a Viterbi decoder is an jointly optimum ML multiuser detector, but its complexity is exponential in the number of users. Suboptimum multiuser detectors were developed, including the linear decorrelating detector (decorrelator) [67], linear minimum mean squared error (MMSE) detector [68], parallel interference cancellation (PIC) detector [119] and the successive interference cancellation (SIC) detector [84].

All the above multiuser detectors have assumed that the receiver knows the exact time delays of all the users in a cell. In practical systems, time delays must be estimated at the receiver. Several time delay estimation algorithms have come forth, including the sliding correlation delay estimator [86] [87], two approximate ML algorithms, the approximate maximum likelihood (AML) algorithm [48] [61] and the large sample maximum likelihood (LSML) algorithm [134], subspace-based algorithms [4] [110] and MMSE-based algorithms [71].

Since time delays cannot be estimated exactly at the receiver due to the MAI

and noise, there always exists timing delay estimation errors (delay mismatch). The performance of multiuser detectors under delay mismatch has been studied for the ML detector [34], the decorrelating detector [85] [136] and the multistage detectors [34] (PIC [8] [53] and SIC [13]). Wang simulated a SAGE-based space-time multiuser decorrelating detector bit error rate (BER) performance under delay mismatch in his Ph.D. thesis [123]. When the delay mismatch is minor, the multiuser detector may still perform better than the conventional matched filter receiver. However the matched filter receiver is more robust to delay mismatch: BER performance does not degrade as steeply as in the case of multiuser detectors [8] [13] [34] [85]. Some modified multiuser detectors have shown some robustness to timing errors. However, they are either not truly near-far resistant or have a capacity limit of less than half of the spreading factor. A multiuser detector that is not affected by the near-far problem under delay mismatch and has capacity larger than 50% of the spreading factor does not exist in the open literature.

Multistage successive interference cancellation (SIC) is one of the most efficient ways to perform multiuser detection as it can be applied to both long code and short code CDMA systems. Linear multiuser detectors such as the decorrelating detector and the MMSE detector, on the other hand, need to perform matrix inversion every symbol for long code CDMA, so are not suitable for such systems. The complexity of multistage SIC is lower compared to that of the decorrelating detector. However, the use of a hard-limiter decision function for data bit decision in the SIC iterations leads to error propagation, which cause a bit error rate (BER) error floor. A number of methods have been proposed to combat error propagation, including partial cancellation [19] and soft-decision [45]. However, those methods need complex control of the parameters which are impractical and may not lead to adequate performance.

Linear space-time coding is a low complexity multiple input multiple output (MIMO) system to achieve high spectral efficiency over rich scattering wireless channels. One important MIMO system concept is the Bell Labs layered space-time system (BLAST), which requires that the number of receive antennas to be larger than the

number of transmitting antennas. Recently, BLAST has been generalized to the case where the number of receiving antennas can be less than the number of transmitting antennas. The original ordered SIC detection method is too complex to be used for the high-rate applications, and its iterated nulling and cancellation can lead to numerical instability for large numbers of antennas. A square-root method which has reduced complexity and increased numerical stability was reported in [38]. We propose to apply decision-feedback multiuser detection methods originally proposed for synchronous CDMA systems to the detection in BLAST systems. To get optimum decision-feedback ordering, which is the same as optimum SIC ordering, we further propose using a series of numerically stable unitary transformations to permute the decision-feedback matrix. This provides further complexity reduction and numerical stability increase over the square-root method.

1.2 Summary of Contributions

This thesis investigates the problem of improving existing CDMA multiuser detection methods to be robust to time delay errors as well as the problem of reducing the complexity of BLAST detection. We develop a robust SIC multiuser receiver that is near-far resistant under time delay estimation errors. A new soft-decision function to improve the BER performance of multistage SIC receivers is incorporated into the delay-robust SIC framework. A new reduced complexity BLAST detection method is also proposed based on our improvements to decision-feedback CDMA multiuser detection methods. The primary contributions are summarized as follows:

- An equivalent two-virtual-users model is introduced for the discrete-time received multiuser signal when there are time delay errors for the case of a rectangular transmitted chip pulse shape. A delay-robust SIC detector is proposed. The delay-robust SIC is generalized to general band-limited chip pulse shapes.

- A new soft-decision function is proposed to mitigate the disastrous error propagation of the hard-limiter function in multistage SIC. The steady-state performance of the new soft-decision SIC with amplitude averaging is analyzed. The new soft-decision function is combined with the delay-robust SIC technique to also mitigate time delay errors.

- The delay-robust SIC is applied to delay error estimation. The Cramér-Rao lower bound (CRLB) is derived as its performance lower bound. The delay-robust SIC is applied to track the time delays of multiple users in CDMA fading channels.

- A CDMA decision-feedback multiuser detection method is improved and applied to the linear MIMO - BLAST (Bell Labs Layered Space-Time) system, to reduce computational complexity and improve numerical stability.

1.3 Thesis Overview

This thesis consists of six chapters, which describe the problem of robust CDMA multiuser detection under time delay errors, improvements to CDMA multistage SIC detection by using a new soft-decision function, and complexity reduction using a modified decision-feedback method for the BLAST system.

In Chapter 2, existing multiuser detection algorithms, approaches to timing delay estimation methods for the asynchronous MAI CDMA channel, performance analysis of different multiuser detection algorithms under time delay errors (delay mismatch) and improved multiuser detectors for mismatched delay are reviewed.

Chapter 3 proposes a robust method for multiuser detection when there exists time delay error. We introduce a two-virtual-user equivalent model. A delay-robust decorrelator is derived based on this model which has a capacity limit of half the spreading factor. An alternative expression for the two virtual user model is derived, and a multistage delay-robust decorrelator is obtained which has a larger system capacity than the delay-robust decorrelator. We apply the space-alternating generalized

expectation-maximization (SAGE) algorithm [24] to derive an efficient delay-robust SIC implementation of the multistage delay-robust decorrelator. Asymptotic multiuser efficiency (AME) [67], BER, and CRLB are derived for the delay-robust SIC. The delay-robust SIC is extended both to integer PN chip delay uncertainty for rectangular chip pulse shapes and to generalized band-limited chip pulse shapes.

Chapter 4 introduces a new soft-decision function to be used in the multistage SIC detector. We first compare the advantages and disadvantages of the existing decision functions, then combine their advantages to arrive at our proposed new soft-decision function, which is a generalization of the unit-clipper [78] [133]. Time averaged amplitude estimation is used in the soft-decision SIC to improve performance over the decorrelator. Steady-state performance is analyzed and confirmed by computer simulations. The combination of the new soft-decision function with the delay-robust SIC technique of Chapter 3 gives improved performance, especially at high-load regions. Multi-user delay tracking and detection for both static channel and fast fading multipath channel is addressed.

In Chapter 5, we apply the CDMA multiuser detection methods to multiple antenna systems. We first introduce the ordered SIC and other detection methods for the BLAST linear space-time system. Their complexity and numerical stability are compared. We then apply the decision-feedback method which was originally proposed for synchronous CDMA systems to the BLAST system, by observing the similarity between the BLAST and CDMA systems. To obtain optimal decision-feedback ordering, we modify the decision-feedback method through a series of numerically stable uniform transformations. The BER performance is investigated by simulation.

Finally, Chapter 6 summarizes the conclusions and provides possible directions for future research.

Chapter 2

Overview and Objectives

The first section introduces multiuser detection methods. CDMA time delay estimation methods and their achievable performance are reviewed in Section 2.2. Section 2.3 reviews the performance of various CDMA multiuser detectors under delay mismatch and Section 2.4 presents modified multiuser detection methods to compensate for delay mismatch. In Section 2.5, the objectives of the thesis are stated.

2.1 CDMA Multiuser Detection

We assume that the CDMA channel is asynchronous and binary phase shift keying (BPSK) modulation is used. The received signal at the basestation after downconverting to the baseband is

$$r(t) = S(t, \mathbf{b}) + n(t) \tag{2.1}$$

where

$$S(t, \mathbf{b}) = \sum_{i=1}^{M} \sum_{k=1}^{K} a_k(i) b_k(i) \tilde{s}_k(t - iT_b - \tau_k) \tag{2.2}$$

$n(t)$ is white Gaussian noise with power spectral density σ^2;

$\tilde{s}_k(t)$ is the normalized signature waveform of user k of duration $[0, T_b)$;

T_b is the symbol interval;

$a_k(i)$ is the received signal amplitude of the kth user in the ith symbol interval;

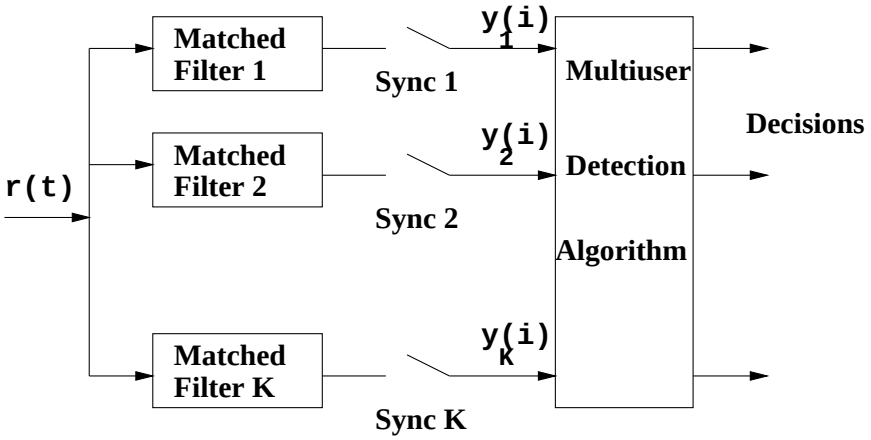

Figure 2.1: Multiuser Detector

$\mathbf{b} = \{\mathbf{b}(i) = [b_1(i), \ldots, b_k(i)],\ b_k(i) \in \{-1, 1\},\ k = 1, \ldots, K;\ i = 1, \ldots, M\}$
is the transmitted bit sequence vector of the K users;
The length of $\mathbf{b}$ is MK;
τ_k is the time delay of user k, where it is assumed that $0 \leq \tau_k < T_b$.

The receiver front-end can be identical for both conventional single-user detector and the multiuser detectors, which is comprised of a bank of K matched filters, matched to the users' spreading waveforms. However, we note that other kinds of receiver front-ends such as chip matched filter that matched to the chip waveform, can also be used in single-user and multiuser detectors. The outputs of the bank of K matched filters are sampled at the symbol rate and collected into a K-dimensional vector for the ith time interval, $\mathbf{y}(i) = [y_1(i), \ldots, y_K(i)]^T$, where $y_k(i)$ is for the ith bit of the kth user

$$y_k(i) = \int_{iT_b+\tau_k}^{(i+1)T_b+\tau_k} r(t)\tilde{s}_k(t - iT_b - \tau_k)dt \tag{2.3}$$

$$= \int_{-\infty}^{\infty} S(t, \mathbf{b})\tilde{s}_k(t - iT_b - \tau_k)dt + \int_{-\infty}^{\infty} n(t)\tilde{s}_k(t - iT_b - \tau_k)dt \tag{2.4}$$

M of such K-vectors are concatenated into a longer signal vector $\mathbf{Y} = [\mathbf{y}(1)^T, \ldots, \mathbf{y}(M)^T]^T$.

The conventional single-user detector uses a decision function following each matched filter and makes symbol decisions separately, treating the MAI terms as white noise. Performance degrades rapidly when the near-far ratio increases, where the near-far

ratio is defined as the ratio of the received signal powers between the strongest user and the weakest user.

The multiuser detectors perform joint detection based on matched filter outputs $\mathbf{Y}$, which are sufficient statistics for detection of all K users' transmitted symbols [22] [75].

Verdú first developed the optimum multiuser detector [120]. If the transmitted sequences of symbols are equiprobable, the maximum-likelihood (ML) detection is the the same as optimum maximum a posterior (MAP) detection [89] [120]. The maximum-likelihood (ML) multiuser detector selects the sequence $\mathbf{b}$ that maximizes the conditional probability $P\left[\{r(t), t \in R\} \mid \mathbf{b}\right]$, and consists of a bank of K matched filters followed by a Viterbi algorithm [89]. The Viterbi algorithm has 2^{MK-1} states, and complexity $O(2^{MK})$, exponential in the number of users.

Because the complexity of ML multiuser detector is too high, suboptimum multiuser detectors with linear complexity have been proposed.

The linear multiuser detector performs a linear transformation on the matched filter output vector $\mathbf{Y}$, as in Fig. 2.2. There are two kinds of linear multiuser detectors: the decorrelating detector [67] and the minimum mean squared error (MMSE) detector [68].

The received signal vector can be expressed in matrix form as

$$\mathbf{Y} = \mathcal{R}\mathbf{A}\mathbf{b} + \mathbf{n} \tag{2.5}$$

The noise vector $\mathbf{n}$ is a zero-mean Gaussian random vector with auto-correlation matrix $\sigma^2\mathcal{R}$, where $\mathcal{R}$ is a $MK \times MK$ symmetric block-Toeplitz matrix:

$$\mathcal{R} = \begin{pmatrix} \mathbf{R}(0) & \mathbf{R}(-1) & & \cdots & 0 \\ \mathbf{R}(1) & \mathbf{R}(0) & \mathbf{R}(-1) & & \vdots \\ 0 & \mathbf{R}(1) & \mathbf{R}(0) & \ddots & 0 \\ \vdots & & \ddots & \ddots & \mathbf{R}(-1) \\ 0 & \cdots & 0 & \mathbf{R}(1) & \mathbf{R}(0) \end{pmatrix} \tag{2.6}$$

and $\mathbf{A}$ is a $MK \times MK$ diagonal matrix:

$$\mathbf{A} = diag\left([a_1(1), \ldots, a_K(1), \ldots, a_1(M), \ldots, a_K(M)]\right) \tag{2.7}$$

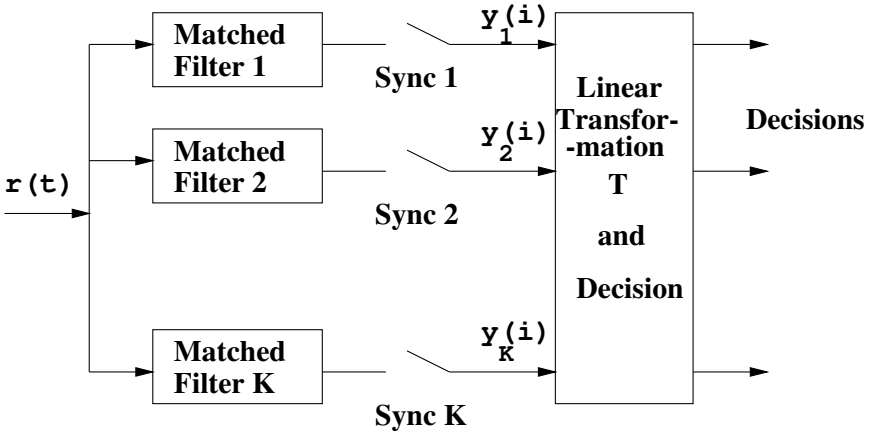

Figure 2.2: Linear Multiuser Detector

In (2.6), the (k,j)th element of the $K \times K$ signal correlation matrix $\mathbf{R}(l)$ is:

$$R_{kj}(l) = \int_{-\infty}^{\infty} \tilde{s}_k(t-\tau_k)\tilde{s}_j(t+lT_b-\tau_j)dt \tag{2.8}$$

and $\mathbf{R}(l)$ has the following properties:

$$\mathbf{R}(l) = 0, \forall |l| > 1 \tag{2.9}$$

$$\mathbf{R}(-l) = \mathbf{R}^T(l) \tag{2.10}$$

Let $\mathbf{T}$ be a linear transformation matrix. The decision vector is

$$\mathbf{d} = \mathbf{TY} \tag{2.11}$$

For the decorrelating detector, the linear transform matrix $\mathbf{T}$ is the inverse of the correlation matrix [67]

$$\mathbf{T} = \mathcal{R}^{-1} \tag{2.12}$$

The decision vector is then

$$\mathbf{d} = \mathcal{R}^{-1}(\mathcal{R}\mathbf{A}\mathbf{b} + \mathbf{n}) = \mathbf{A}\mathbf{b} + \mathcal{R}^{-1}\mathbf{n} \tag{2.13}$$

The noise vector $\mathcal{R}^{-1}\mathbf{n}$ has covariance matrix

$$E[(\mathcal{R}^{-1}\mathbf{n})(\mathcal{R}^{-1}\mathbf{n})^H] = \sigma^2\, \mathcal{R}^{-1} \tag{2.14}$$

where the noise power is enhanced by $\mathcal{R}^{-1}$.

Since BPSK modulation is used, the decisions are made by the sign of the decision vector

$$\hat{\mathbf{b}} = sign\ (\mathbf{d}) = sign\ (\mathbf{A}\mathbf{b} + \mathcal{R}^{-1}\mathbf{n}) \tag{2.15}$$

Since the symbol decision of the kth user is not affected by the energies of the interfering users, the decorrelating detector is near-far resistant [67]. A multiuser detector is said to be near-far resistant only if its near-far resistance is not zero [67].

The linear transformation matrix $\mathbf{T}$ for the MMSE detector is chosen to minimize the mean squared error between the transmitted symbol and the symbol estimation [68]

$$\mathbf{T} = \min_{\mathbf{T}}\ E[(\mathbf{b} - \hat{\mathbf{b}})^T(\mathbf{b} - \hat{\mathbf{b}})] \tag{2.16}$$

The solution to the above equation is

$$\mathbf{T} = (\mathcal{R} + \sigma^2(\mathbf{A}^H\mathbf{A})^{-1})^{-1} \tag{2.17}$$

The MMSE detector maximizes the output signal-to-interference ratio (SIR). Performance is superior to that of the decorrelating detector because the MMSE detector does not have the noise enhancement problem of decorrelating detector [70] [89]. As the noise vanishes, the MMSE detector converges to the decorrelating detector. When the noise goes to infinity, the MMSE detector degrades to the conventional matched filter single-user receiver.

Iterative multistage receivers have received significant interest recently. This is a suboptimum solution for maximizing the log-likelihood function [78] [113] [119] [124]. At each stage, the estimated interference from other users is subtracted before estimating the desired user's transmitted data bit.

Assume the jth stage estimate of bits $b_k(m)$ to be $\hat{b}_k^{(j)}(m)$ for user k. The $(j+1)$st stage estimate of $b_k(m)$ is then

$$\hat{b}_k^{(j+1)}(m) = arg \max_{b_l(m)=\hat{b}_l^{(j)}(m)} \{\Omega(\mathbf{b})\} \tag{2.18}$$

where $\Omega(\mathbf{b})$ is the log-likelihood function

$$\Omega(\mathbf{b}) = 2\mathbf{b}^T\mathbf{Y} - \mathbf{b}^T\mathcal{R}\mathbf{b} \tag{2.19}$$

Using a hard decision detector, this can be calculated as:

$$\hat{b}_k^{(j+1)}(m) = sign\,[y_k^{(j)}(m)] \tag{2.20}$$

where

$$y_k^{(j)}(m) = y_k^{(0)}(m) - \sum_{l=k+1}^{K} \mathbf{R}_{kl}(1)\hat{b}_l^{(j)}(m-1) - \sum_{l\neq k} \mathbf{R}_{kl}(0)\hat{b}_l^{(j)}(m) - \sum_{l=1}^{k-1} \mathbf{R}_{kl}(-1)\hat{b}_l^{(j+1)}(m+1) \tag{2.21}$$

The initial estimate $\hat{b}_k^{(1)}(m)$ can be obtained from the conventional detector output

$$\hat{b}_k^{(1)}(m) = sign\,[y_k^{(0)}(m)] \tag{2.22}$$

Depending on the interference cancellation procedure used in each stage, there are two kinds of multistage iterative receivers: successive interference cancellation (SIC) [84] and parallel interference cancellation (PIC) [119].

For multistage SIC receiver, the signals of users are detected and cancelled in the order of decreasing powers at each stage. The SIC is similar in structure to the space-alternating generalized expectation-maximization (SAGE) based receiver [24] [78] [124].

The PIC differs from SIC in that it detects the transmitted bits of all users in parallel at each stage [119]. The PIC is similar in structure to the expectation-maximization (EM) based receiver [23] [78]. Although PIC is more complex than SIC [84], PIC can use parallel computation to reduce processing delay [8].

When a linear decision function is used in the multistage interference cancellation detector, the linear SIC and PIC correspond to applying the Gauss-Seidel and Jacobi iteration to approximate the matrix inversion [37] [93] [125].

2.2 CDMA Time Delay Estimation

All the multiuser detectors described in the previous section have assumed exact knowledge of user time delays. Once the time delays are known, other parameters such

as the channel attenuation and phase offsets can be easily obtained [74]. Therefore, an important problem of CDMA multiuser detection is to accurately estimate all users' time delays.

Existing delay estimation methods include the sliding correlation algorithm [87], maximum-likelihood (ML) algorithms [90] [110], approximate ML (AML) algorithms [5] [134], subspace-based algorithms [4] [110] and minimum mean squared error (MMSE) based algorithms [69] [71] [105] [106]. For an observation length of 100 symbols, current sliding correlation delay estimation methods [87] can achieve a delay estimation error within one fifth of a chip duration, 0.2 T_c, and the subspace-based MUSIC algorithm can achieve 0.03 T_c [110], where T_c is the chip interval.

Sliding correlation is the conventional method of time delay estimation [86] [87], which is only optimum for the single-user channels with additive white Gaussian noise. Since performance is affected by the multiple access interference (MAI), it is near-far limited.

The sliding correlation algorithm requires an all ones training sequence. The received signal is correlated with different shifts of the desired user's code sequence. The time delay is estimated to be at the correlation peak. For a training sequence length of 100 symbols, the sliding correlation algorithm can achieve a root mean squared error (RMSE) of $0.2T_c$, where T_c is the chip interval [110].

The maximum-likelihood (ML) estimator maximizes the log-likelihood function over all parameters, i.e., data bits, amplitudes and time delays of all users [90] [110]:

$$\begin{bmatrix} \hat{\mathbf{b}}^{ML} \\ \hat{\boldsymbol{\tau}}^{ML} \\ \hat{\mathbf{a}}^{ML} \end{bmatrix} = arg \min_{\substack{\mathbf{b} \\ \boldsymbol{\tau} \\ \mathbf{a}}} \|\mathbf{Y} - \mathcal{R}\mathbf{A}\mathbf{b}\|^2 \tag{2.23}$$

Eq. (2.23) jointly estimates the time delays $\boldsymbol{\tau}$, complex amplitudes $\boldsymbol{\alpha}$ and data bits $\mathbf{b}$. Since the ML estimator exploits the full structure of the problem, it may achieve the Cramér-Rao lower bound (CRLB) [110]. Since (2.23) is a mixed type optimization problem with both continuous and discrete valued parameters, its maximization is difficult to obtain. Similar to the ML multiuser detector, complexity is exponential

in the number of users.

A suboptimum solution of the above ML problem is by alternatively iterating between an expectation-maximization (EM) algorithm which estimates complex amplitudes and time delays, and a multistage detection algorithm which detects the data bits [55] [90]. This requires an initial estimate which is reasonably close to the true parameter value to be able to converge.

The approximation that all parameters are treated as a continuous signal simplifies the problem of mixed type parameter maximization. There are two kinds of simplified maximum-likelihood algorithms based on this approximation: the approximate maximum likelihood (AML) algorithm [48] [61] and the single-user maximum likelihood algorithm [5] [134]. Because of the approximation, it has been observed that the performance of those estimators may not be as high as that of the ML estimator [110].

The complexity of the AML algorithm is lower than that of the ML algorithm. However, the AML algorithm estimates all users' delays simultaneously, so it is still a difficult multi-dimensional maximization problem [48] [61].

The single-user maximum-likelihood algorithm is less computationally complex than the AML as it uses a one-dimensional search to find the time delay [5] [134]. For the desired user, a training sequence is transmitted. The MAI is approximated as colored Gaussian noise, and whitened by a whitening filter before delay estimation. Only one user's delay can be estimated at a time by the single-user ML algorithm.

Subspace-based methods were originally used in array signal processing problems. Only recently have they been applied to CDMA delay estimation [4] [110] using the well known MUltiple SIgnal Classification (MUSIC) algorithm [99]. The advantage of subspace-based estimation is that no training sequences are needed and all users' delays can be estimated simultaneously. The disadvantage is that performance is unsatisfactory when the SNR is low [4] [134], and cannot be used when $K > \frac{1}{2}N$, since there is no dimensionality left for the noise subspace.

The dimensionality limitation problem described above was solved recently by

a differential correlation MUSIC (DC-MUSIC) algorithm, which can be used when the number of users is larger than half the spreading gain [94]. The MUSIC delay estimator was also extended from rectangular chip pulse shapes to bandlimited chip pulse shapes in [83].

Minimum mean squared error (MMSE) interference suppression can also be used for both timing acquisition and data bit demodulation. MMSE-based delay estimation algorithms use either a training sequence [71] [105] [106] or blind adaptation [69].

The training based adaptive MMSE delay estimator was proposed in [105] and analyzed in [106].

The blind adaptive MMSE delay estimator requires only the knowledge of the desired signature sequence [69]. However, it is sensitive to the choice of internal parameters.

2.3 CDMA Multiuser Detection under Delay Mismatch

Since time delays cannot be estimated exactly at the receiver in practice, there always exists some amount of time delay estimation error (delay mismatch). Compared to amplitude mismatch and phase mismatch, delay mismatch has a more severe impact on the performance of multiuser detectors [34]. If the delay mismatch is larger than one half of the chip interval, the multiple access interference (MAI) may not be canceled, but instead may actually be increased [13].

The impact of timing errors on detector performance was investigated for the ML detector in [34], for the linear decorrelating detector in [85] [136], and for the multistage detectors (including PIC [8] and SIC [13]).

The performance degradation of the linear multiuser detector especially the linear decorrelating detector due to timing errors was analyzed in both [85] and [136].

Denote the estimated time delay for user k as $\hat{\tau}_k$, and the delay error as $\tilde{\tau}_k = \tau_k - \hat{\tau}_k$. It can be assumed that the delay estimates of different users are independent. The

delay error can be modeled as a zero-mean Gaussian random variable with variance $\sigma^2_{\tilde{\tau}_k}$ [14].

Analogous to Equation (2.8), define the elements of the estimated correlation matrices as

$$\hat{R}_{kj}(l) = \int_{-\infty}^{\infty} \tilde{s}_k(t - \hat{\tau}_k)\tilde{s}_j(t + lT - \tau_j)dt \tag{2.24}$$

$$\hat{\hat{R}}_{kj}(l) = \int_{-\infty}^{\infty} \tilde{s}_k(t - \hat{\tau}_k)\tilde{s}_j(t + lT - \hat{\tau}_j)dt \tag{2.25}$$

When delay mismatch exists, the matched filter front-end is aligned with the estimated time delay and its output is sampled at the estimated time delay. The sampled matched filter output expressed in vector form is

$$\mathbf{Y} = \hat{\mathcal{R}}\mathbf{A}\mathbf{b} + \mathbf{n} \tag{2.26}$$

where

$$\hat{\mathcal{R}} = \begin{pmatrix} \hat{\mathbf{R}}(0) & \hat{\mathbf{R}}(-1) & \cdots & \hat{\mathbf{R}}(-2M) \\ \hat{\mathbf{R}}(1) & \hat{\mathbf{R}}(0) & \cdots & \hat{\mathbf{R}}(-2M+1) \\ \vdots & \ddots & \ddots & \\ \hat{\mathbf{R}}(2M) & \cdots & \hat{\mathbf{R}}(1) & \hat{\mathbf{R}}(0) \end{pmatrix} \tag{2.27}$$

The noise vector is zero-mean Gaussian with covariance matrix $E[\mathbf{n}\mathbf{n}^H] = \frac{N_0}{2}\hat{\hat{\mathcal{R}}}$. Where $\hat{\hat{\mathcal{R}}}$ is similar to $\hat{\mathcal{R}}$ with $\hat{\hat{R}}_{kj}(l)$ replacing $\hat{R}_{kj}(l)$.

For the linear detectors, the data bit estimate and decision for the kth users's ith bit are given by

$$d_k(i) = \mathbf{u}^T_{k,i}\mathbf{T}\mathbf{y} = \mathbf{u}^T_{k,i}\mathbf{T}\hat{\mathcal{R}}\mathbf{A}\mathbf{b} + \mathbf{u}^T_{k,i}\mathbf{T}\mathbf{n} \tag{2.28}$$

and

$$\hat{b}_k(i) = sign\ (d_k(i)) \tag{2.29}$$

where $\mathbf{u}_{k,i}$ is a unit vector with a '1' in the $((i+M)K+k)$th position and zeros elsewhere, and the noise term is a zero-mean Gaussian random variable with variance

$$E[(\mathbf{u}^T_{k,i}\mathbf{T}\mathbf{n})^2] = \frac{N_0}{2}\mathbf{u}^T_{k,i}\mathbf{T}\hat{\hat{\mathcal{R}}}\mathbf{T}^T\mathbf{u}_{k,i} \tag{2.30}$$

Based on the above model, two bit error rate (BER) analyses were carried out using a direct approach [85] [136] and a Taylor series expansion approach [136].

The impact of timing errors on multistage detectors was studied by [8] [34] [53] on PIC, and by [13] on SIC.

In [8], a PIC multistage detector was examined. To simplify the analysis, it is assumed that each user has the same timing error ϵ, $0 \leq \epsilon < T_c$. A closed-form expression for probability of bit error is obtained for the multistage PIC detector based on a Gaussian approximation for the multiple-access interference.

A similar approach is adopted in [13] to analyze the performance degradation of multistage SIC detector due to timing errors. However, the timing errors are assumed to be i.i.d. zero mean Gaussian random variables with variance σ_τ^2 in [13].

Wang simulated the BER performance of a SAGE-based space-time multiuser decorrelating detector under delay mismatch [123]. It was found that delay mismatch as small as $\frac{1}{8}T_c$ can severely degrade space-time multiuser detector performance [123]. This observation is also consistent with our simulation results in Fig. 3.13.

The robustness of multiuser detectors under both synchronization and phase errors was simulated in [81], which compares the decorrelating detector, the MMSE detector, the SIC, the PIC and the conventional matched filter. Simulation results show that synchronization errors have caused more severe performance degradation than phase errors. All multiuser detectors are equally sensitive to the time delay errors, and they are all near-far limited. The decision statistics of multiuser detectors depend on the powers of the interfering users under delay mismatch, so it is important to apply strict power control to minimize the impact of time delay errors [136].

2.4 Improved CDMA Multiuser Detection in the Presence of Time Delay Error

There are two approaches to improve the robustness of a multiuser detector in the presence of time delay errors: one is based on stochastic delay error modeling, and

the other is based on deterministic delay error modeling.

The research on robust multiuser detection based on stochastic delay error modeling has been focused mainly on the MMSE detector. Modified MMSE multiuser structures that are robust to delay mismatch were proposed in [14] [46] [82].

An MMSE receiver for quasi-synchronous CDMA is proposed in [46], which averages over all possible delay offsets. The delays are assumed to be uniformly distributed over a small fraction of a chip duration. Performance when the signal-to-noise ratio (SNR) is low is analyzed.

For moderate to large signal-to-noise ratios, an improved MMSE detector that is robust to delay errors was proposed in [14]. The improved linear MMSE receiver $\mathbf{w}$ for bit *0* of the first user satisfies

$$E_{\mathbf{b},\mathbf{n},\tilde{\boldsymbol{\tau}}}\left\{(\mathbf{w}^T\mathbf{r} - b_1(0))\mathbf{w}^T\mathbf{r}\right\} = 0 \tag{2.31}$$

where $\mathbf{b} = [b_1(-1), b_1(0), b_1(1), \ldots, b_K(-1), b_K(0), b_K(1)]^T$ and $\tilde{\boldsymbol{\tau}} = [\tilde{\tau}_1, \ldots, \tilde{\tau}_K]^T$.

In (2.31), $E_{\mathbf{b},\mathbf{n},\tilde{\boldsymbol{\tau}}}$ is averaged over all possible data bits, noise, and delay errors. This improved MMSE detector takes into account the timing errors, so its average BER is lower than that of the original MMSE, $E_{\mathbf{b},\mathbf{n}}$, which only averages over data bits and noise.

In [82], the linear transformation matrices of the MMSE and the decorrelating detector are modified where the correlation matrix $\mathcal{R}$ is expanded by a Taylor series when the timing error is small.

Although the stochastic approach improves the average BER for a large delay error distribution, the residual MAI caused by timing error is not completely eliminated and the detector is therefore not near-far resistant.

The research on robust multiuser detector based on deterministic delay error modeling has been focused mainly on the decorrelating detector. The decorrelating detector [46] and delay-independent decorrelating detector [40] for the quasi-synchronous CDMA (QS-CDMA) channel was proposed for a rectangular chip pulse shaped CDMA system.

The chip-asynchronous user signal is modeled as the sum of signals from two equivalent chip-synchronous virtual users. The multiple-access interference (MAI) is completely rejected when the true delay and estimated delay are in the same chip interval. However, because they double the number of PN codes used, the noise enhancement problem of the decorrelating detector is more severe, and their capacity will not exceed 50% of the spreading factor [40].

2.5 Objectives

The objectives of this thesis are to develop a base-station multiuser receiver for an asynchronous CDMA channel when the estimated time delay has mismatch. The time delay error in a synchronous CDMA system can be viewed as a special case of the asynchronous CDMA system. The delay-robust multiuser detector should have a large capacity and be near-far resistant.

The decision function used in the multistage SIC receiver determines performance. No accurate analysis exists in how close the multistage soft-decision SIC performance approaches the optimum multiuser detector. We would like to investigate a soft-decision function that has good performance and is easy to analyze.

Multi-user delay tracking is a difficult task because of the MAI. A practical multiuser delay tracking detector will be investigated.

Recently, there is much interest to apply CDMA multiuser detection methods to multiple antenna system. We consider the application to a linear multiple input multiple output (MIMO) system that has similarity with a synchronous CDMA system. One promising example of a linear MIMO system is the Bell Labs Layered Space-Time (BLAST) System. An ordered SIC CDMA multiuser detection method was applied to the BLAST. However, its complexity is too high since after each SIC step the cancellation ordering has to be recomputed. This thesis wraps up by proposing a reduced complexity detection method for BLAST which has the same performance as the ordered SIC method.

Chapter 3

Multiuser Receivers that are Robust to Delay Mismatch

We investigate a new delay-robust multiuser signal detector for asynchronous CDMA uplink channels under delay mismatch in this chapter. We first formulate a delay-robust decorrelating detector by dividing each user into two virtual users with rectangular chip pulse shapes. To increase the system capacity, a multistage version of the delay-robust decorrelating detector is derived, which can achieve capacity of up to $M/(M+1)$ of the spreading factor, where M is the observation block length. We further propose a delay-robust successive interference cancellation (SIC) implementation of the multistage delay-robust decorrelator. The proposed delay-robust SIC detector adds a residual error signal estimation and cancellation procedure onto the standard SIC detector, so its computational complexity is close to that of the standard SIC. Performance is investigated via analysis and simulation. Computer simulation results showed that our proposed delay-robust SIC detector outperforms the conventional decorrelating detector when delay estimation error is present, and its performance is close to that of the decorrelating detector with perfect time delay information. Finally, we generalize the delay-robust SIC detector to the case of non-rectangular chip pulse shapes.

3.1 Introduction

We consider multiuser detection for the asynchronous CDMA uplink under delay mismatch using a similar approach as in [40] and [46], using chip-matched sampling and filtering. We assume that the delays of all users are estimated to within the same chip interval of the true delay. Our proposed delay-robust multiuser detector is insensitive to time delay estimation errors, with a capacity close to 100% of the spreading factor, and can be applied to band-limited chip pulse shapes as well.

Without loss of generality, we consider an asynchronous single-path uplink CDMA channel, assuming K active users. We note that an L-path, K-user system can be modeled as an equivalent single-path system with $K \times L$ users.

For rectangular chip pulses, the equivalent discrete-time user signal can be expressed as the sum of signals from two equivalent virtual users. We divide the two *virtual* users into an *estimated virtual user* with signature waveform at the estimated delay, and one *error virtual user* with signature waveform as the error vector corresponding to the difference between the true time delay and the estimated time delay. Thus, we view a signal from one propagation path as signals arriving from two virtual paths. Since the time delay error will only affect the amplitude of those two virtual users' signals, and since it is well known that the decorrelating detector does not require user amplitude information, it is possible to design a delay-robust decorrelating detector for those $2K$ virtual users and eliminate the MAI completely [40]. However, the delay-robust decorrelator has a capacity limitation of 50% of the spreading factor.

To increase capacity beyond 50% of the spreading factor, we use a block of M symbols, and apply the new delay-robust decorrelating detector on a block in a multistage fashion. In each stage, M separate error vectors are combined into an M-symbol long error vector using tentative data bit decision-feedback from the current stage. The result is an equivalent $(M+1)K/M$ user CDMA system, and the system capacity is increased to $M/(M+1)$ of the spreading factor.

Since the multistage decorrelating detector is extremely complex to compute, we

propose a delay-robust successive interference cancellation (SIC) implementation. At each SIC iteration, the interference due to time delay error is estimated and cancelled. We also show that the delay-robust SIC is a maximum-likelihood estimate of the data bits and the time delay error introduced interference. This estimate can be computed through the space alternating generalized expectation-maximization (SAGE) algorithm [24] with known convergence properties.

Unlike [14] and [46], the delay-robust SIC detector does not require an assumed delay error distribution, so it is near-far resistant under arbitrary delay error distributions. We also propose this delay-robust SIC as a delay error estimator, and its root mean square error (RMSE) performance is compared to the Cramér-Rao lower bound (CRLB). For large time delay errors, the delay-robust SIC is improved by applying a local decorrelation operation into the delay-robust SIC iterations to decouple the estimated user signal and the time delay introduced interfering signal of the same user. The delay-robust SIC technique is then generalized to band-limited chip pulse shapes.

This chapter is organized as follows. In Section 3.2, the system models are described. Section 3.3 proposes the delay-robust SIC multiuser detector under delay mismatch, which is analyzed in Section 3.4. Section 3.5 considers the large delay mismatch case. Section 3.6 generalizes the new detector to band-limited chip pulse shapes, while Section 3.7 provides simulation results.

3.2 System Model

We consider a basestation uplink receiver that has knowledge of the spreading codes of all users. It is assumed that the time delays of all users are under acquisition, i.e., estimated to within half chip interval of the true delays. For clarity and brevity, we consider a single-path channel. However, the method can be extended to the case of multipath channels in a straightforward manner.

Using a similar system model to that of [67], the received signals are assumed to

be carrier phase synchronized and coherently received, so the equivalent base-band signal is real

$$r(t) = \sum_{i} \sum_{k=1}^{K} a_k(i) b_k(i) \tilde{s}_k(t - iT - \tau_k) + n(t) \tag{3.1}$$

where $a_k(i) \in \mathcal{R}$ and $b_k(i) \in \{+1, -1\}$ are the kth user's received signal amplitude and data bit for the ith time interval respectively, $\tau_k \in [0, T)$ is the kth user's propagation delay, T is the bit duration, K is the total number of users and $n(t)$ is the white Gaussian noise. We note that carrier phase-synchronized MAI is a worst-case scenario.

We consider only rectangular chip pulse shapes here. The more general case of band-limited chip pulse shapes is considered later in Section 3.6. In (3.1), the normalized signature waveform of user k, $\tilde{s}_k(t)$, is

$$\tilde{s}_k(t) = \sum_{j=0}^{N-1} c_k(j) h(t - jT_c) \tag{3.2}$$

where $N = T/T_c$ is the spreading factor, T_c is the chip duration, $\{c_k(j)\}_{j=0}^{N-1}$ is the spreading code, and $h(t)$ is a rectangular pulse with duration $[0, T_c)$.

The decorrelating detector for asynchronous CDMA channels in [67] is based on an infinite-length bit sequence. Near-far resistance is destroyed, however, when applied to a finite-length observation window, because of the edge effect [101]. To focus on the effect of timing errors, we eliminate edge effects by using an isolation bit insertion (IBI) receiver [135], where a blank bit interval is inserted into the bit stream every M bit intervals. We want to recover the M transmitted data bits from each user, and select the received signal observation window to be $(M + 1)T$ sec. long for demodulation.

Assuming that the channel changes relatively slowly, we can model the received signal power as a constant for this $(M+1)$-bit interval, i.e., $a_k(i) = a_k$ for $i = 1, \ldots, M$.

After chip-matched filtering and chip-rate sampling, in vector form we obtain the discrete-time received signal:

$$\mathbf{r} = \sum_{i=1}^{M+1} \sum_{k=1}^{K} a_k b_k(i) \mathbf{d}_k(i) + \mathbf{n} \tag{3.3}$$

where

$$\mathbf{r} = [\mathbf{r}^T(1)\ \mathbf{r}^T(2)\ \ldots\ \mathbf{r}^T(M+1)]^T \in \mathcal{R}^{(M+1)N} \tag{3.4}$$

$$\mathbf{n} = [\mathbf{n}^T(1)\ \mathbf{n}^T(2)\ \ldots\ \mathbf{n}^T(M+1)]^T \in \mathcal{R}^{(M+1)N} \tag{3.5}$$

The vector $\mathbf{r}(m)$ in (3.4) for the mth observation interval is

$$\mathbf{r}(m) = [r(mN+1)\ r(mN+2)\ \ldots\ r(mN+N)]^T \in \mathcal{R}^N \tag{3.6}$$

The noise vector $\mathbf{n}$ is a zero-mean Gaussian random vector with

$$E[\mathbf{n}\mathbf{n}^H] = \sigma_n^2 I_{(M+1)N}$$

Assume the actual (true) time delay of the kth user is $\tau_k = (p_k + \delta_k)T_c$, where $p_k \in \{0, 1, \ldots, N-1\}$ is an integer and $\delta_k \in [0, 1)$ is the fractional part. The received signature waveform of the ith bit of the kth user, $\mathbf{d}_k(i) \in \mathcal{R}^{(M+1)N}$, can be expressed as the combination of two adjacent shifted versions of user spreading codes [110]

$$\mathbf{d}_k(i) = \delta_k \mathbf{c}_k(p_k + 1, i) + (1 - \delta_k)\mathbf{c}_k(p_k, i) \tag{3.9}$$

where $\mathbf{c}_k \in \mathcal{R}^{(M+1)N}$ is the kth user's spreading code vector for the $(M+1)T$ second interval defined as

$$\mathbf{c}_k = [c_k(0)\ c_k(1)\ \ldots\ c_k(N-1)\ \underbrace{0\ 0\ \ldots\ 0}_{MN}]^T \tag{3.10}$$

In (3.9), $\mathbf{c}_k(p_k, i)$ is defined as $\mathbf{c}_k$ right-shifted by $(i-1)N + p_k$ chips. The chip-matched filtered and sampled signal of (3.3) can be expressed in more compact matrix-vector form as

$$\mathbf{r} = \mathbf{D}\mathbf{A}\mathbf{b} + \mathbf{n} \tag{3.11}$$

where $\mathbf{b} = [\mathbf{b}^T(1)\ \mathbf{b}^T(2)\ \ldots\ \mathbf{b}^T(M)]^T$, $\mathbf{b}(i) = [b_1(i)\ b_2(i)\ \ldots\ b_K(i)]^T$ is the data bit vector for the ith interval, $\mathbf{A} = \mathbf{I}_M \otimes \mathbf{a}$ is an $MK \times MK$ diagonal matrix of received signal amplitudes, where $\otimes$ denotes the Kronecker product, and $\mathbf{a} = diag(a_1, a_2, \ldots, a_K)$. The code matrix is

$$\mathbf{D} = [\mathbf{d}_1(1)\ \ldots \mathbf{d}_K(1)\ \mathbf{d}_1(2)\ \ldots\ \mathbf{d}_K(2)\ \ldots\ \mathbf{d}_1(M)\ \ldots\ \mathbf{d}_K(M)] \in \mathcal{R}^{(M+1)N \times MK} \tag{3.12}$$

The decorrelating detector (decorrelator) with perfect time delay information is constructed as [67]

$$\hat{\mathbf{b}} = sign\ ([\mathbf{D}^H\mathbf{D}]^{-1}\mathbf{D}^H\mathbf{r}) \tag{3.13}$$

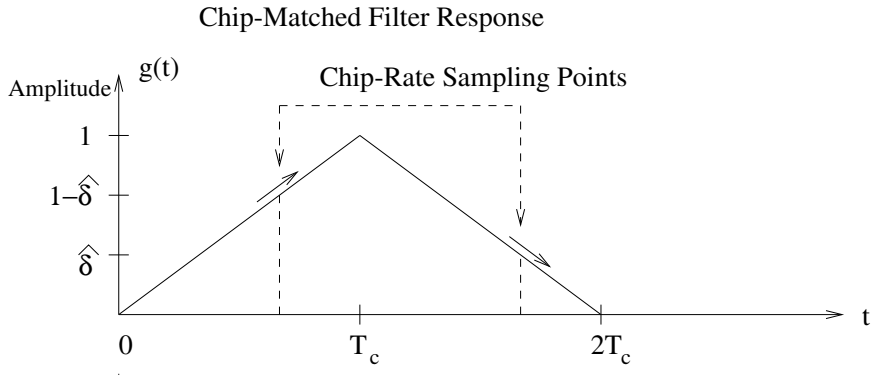

Figure 3.1: Sampling of the chip-matched filter response for rectangular chip-pulse shapes. The solid arrows represent the error in chip-matched filter response at the sampling points due to time delay mismatch.

3.3 Delay-Robust Multiuser Detectors

3.3.1 Prediction Error Approach

Denote the estimated time delay of the kth user as $\hat{\tau}_k = (_k + \hat{\delta}_k)T_c$, where $p_k \in \{0, 1, \ldots, N-1\}$ and $\hat{\delta}_k \in [0, 1)$ is the fractional part. Here we have assumed that all true delays and estimated delays occur in the same chip sampling interval (fractional delay uncertainty) where $\hat{p}_k = p_k$ for $1 \leq k \leq K$. The kth user's signature waveform for the ith interval $\mathbf{d}_k(i)$ can be expressed as the weighted sum of two signals, as shown in Fig. 3.1.

$$\begin{aligned}
\mathbf{d}_k(i) &= \delta_k \mathbf{c}_k(p_k+1, i) + (1-\delta_k)\mathbf{c}_k(p_k, i) \\
&= \left[\hat{\delta}_k \mathbf{c}_k(p_k+1, i) + (1-\hat{\delta}_k)\mathbf{c}_k(p_k, i)\right] + (\delta_k - \hat{\delta}_k)\left[\mathbf{c}_k(p_k+1, i) - \mathbf{c}_k(p_k, i)\right] \\
&\stackrel{\text{def}}{=} \hat{\mathbf{d}}_k(i) + (\delta_k - \hat{\delta}_k)\Delta\mathbf{d}_k(i) \qquad (3.14)
\end{aligned}$$

From (3.14), we can view each user as the combination of two virtual users, one with estimated code vector $\hat{\mathbf{d}}_k(i)$, and the other with error code vector $\Delta\mathbf{d}_k(i)$.

3.3.2 Two Virtual User Approach

Similar to [40] and [46], these two virtual users can also be the chip-synchronous adjacent shifted versions of that user's spreading code signal, i.e.,

$$\begin{aligned}\mathbf{d}_k(i) &= \delta_k \mathbf{c}_k(p_k+1,i) + (1-\delta_k)\mathbf{c}_k(p_k,i) \\ &\stackrel{\text{def}}{=} \delta_k \mathbf{d}'_{2k}(i) + (1-\delta_k)\mathbf{d}'_{2k-1}(i) \end{aligned} \tag{3.15}$$

Since a rectangular chip pulse is used, the expressions in (3.14) and (3.15) are exact [82].

3.3.3 Hybrid Approach

However, $\hat{p}_k = p_k$ is not always satisfied since the fractional delay error may across the integer chip boundary (integer fractional delay uncertainty). Consider the example that the true delay is $2.04T_c$ while the estimated delay is at $1.95T_c$, the estimated integer delay is one unit smaller than the true integer delay, $\hat{p}_k = p_k - 1$. Alternatively, rather than (3.14), the kth user's signature waveform for the ith interval $\mathbf{d}_k(i)$ can be expressed as a mixture between the previous two cases, i.e.,

$$\begin{aligned}\mathbf{d}_k(i) &= (1-\delta_k)\mathbf{c}_k(p_k,i) + \delta_k \mathbf{c}_k(p_k+1,i) \\ &= (1-\delta_k)\Big[(\hat{\delta}_k \mathbf{c}_k(p_k,i) + (1-\hat{\delta}_k)\mathbf{c}_k(p_k-1,i)) \\ &\quad +(1-\hat{\delta}_k)(\mathbf{c}_k(p_k,i) - \mathbf{c}_k(p_k-1,i))\Big] + \delta_k \mathbf{c}_k(p_k+1,i) \\ &\stackrel{\text{def}}{=} (1-\delta_k)\Big[\hat{\mathbf{d}}_k(i) + (1-\hat{\delta}_k)\Delta\mathbf{d}_k(i)\Big] + \delta_k \mathbf{c}_k(p_k+1,i) \end{aligned} \tag{3.16}$$

Each user can now be viewed as the combination of three virtual users with code vectors $\hat{\mathbf{d}}_k(i)$, $\Delta\mathbf{d}_k(i)$ and $\mathbf{c}_k(p_k+1,i)$. We denote the vector $\mathbf{c}_k(p_k+1,i)$ of the third virtual user as the *guard vector*. The robust SIC detector based on (3.16) uses a similar technique as the prediction error approach.

The above decomposition has the advantage in that it contains the additional term $\mathbf{c}_k(p_k+1,i)$, which allows for fractional delay error correction across integer

chip boundaries. Its disadvantage over Eg. (3.14) is noise enhancement when there is no integer chip error.

3.3.4 Delay-Robust Decorrelating Detector

For simplicity, we consider fractional delay uncertainty only. In view of (3.14), the vector of received signal (3.11) is modified as

$$\mathbf{r} = \mathbf{D}'\mathbf{A}'\mathbf{b}' + \mathbf{n} \tag{3.17}$$

where $\mathbf{b}' = [\mathbf{b}^T(1)\ \mathbf{b}^T(2)\ \ldots\ \mathbf{b}^T(M)\ \mathbf{b}^T(1)\ \mathbf{b}^T(2)\ \ldots\ \mathbf{b}^T(M)]^T \in \mathcal{R}^{2MK}$, $\mathbf{A}' = \mathbf{I}_M \otimes \mathbf{a}'$, $\mathbf{a}' = diag(\, a_1, a_2,\ \ldots,\ a_K, (\delta_1 - \hat{\delta}_1)a_1, (\delta_2 - \hat{\delta}_2)a_2,\ \ldots,\ (\delta_K - \hat{\delta}_K)a_K\,)$, and code matrix

$$\begin{aligned}\mathbf{D}' \ = \ & [\hat{\mathbf{d}}_1(1)\ \ldots\ \hat{\mathbf{d}}_K(1)\ \hat{\mathbf{d}}_1(2)\ \ldots\ \hat{\mathbf{d}}_K(2)\ \ldots\ \hat{\mathbf{d}}_1(M)\ \ldots\ \hat{\mathbf{d}}_K(M) \\ & \Delta\mathbf{d}_1(1)\ \ldots\ \Delta\mathbf{d}_K(1)\ \Delta\mathbf{d}_1(2)\ \ldots\ \Delta\mathbf{d}_K(2)\ \Delta\mathbf{d}_1(M)\ \ldots\ \Delta\mathbf{d}_K(M)] \\ & \in \mathcal{R}^{(M+1)N\times 2MK}\end{aligned} \tag{3.18}$$

We can now construct a delay-robust decorrelating detector as

$$\hat{\mathbf{b}}' = sign\ ([\mathbf{D}'^H\mathbf{D}']^{-1}\mathbf{D}'^H\mathbf{r}) \tag{3.19}$$

Since the signal energy in the error signal (signal in the error vector direction) may be small, we only use the signal energy in the estimated virtual user for bit detection, i.e.,

$$\hat{b}_k(i) = \hat{b}'_k(i)\ , \qquad\qquad k = 1, \ldots, K, \text{ and } i = 1, \ldots, M \tag{3.20}$$

Since (3.19) is a decorrelating detector, it does not depend on amplitude information and is near-far resistant under delay mismatch. However, since each user is decomposed into two virtual users, the total number of users that can be detected is upper bounded by $N/2$, where N is the spreading factor [40]. The computational complexity of delay-robust decorrelating detector is dominated by the doubled dimension matrix inversion, which is 8 times that of the standard decorrelating detector.

3.3.5 Multistage Delay-Robust Decorrelating Detector

One possible way to improve capacity and performance is to use a multistage version of the above delay-robust decorrelating detector. At each stage, the M error vectors of each user for different bit interval are combined into a "long" error vector based on the tentative data bit decision-feedback, $\hat{b}_k(i)$, as

$$\mathbf{e}_k = \sum_{i=1}^{M} \Delta\mathbf{d}_k(i)\hat{b}_k(i) \tag{3.21}$$

We construct a new code matrix $\mathbf{D}''$, but with a smaller dimension than that of (3.18)

$$\begin{aligned} \mathbf{D}'' \;=\; & [\hat{\mathbf{d}}_1(1)\ \ldots\ \hat{\mathbf{d}}_K(1)\,\hat{\mathbf{d}}_1(2)\ \ldots\ \hat{\mathbf{d}}_K(2)\ \ldots\ \hat{\mathbf{d}}_1(M)\ \ldots\ \hat{\mathbf{d}}_K(M) \\ & \mathbf{e}_1\ \ldots\ \mathbf{e}_K] \in \mathcal{R}^{(M+1)N\times(M+1)K} \end{aligned} \tag{3.22}$$

The vector of received signal (3.11) is expressed in $\mathbf{D}''$ as

$$\mathbf{r} = \mathbf{D}''\mathbf{A}''\mathbf{b}'' + \mathbf{n} \tag{3.23}$$

The multistage delay-robust decorrelating detector is implemented by the following procedure:

(1) Use the standard decorrelating detector (3.13) with estimated time delay to obtain the initial estimate:

$$\hat{\mathbf{b}} = sign\ ([\hat{\mathbf{D}}^H\hat{\mathbf{D}}]^{-1}\hat{\mathbf{D}}^H\mathbf{r}) \tag{3.24}$$

where $\hat{\mathbf{D}}$ is defined as in (3.12) but with $\hat{\mathbf{d}}_k(i)$ replacing $\mathbf{d}_k(i)$ for all k and i.

(2) Construct code matrix $\mathbf{D}''$ using (3.21) and (3.22) based on the tentative data bit decisions from the previous stage.

(3) Obtain tentative data bit decisions for the next stage via

$$\hat{\mathbf{b}}'' = sign([\mathbf{D}''^H\mathbf{D}'']^{-1}\mathbf{D}''^H\mathbf{r}) \tag{3.25}$$

(4) If the change of $\hat{\mathbf{b}}''$ from the previous stage is small enough, end the calculation. Otherwise go to step (2).

The number of users that can be supported is now $\frac{M}{M+1}N$. For moderate block lengths, such as $M = 9$, the capacity is now 90% of the spreading factor. Usually the above multistage delay-robust detector converges to a fixed point in 3-4 iterations. However, the inversion of a $(M+1)K \times (M+1)K$ matrix in (3.25) is still computationally complex.

3.3.6 Delay-Robust SIC Detector

The decorrelating detector is the maximum-likelihood estimator when the user amplitude information is unknown at the receiver [67]. The linear successive interference cancellation (SIC) receiver is a computationally attractive iterative implementation of the decorrelating detector with proven convergence properties [93] [125]. Since our proposed delay-robust SIC is based on a linear SIC implementation, where reordering of the users according to signal-to-noise ratio (SNR) at each iteration is not necessary [93], reordering is not performed here to reduce complexity. However, we note that although the delay-robust implementation is based on improving a linear SIC, it is not a linear SIC as a nonlinear decision is made in its iterations.

We propose the following multistage delay-robust SIC implementation of the above multistage delay-robust decorrelating detector:

Initialization:

Set:

$$\begin{aligned}
\Delta\mathbf{d}_l(i) &= \mathbf{c}_l(\hat{p}_l+1,i) - \mathbf{c}_l(\hat{p}_l,i), && 1 \le l \le K, 1 \le i \le M \\
\hat{\mathbf{d}}_l(i) &= \hat{\delta}_l \mathbf{c}_l(\hat{p}_l+1,i) + (1-\hat{\delta}_l)\mathbf{c}_l(\hat{p}_l,i), && 1 \le l \le K, 1 \le i \le M \\
\hat{a}_l^0(i) &= 0, && 1 \le l \le K, 1 \le i \le M \\
\hat{b}_l^0(i) &= 0, && 1 \le l \le K, 1 \le i \le M \\
\widehat{\Delta a}_l^{\,0} &= 0, && 1 \le l \le K
\end{aligned}$$

Iteration:

For $j = 0, 1, \ldots$ do:

For $k = 1, 2, \ldots, K$ do:

Steps (1) through (4):

(1) Estimate user k's received signal for the $(j+1)$st iteration by subtracting other users' reconstructed signals and the error signals from the received signal:

$$\mathbf{r}_k^{j+1} = \mathbf{r} - \sum_{l=1}^{k-1} (\hat{\mathbf{r}}_l^{j+1} + \widehat{\Delta a}_l^{j+1} \mathbf{e}_l^{j+1}) - \sum_{l=k+1}^{K} (\hat{\mathbf{r}}_l^{j} + \widehat{\Delta a}_l^{j} \mathbf{e}_l^{j}) - \widehat{\Delta a}_k^{j} \mathbf{e}_k^{j} \tag{3.26}$$

where $\mathbf{e}_l^j = \sum_{i=1}^{M} \Delta \mathbf{d}_l(i) \hat{b}_l^j(i)$ and $\hat{\mathbf{r}}_l^j = \sum_{i=1}^{M} \hat{b}_l^j(i) \hat{a}_l^j(i) \hat{\mathbf{d}}_l(i)$ for $l \geq k$, and $\mathbf{e}_l^{j+1} = \sum_{i=1}^{M} \Delta \mathbf{d}_l(i) \hat{b}_l^{j+1}(i)$, $\hat{\mathbf{r}}_l^{j+1} = \sum_{i=1}^{M} \hat{b}_l^{j+1}(i)$ $\hat{a}_l^{j+1}(i) \hat{\mathbf{d}}_l(i)$ and $\hat{b}_l^{j+1}(i) = sign\ ((\hat{\mathbf{d}}_{l-dec}(i))^H \mathbf{r}_l^{j+1})$ for $l < k$.

(2) Update user k's signal amplitudes and data bits:

$$\hat{a}_k^{j+1}(i) = abs\ ((\hat{\mathbf{d}}_k(i))^H\ \mathbf{r}_k^{j+1}) \tag{3.27}$$

$$\hat{b}_k^{j+1}(i) = sign\ ((\hat{\mathbf{d}}_k(i))^H\ \mathbf{r}_k^{j+1}) \tag{3.28}$$

where $abs(\ )$ and $sign(\ )$ take the absolute value and the sign, respectively.

(3) Estimate the error signal of the kth user due to timing error as:

$$\Delta \mathbf{r}_k^{j+1} = \mathbf{r}_k^{j+1} - \hat{\mathbf{r}}_k^{j+1} + \widehat{\Delta a}_k^{j} \mathbf{e}_k^{j} \tag{3.29}$$

(4) Update the amplitude of the error signal:

$$\mathbf{e}_k^{j+1} = \sum_{i=1}^{M} \Delta \mathbf{d}_k(i) \hat{b}_k^{j+1}(i)$$

$$\widehat{\Delta a}_k^{j+1} = \frac{1}{M} (\mathbf{e}_k^{j+1})^H (\Delta \mathbf{r}_k^{j+1}) \tag{3.30}$$

If for all $k = 1$ to K and $i = 1$ to M, $|\hat{a}_k^{j+1}(i) - \hat{a}_k^j(i)|$ are below a threshold, end the calculation.

The standard multistage linear SIC is an iterative version of the decorrelating detector, and it is guaranteed to converge to the decorrelating detector [93]. Our

delay-robust SIC adds an error signal estimation and cancellation procedure to the standard linear SIC. When the tentative data bit decision-feedback at the jth iteration are all correct, then the estimated error vector signal will have an interference cancellation factor of 100%. When some bits of the tentative data bit decision-feedback are incorrect, the estimated amplitude of the error signal will be smaller than the actual value, which is equivalent to soft cancellation with a factor less than 100%. So this delay-robust SIC implicitly incorporates soft interference cancellation into its iterations, and will likely converge to the multistage delay-robust decorrelating detector output. In the case when it does not converge to global maximum, good performance will still be expected: strong users are more likely to have an accurate residual error signal estimate and cancellation. As a result, error signal due to delay mismatch will be mostly cancelled out, and the local maximum will be close to the multistage delay-robust decorrelating detector output.

The proposed delay-robust SIC detector adds modest complexity to the standard multistage linear SIC detector, but with interference caused by the timing errors dramatically reduced. Its capacity is close to the ideal decorrelating detector with the perfect time delay estimates, when the block size M is not too small.

The above delay-robust SIC detector can be extended to multipath channels as well. Each path is divided into two virtual paths, and the delay error introduced interference is estimated and cancelled for each path. The multipath signals are combined using maximum ratio combining before the data bit decision. The complexity increase from the single path case is proportional to the number of multipaths.

We note that since $\widehat{\Delta a}_k = a_k(\delta_k - \hat{\delta}_k)$ from (3.14), the estimate of the error vector amplitude $\widehat{\Delta a}_k$ at $(j+1)$st iteration in (3.30) can be used to improve the delay estimate. The delay error $\delta_k - \hat{\delta}_k$ can be estimated as $\widehat{\Delta a}_k / a_k$. Since the true amplitude a_k is not known, a_k can be approximated as the time average of amplitude estimates over an M-bit long window: $a_k \approx \frac{1}{M}\sum_{i=1}^{M} \hat{a}_k(i)$, where $\hat{a}_k(i)$ is obtained from (3.27).

3.3.7 Convergence of the Delay-Robust SIC

To give insight into the convergence of the delay-robust SIC, we derive the algorithm by maximizing the log-likelihood function and employing the space alternating generalized expectation-maximization (SAGE) algorithm [24] as applied to the space-time decorrelation detector [122] [124].

The SAGE algorithm is a computational tool for maximum-likelihood estimation. This method divides the parameters to be estimated into several smaller hidden-data spaces specified by index sets, and sequentially updates these groups of parameters.

The derivation of the delay-robust SIC CDMA detector based on SAGE algorithm follows the procedure of [122] [123] [124]. If we choose user index k as the index set, the admissible hidden-data space for index k is

$$\mathbf{r}_k^S(i) \sim N(a_k(i)b_k(i)\hat{\mathbf{d}}_k(i), \sigma^2\mathbf{I}_M), \text{ for } i = 1, \ldots, M \tag{3.31}$$

and

$$\Delta\mathbf{r}_k^S \sim N(\Delta a_l \sum_{i=1}^{M} b_k(i)\Delta\mathbf{d}_k(i), \sigma^2\mathbf{I}_M) \tag{3.32}$$

At the jth iteration, given the amplitude estimations , $\hat{a}_k^j(i)$, data bit decisions, $\hat{b}_k^j(i)$, and the amplitude estimates of the error signals, $\widehat{\Delta a}_k^j$, for $k = 1, \ldots, K$ and $i = 1, \ldots, M$, the conditional expectation of $\mathbf{r}_k^S(i)$ and $\Delta\mathbf{r}_k^S$ is obtained as

$$\begin{aligned} \hat{\mathbf{r}}_k^S(i) &= \mathbf{r} - \sum_{m=1, m\neq i}^{M} \sum_{l=1, l\neq k}^{K} \hat{a}_l^j(m)\hat{b}_l^j(m)\hat{\mathbf{d}}_l(m) \\ &\quad - \sum_{l=1}^{K} \widehat{\Delta a}_l^j \sum_{m=1}^{M} \hat{b}_l^j(m)\Delta\mathbf{d}_l(m) \ , \qquad \text{for } i = 1, \ldots, M \end{aligned} \tag{3.33}$$

and

$$\widehat{\Delta\mathbf{r}}_k^S = \mathbf{r} - \sum_{m=1}^{M}\sum_{l=1}^{K} \hat{a}_l^j(m)\hat{b}_l^j(m)\hat{\mathbf{d}}_l(m) - \sum_{l=1, l\neq k}^{K} \widehat{\Delta a}_l^j \sum_{m=1}^{M} \hat{b}_l^j(m)\Delta\mathbf{d}_l(m) \tag{3.34}$$

The log-likelihood function of the received signal vector $\mathbf{r}$ is

$$ln\Omega(\mathbf{r}) = -(M+1)Nln\sigma^2 - \frac{1}{\sigma^2}(\mathbf{r} - \mathbf{D}'\mathbf{A}'\mathbf{b}')^H(\mathbf{r} - \mathbf{D}'\mathbf{A}'\mathbf{b}') \tag{3.35}$$

The log-likelihood function of $\hat{\mathbf{r}}_k^S(i)$ and $\widehat{\Delta\mathbf{r}}_k^S$ after removing the fixed terms is

$$\begin{aligned} ln\Omega(\hat{\mathbf{r}}_k^S(1),\ldots,\hat{\mathbf{r}}_k^S(M),\widehat{\Delta\mathbf{r}}_k^S) &= -\frac{1}{\sigma^2}\{(\sum_{i=1}^{M}(\hat{\mathbf{r}}_k^S(i)-a_k(i)b_k(i)\hat{\mathbf{d}}_k(i))+\widehat{\Delta\mathbf{r}}_k^S \\ &\quad -\widehat{\Delta a}_k\sum_{i=1}^{M}\hat{b}_k(i)\Delta\mathbf{d}_k(i))^H\ (\sum_{i=1}^{M}(\hat{\mathbf{r}}_k^S(i)-a_k(i)b_k(i)\hat{\mathbf{d}}_k(i)) \\ &\quad +\widehat{\Delta\mathbf{r}}_k^S-\widehat{\Delta a}_k\sum_{i=1}^{M}\hat{b}_k(i)\Delta\mathbf{d}_k(i))\} \end{aligned} \tag{3.36}$$

The maximization step (M-step) of SAGE maximizes the conditional expectation while keeping the other parameters fixed:

$$\hat{a}_l^{j+1}(m)=\hat{a}_l^j(m),\ \hat{b}_l^{j+1}(m)=\hat{b}_l^j(m) \qquad \text{for } (l,m)\neq(k,i) \tag{3.37}$$

The maximization results at the next iteration are given by

$$[\hat{\mathbf{a}}_k^{j+1},\hat{\mathbf{b}}_k^{j+1},\widehat{\Delta a}_k^{j+1}]=arg\max_{\mathbf{a}_k,\mathbf{b}_k,\Delta a_k} ln\Omega(\hat{\mathbf{r}}_k^S(1),\ldots,\hat{\mathbf{r}}_k^S(M),\widehat{\Delta\mathbf{r}}_k^S) \tag{3.38}$$

Since the correlation between $\sum_{i=1}^{M}(\hat{\mathbf{r}}_k^S(i)-a_k(i)b_k(i)\hat{\mathbf{d}}_k(i))$ and $\widehat{\Delta\mathbf{r}}_k^S-\widehat{\Delta a}_k\sum_{i=1}^{M}\hat{b}_k(i)\Delta\mathbf{d}_k(i)$ is very small when the time delay error is small, we assume those two vectors to be uncorrelated. With this assumption, equating the derivative of (3.38) to zero with respect to $a_k(i)b_k(i)$, for $i=1,\ldots,M$, we get

$$\hat{a}_k^{j+1}(i)\hat{b}_k^{j+1}(i)=\hat{\mathbf{d}}_k^H(i)\hat{\mathbf{r}}_k^S(i) \tag{3.39}$$

Since $b_k(i)\in\{-1,+1\}$, the data bit decisions are given by

$$\hat{b}_k^{j+1}(i)=sign\ (\hat{\mathbf{d}}_k^H(i)\hat{\mathbf{r}}_k^S(i)) \tag{3.40}$$

and the amplitude estimates are given by

$$\hat{a}_k^{j+1}(i)=abs\ (\hat{\mathbf{d}}_k^H(i)\hat{\mathbf{r}}_k^S(i)) \tag{3.41}$$

Equating the derivative of (3.38) to zero with respect to Δa_k, we get

$$\widehat{\Delta a}_k^{j+1}=(\sum_{i=1}^{M}\hat{b}_k^{j+1}(i)\Delta\mathbf{d}_k(i))^H\widehat{\Delta\mathbf{r}}_k^S \tag{3.42}$$

Equations (3.33), (3.34) and (3.37) are similar to equations (3.26) and (3.29), so steps (1) and (3) of the delay-robust SIC are equivalent to the expectation step (E-step) of the SAGE algorithm.

Equations (3.40), (3.41), (3.42) and (3.37) are similar to equations (3.27),(3.28) and (3.30), so steps (2) and (4) of the delay-robust SIC are equivalent to the maximization step (M-step) of the SAGE algorithm.

The SAGE algorithm produces a monotonically non-decreasing sequence of likelihood functions at each iteration, and is guaranteed to converge at least to a fixed stationary point or a local maximum [24]. Improved convergence rate over the expectation-maximization (EM) algorithm has been demonstrated by sequentially updating less informative hidden-data spaces in [122] [124]. Therefore, it is expected that the delay-robust SIC will converge at a fast rate.

3.4 Performance Analysis

In this section, we derive the the asymptotic multiuser efficiency (AME) [120] and bit error rate (BER) performance for the delay-robust SIC detector. We also calculate the Cramér-Rao lower bound (CRLB) for the delay-robust SIC as a delay error estimator and calculate the probability of the occurrence of an integer and fractional uncertainty delay estimate. Implementation complexity is then compared to other delay-robust multiuser detection methods.

3.4.1 AME and BER

Performance of CDMA multiuser detection methods can be measured by asymptotic multiuser efficiency (AME) [120]. AME is the asymptotic signal power loss of the multiuser detector compared to the single-user channel receiver as the background noise vanishes. The value of AME falls in the range $[0, 1]$. The AME of the ML multiuser detector is 1, which means the ML multiuser detector has no loss compared to the single-user lower bound. The AME of the conventional matched-filter is 0,

which means it may not correctly detect transmitted data bits regardless how large the signal power is. The AME for user k is defined as [120]

$$\eta_k = sup\left\{0 \le r \le 1 : \lim_{\sigma \to 0} \frac{P_k(\sigma)}{\mathcal{Q}(\sqrt{\frac{r\ a_k^2}{\sigma^2}})} < +\infty\right\} \tag{3.43}$$

where a_k is the received signal amplitude of user k, σ^2 is the white Gaussian noise variance, $P_k(\sigma)$ is the BER of user k at the multiuser detector output and $\mathcal{Q}(x) = \int_x^\infty \frac{1}{\sqrt{2\pi}} e^{-\frac{y^2}{2}} dy$.

For the fractional chip uncertainty delay estimate case, the AME and BER of the proposed delay-robust decorrelating detector are obtained similarly as the decorrelating detector [67]. The BER and AME for the ith bit of the kth user of the decorrelating detector with perfect time delay are, respectively [67]

$$P_{k,i}(\sigma) = \mathcal{Q}\left(\frac{a_k}{\sigma\sqrt{(\mathbf{D}^H\mathbf{D})^{-1}_{(i-1)K+k}}}\right) \tag{3.44}$$

and

$$\eta_{k,i} = max^2\left\{0, \frac{1}{\sqrt{(\mathbf{D}^H\mathbf{D})^{-1}_{(i-1)K+k}}}\right\} = \frac{1}{(\mathbf{D}^H\mathbf{D})^{-1}_{(i-1)K+k}} \tag{3.45}$$

where $(\mathbf{D}^H\mathbf{D})^{-1}_{(i-1)K+k}$ denotes the $[\ (i-1)K+k, (i-1)K+k\ ]$th element of the matrix $(\mathbf{D}^H\mathbf{D})^{-1}$.

For the delay-robust decorrelating detector and the multistage decorrelating detector (assume that at convergence, its tentative decision-feedback data bits are all correct), the AME and BER can be defined similarly as [67]

$$P_{k,i}(\sigma) = \mathcal{Q}(\frac{a_k}{\sigma\sqrt{(\mathbf{D}'^H\mathbf{D}')^{-1}_{(i-1)K+k}}}) \tag{3.46}$$

and

$$\eta_{k,i} = \frac{1}{(\mathbf{D}'^H\mathbf{D}')^{-1}_{(i-1)K+k}} \tag{3.47}$$

In [76], it was shown that for a K-user CDMA system using independent and identically distributed random spreading codes with spreading factor N, the average AME of a decorrelating detector is $\eta_K = \frac{N-K}{N-1}$. Similar asymptotic results were

obtained in a large-system analysis of a synchronous CDMA system with random spreading codes in [118] [121]. Therefore, the AME is inversely proportional to the number of users. The delay-robust decorrelating detector has an equivalent of $2K$ users. The multistage decorrelating detector described in Section 3.3 assuming correct tentative decision-feedback data bits has an equivalent of $\frac{M+1}{M}K$ users. The robust SIC detector is an iterative implementation of the multistage decorrelating detector, so its performance would be upper bounded by the multistage decorrelator.

Note that in (3.27) we have estimated $\hat{a}_k(i)$ independently at different time intervals, $1 \leq i \leq M$, which corresponds to use a linear decision function. If we use the constant amplitude property to average the $\hat{a}_k(i)$s, i.e., $\hat{a}_k = \frac{1}{M}\sum_{i=1}^{M} \hat{a}_k(i)$, or use exact amplitude information a_k (if it is available), then there will be less noise enhancement, and the delay-robust SIC detector may outperform the corresponding decorrelating detector (this will be shown in Chapter 4). However, convergence of such a smoothing procedure is not guaranteed.

The BER and AME for the ith bit of the kth user of the decorrelating detector with estimated time delay is calculated using the same method as in [85]. The conditional BER based on estimated time delay can be shown to be [85]

$$P_{e|\tau} = \frac{1}{2^{MK-1}} \sum_{\mathbf{b}\in\{-1,1\}^{MK}, b_k(i)=1} \mathcal{Q}\left(\frac{\mathbf{u}_{k,i}^T(\hat{\mathbf{D}}^H\hat{\mathbf{D}})^{-1}\hat{\mathbf{D}}\mathbf{D}\mathbf{A}\mathbf{b}}{\sigma\sqrt{(\hat{\mathbf{D}}^H\hat{\mathbf{D}})^{-1}_{(i-1)K+k}}}\right) \tag{3.48}$$

where $\mathbf{u}_{k,i} \in \mathcal{R}^{MK}$ is a unit vector with a '1' in the $((i-1)K+k)$th position and zeros elsewhere.

Denote $\mathbf{u}_{k,i}^T(\hat{\mathbf{D}}^H\hat{\mathbf{D}})^{-1}\hat{\mathbf{D}}\mathbf{D} = \mathbf{x}^T = [\mathbf{x}^T(1) \ \ldots \ \mathbf{x}^T(M)]$ and $\mathbf{x}(i) = [x_1(i) \ \ldots \ x_K(i)]^T$. The total BER, P_e, is calculated by averaging the conditional BER $P_{e|\tau}$ over the distribution of delay estimation errors. Since $P_{e|\tau}$ is dominated by the $\mathcal{Q}$-function with the smallest argument, the conditional AME for the ith bit of the kth user is

$$\eta_{k,i|\tau} = max^2\left\{0, \frac{x_k(i)a_k - \sum_{(l,j)\neq(k,i)}|x_l(j)|a_l}{a_k\sqrt{(\hat{\mathbf{D}}^H\hat{\mathbf{D}})^{-1}_{(i-1)K+k}}}\right\} \tag{3.49}$$

The average AME for the ith bit of the kth user is the conditional AME $\eta_{k,i|\tau}$ averaged over the distribution of the delay errors. As the AME of the decorrelating

detector with estimated delay depends on the powers of the other users, it is not near-far resistant.

To calculate the AME of the delay-robust SIC for the numerical results in Section 3.7, we use Eq. (3.49) with $\mathbf{D}''$ replacing $\hat{\mathbf{D}}$ to calculate the conditional AME, and then average over different delay errors. In the conditional AME calculation, we perform the following steps (1) - (3):

(1) The delay-robust SIC algorithm is used to obtain the data bit estimates $b_k(i)$.

(2) These $b_k(i)$ are substituted into (3.21) and (3.22) to obtain the code matrix $\mathbf{D}''$.

(3) The conditional AME of the delay-robust SIC is calculated using Eq. (3.49) with $\mathbf{D}''$ replacing $\hat{\mathbf{D}}$.

The steps (1) - (3) are run a large number of times, typically hundreds, with different time delays for each run to get an estimate of the average AME for the delay-robust SIC. We note that in Eq. (3.49), the noise power σ^2 is not used since it approaches zero in the definition of (see Eq. (3.43)) the AME. We also note that (3.45) and (3.47) are just special cases of (3.49) where the off-diagonal elements $x_l(j)$ are exactly zero for $(l, j) \neq (k, i)$.

3.4.2 Time Delay Error Variance Bound

To assess the proposed detector's robustness to time delay errors, we compare the observed time delay error variance to the Cramér-Rao lower bound (CRLB). The CRLB gives the lower bound on the variance for a scalar parameter or covariance matrix for parameter vectors that any unbiased estimator can attain [88]. Since our delay-robust SIC detector is an iterative implementation of the multistage delay-robust decorrelating detector with the correct tentative data bits decisions, and the decorrelating detector performs a linear transformation, it is easy to see that the decorrelating detector is an unbiased estimator and so the delay-robust SIC detector

is approximately unbiased as an iterative calculation of the multistage delay-robust decorrelating detector. The CRLB can therefore be used as a meaningful measure of the performance of the delay-robust SIC detector, and is derived as follows.

Let the kth user's signal amplitude be a_k, then by (3.14) the kth user's signal can be decomposed into two terms as

$$a_k \mathbf{d}_k(i) = a_k \hat{\mathbf{d}}_k(i) + a_k(\delta_k - \hat{\delta}_k)\Delta\mathbf{d}_k(i) \tag{3.50}$$

Define the amplitudes of the error signal as $\Delta a_k = a_k(\delta_k - \hat{\delta}_k)$. Clearly the time delay error is proportional to Δa_k.

For the problem we are considering, the parameters to be estimated are noise variance σ^2, user amplitudes $\mathbf{a} = [a_1 \ a_2 \ldots a_K]^T$ and the amplitudes of the error signals, $\Delta\mathbf{a} = [\Delta a_1 \ \Delta a_2 \ldots \Delta a_K]^T$. These parameters to be estimated are organized in a vector ψ

$$\psi = [\sigma^2 \ \ \mathbf{a}^T \ \ \Delta\mathbf{a}^T]^T \tag{3.51}$$

The observed data is the received vector $\mathbf{r} = [\mathbf{r}^T(1) \ \mathbf{r}^T(2) \ \ldots \ \mathbf{r}^T(M+1)]^T \in \mathcal{R}^{(M+1)N}$ in (3.3). The log-likelihood function is

$$ln\Omega(\mathbf{r}) = -(M+1)Nln\sigma^2 - \frac{1}{\sigma^2}(\mathbf{r} - \mathbf{d}\ \mathbf{a} - \Delta\mathbf{d}\ \Delta\mathbf{a})^H(\mathbf{r} - \mathbf{d}\ \mathbf{a} - \Delta\mathbf{d}\ \Delta\mathbf{a}) \tag{3.52}$$

where

$$\mathbf{d} = [\sum_{i=1}^{M}\mathbf{d}_1(i)b_1(i)\ldots\sum_{i=1}^{M}\mathbf{d}_k(i)b_k(i)\ldots\sum_{i=1}^{M}\mathbf{d}_K(i)b_K(i)] \tag{3.53}$$

and

$$\Delta\mathbf{d} = [\sum_{i=1}^{M}\Delta\mathbf{d}_1(i)b_1(i)\ldots\sum_{i=1}^{M}\Delta\mathbf{d}_k(i)b_k(i)\ldots\sum_{i=1}^{M}\Delta\mathbf{d}_K(i)b_K(i)] \tag{3.54}$$

The details of the derivation of the CRLB are in Appendix A. It is shown that the CRLB is the inverse of the Fisher information matrix $\mathbf{J} = E\left[\left(\frac{\partial ln\Omega(\mathbf{r})}{\partial\psi}\right)\left(\frac{\partial ln\Omega(\mathbf{r})}{\partial\psi}\right)^T\right] \in \mathcal{R}^{(1+2K)\times(1+2K)}$, which can be written as

$$\mathbf{J} = \begin{bmatrix} (M+1)N/\sigma^4 & \mathbf{0} & \mathbf{0} \\ \mathbf{0} & \mathbf{J}_{\mathbf{aa}} & \mathbf{J}_{\mathbf{a}\Delta\mathbf{a}} \\ \mathbf{0} & \mathbf{J}^H_{\mathbf{a}\Delta\mathbf{a}} & \mathbf{J}_{\Delta\mathbf{a}\Delta\mathbf{a}} \end{bmatrix} \tag{3.55}$$

where the matrices $\mathbf{J_{aa}}, \mathbf{J_{a\Delta a}}, \mathbf{J_{\Delta a\Delta a}} \in \mathcal{R}^{K\times K}$ are defined as

$$\mathbf{J_{aa}} = \frac{2}{\sigma^2}\mathbf{a}^H\mathbf{d}^H\mathbf{d}\ \mathbf{a} \tag{3.56}$$

$$\mathbf{J_{a\Delta a}} = \frac{2}{\sigma^2}\mathbf{a}^H\mathbf{d}^H\Delta\mathbf{d}\ \Delta\mathbf{a} \tag{3.57}$$

$$\mathbf{J_{\Delta a\Delta a}} = \frac{2}{\sigma^2}\Delta\mathbf{a}^H\Delta\mathbf{d}^H\Delta\mathbf{d}\ \Delta\mathbf{a} \tag{3.58}$$

We note that the CRLB is conditioned on known data symbols $b_k(i)$ and is interpreted as the lower variance bound given the knowledge of $b_k(i)$. In Section 3.7, the CRLB will be compared to simulated delay-robust SIC performance.

3.4.3 Probability of the Integer and Fractional Uncertainty Delay Estimate

When the estimated delay is not in the same chip interval of the true delay, i.e., $\hat{p}_k \neq p_k$, and the delay-robust SIC detector designed for fractional delay uncertainty case is used for this integer and fractional delay uncertainty case, there will be residual MAI. If this residual MAI is not eliminated, the performance will degrade.

For MUSIC-based delay estimation, it is shown in [110] that the probability of $p_k \neq \hat{p}_k$ is very small for $SNR_1 = 15$ dB and $M = 100$ observation lengths at near-far ratio of 20 dB. So in [15], this case is not included in performance evaluation of the MUSIC-based delay estimator. However, it is interesting to know how large the probability that $\hat{p}_k \neq p_k$ will be, if we assume the delay error is Gaussian distributed and can across chip boundaries, and a uniformly distributed actual delay position in a chip interval.

Assuming that the delay estimate error is a zero-mean Gaussian random variable with variance σ_τ, the per-user probability that $p_k \neq \hat{p}_k$ is obtained as (see Appendix B)

$$P = 2\left\{\mathcal{Q}(\frac{1}{\sigma_\tau}) + \frac{\sigma_\tau}{\sqrt{2\pi}}(1 - e^{-\frac{1}{2\sigma_\tau^2}})\right\} \tag{3.59}$$

In Section 3.7, we choose $\sigma_\tau = 0.1$, corresponding to $P \approx \frac{2\sigma_\tau}{\sqrt{2\pi}} = 0.08$.

3.4.4 Implementation Complexity

In this subsection, we calculate the computational complexity of the proposed delay-robust SIC and compare it to those of other multiuser detectors.

Note that in the decorrelation in the initialization step there are MK 2×2 matrices, each constructed from multiplying $2 \times N$ and $N \times 2$ matrices, and therefore is $O(MNK)$. Assume that the delay-robust SIC needs J iterations. Each iteration of the robust SIC algorithm takes $O(MNK)$ computations, so the total complexity is $O(JMNK)$. Usually $J = 10$ is enough to get close to steady-state performance. No reordering according to SNR is performed in the algorithm.

The decorrelating detector has complexity $O(M^3K^3)$. The SIC implementation of the decorrelating detector is of complexity $O(JMNK)$ [93], assuming that the number of SIC stages is the same as that of the delay-robust SIC. The delay-robust decorrelating detector [46] and [40] has complexity $O(M^3K^3)$. The improved MMSE (IMMSE) multiuser detector [14] [46] has complexity at least $O(M^3K^3)$.

Successive interference cancellation (SIC) is a low complexity suboptimum CDMA multiuser detection method and has been considered to be practical for actual CDMA basestation implementation [100]. Although the delay-robust SIC approximately doubles both computational complexity and processing delay of those of standard SIC algorithm [84], its complexity is still far less than those of other delay-robust multiuser detectors.

3.5 Larger Delay Errors

The previous delay-robust SIC algorithm is developed under the assumption that the time delay error is small, i.e., with standard deviation $\sigma_\tau = 0.1T_c$. Although this time delay estimation error is typical of the current multi-user delay estimators, and some multi-user delay estimators have a smaller standard deviation than $0.1T_c$, it is beneficial to evaluate the performance of the delay-robust SIC under larger time delay estimation errors. In this subsection, we simulate the delay-robust SIC performance

as a function of the time delay error for rectangular chip pulse shapes, and observe when the delay-robust SIC breaks down. Based on the simulation results, we find the reason for breakdown and propose an enhancement to the delay-robust SIC so that it can operate under larger time delay error conditions.

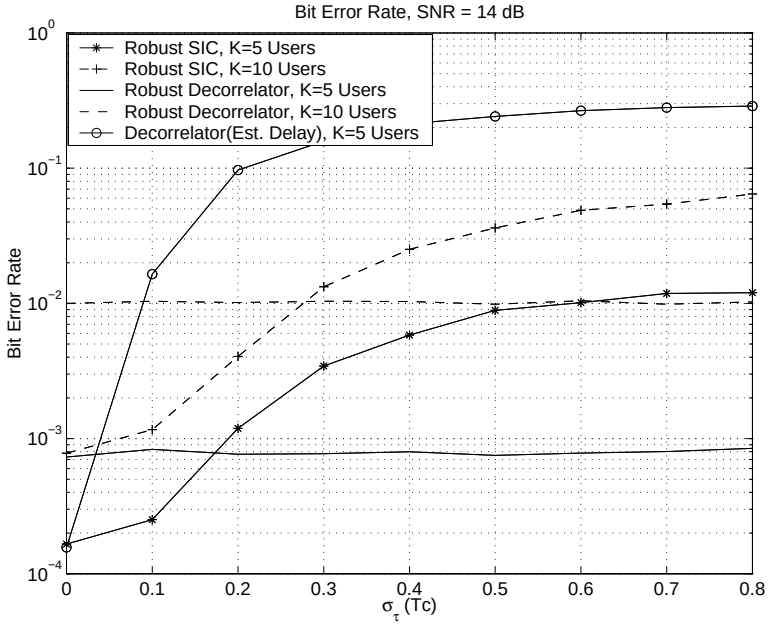

Figure 3.2: Bit Error rate (BER) of user 1 as a function of the delay error standard deviation σ_τ. Near-far ratio 20 dB.

In Fig. 3.2, the BER performance of the delay-robust SIC and the delay-robust decorrelator are simulated as a function of the time delay error standard deviation from $\sigma_\tau = 0.0T_c$ to $0.8T_c$ for both $K = 5$ users and $K = 10$ users. As a comparison, curves for the decorrelator with estimated delay information are also shown for the $K = 5$ user case. The delay error is truncated to lie within $\pm 0.5T_c$ as all users are assumed under acquisition. As we can see, the BER of the delay-robust SIC gets worse as σ_τ increases. This degradation slows after σ_τ reaches $0.5T_c$. However, the BER of the delay-robust decorrelator remains constant.

We conjecture that the reason for this difference is that when the time delay error becomes larger, correlation between the signal at the estimated vector direction and the residual interference signal due to timing error in the error vector direction

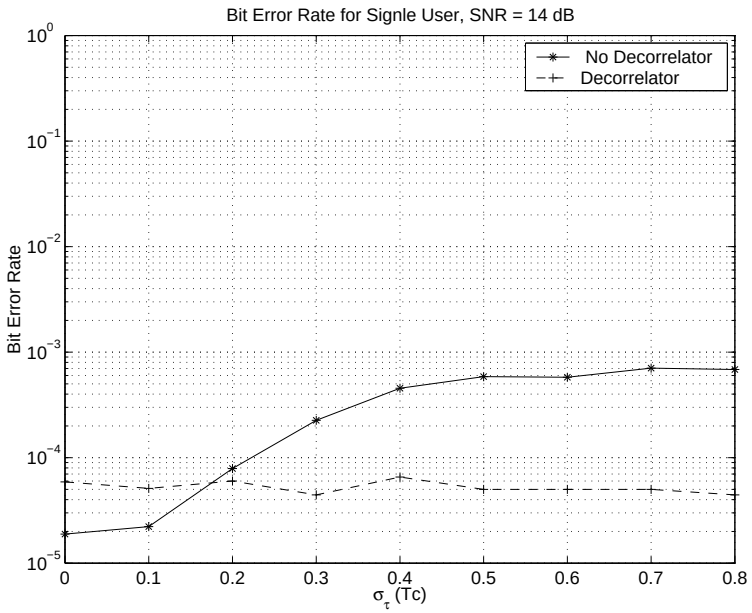

Figure 3.3: Bit Error rate (BER) of single user channel as a function of the delay error standard deviation σ_τ.

becomes larger. Since the delay-robust decorrelator performs decorrelation between those two signals, it is not affected by this correlation. To prove that the degradation is mainly caused by the residual self-interference introduced by timing error, we simulated a single-user scenario where the matched-filter receiver is matched to the estimated time delay. The BER is shown as a function of the delay error standard deviation σ_τ in Fig. 3.3. Almost the same amount of BER increase is observed for the single-user case without decorrelation as the delay-robust SIC in the multi-user case. In Fig. 3.3, we also simulated a decorrelator which decouples the two signals from the same user. Due to the decorrelation, the desired signal is not affected by the residual self-interference, and so the BER curve is almost constant.

We therefore propose to insert a local decorrelation operation between the signals of the same user into the delay-robust SIC algorithm. Denote $\hat{\mathbf{d}}_{k-dec}(i) = \mathbf{D}(i)[\mathbf{D}(i)^H\mathbf{D}(i)]^{-1}[1\ 0]^H$, where $\mathbf{D}(i) = [\hat{\mathbf{d}}_k(i)\ \ \Delta\mathbf{d}_k(i)]$. The decorrelation $[\mathbf{D}(i)^H\mathbf{D}(i)]^{-1}$ is used to separate the signals in the $\hat{\mathbf{d}}_k(i)$ and $\Delta\mathbf{d}_k(i)$ directions, to prevent the self-interference from the residual signal due to timing error. Note this local decorrelation

is similar to the local multipath decorrelation used to decouple multipath signals from the same user in the multistage SIC receiver in [123] and [126].

The original delay-robust SIC in Section 3.3.6 is modified by replacing $\hat{\mathbf{d}}_k(i)$ with $\hat{\mathbf{d}}_{k-dec}(i)$ in (3.27) and (3.28) to incorporate the local decorrelation. We remark that $\hat{\mathbf{d}}_{k-dec}(i)$ only needs to be calculated once at the beginning of the algorithm.

When $\sigma_\tau < 0.2T_c$, the self-interference from the timing error residual signal is small, and it is advantageous to use $\hat{\mathbf{d}}_k(i)$ instead of $\hat{\mathbf{d}}_{k-dec}(i)$ in (3.27) and (3.28) to avoid noise enhancement due to the extra decorrelation step. The performance of the improved delay-robust SIC under large timing errors is shown in Section 3.7.

3.6 Delay-Robust SIC Detector for Band-limited Chip Pulse Shapes

Few research results have been reported on delay-robust multiuser detectors with different chip pulse shapes. In [16], an approach similar to the IMMSE detector of [14] was extended to a pulse-shaping system, and a modified maximum-likelihood sequence detection (M-MLSD) is derived by averaging over the time delay error distributions. In this section, we will construct a generalized system model for a band-limited chip pulse shapes CDMA system, and extend the proposed robust SIC detector of Section 3.3 to this general case.

The system model is similar to the one used in [16] and [125]. The received signal is

$$r(t) = \sum_i \sum_{k=1}^{K} a_k(i) b_k(i) \tilde{s}_k(t - iT - \tau_k) + n(t) \tag{3.60}$$

The normalized signature waveform of user k is $\tilde{s}_k(t)$

$$\tilde{s}_k(t) = \sum_{j=0}^{N-1} c_k(j) \psi(t - jT_c) \tag{3.61}$$

where $\psi(t)$ is a band-limited chip pulse shape and the other symbols are the same as in (3.2). In the simulations, a square-root raised cosine pulse shape is used for

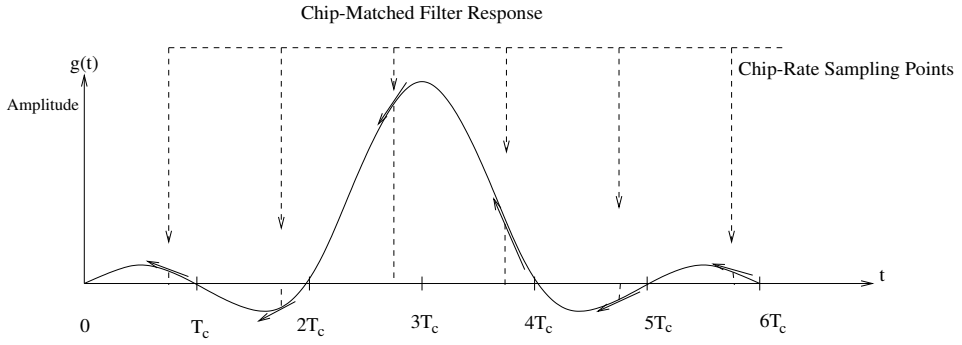

Figure 3.4: Sampling of the chip-matched filter response for truncated band-limited chip-pulse shapes. The solid arrows represent the first order derivative of the chip-matched filter response at the sampling points with estimated timing delay.

the chip-pulse waveform, $\psi(t)$. The receiver front-end is a chip-matched filter with impulse response $\psi^*(t)$. After chip-matched filtering and chip-rate sampling, equation (3.60) can be expressed in vector form as

$$\mathbf{r} = \sum_{i=1}^{M+1} \sum_{k=1}^{K} a_k b_k(i) \mathbf{d}_k(i) + \mathbf{n} \tag{3.62}$$

For the general chip pulse shapes, the received signature waveform of the ith bit of the kth user, $\mathbf{d}_k(i)$, is the convolution of the user spreading codes with the chip-matched filter response at the sampling points, i.e.,

$$\mathbf{d}_k(i) = \mathbf{c}_k(p_k, i) * \mathbf{g}_k \tag{3.63}$$

where vector $\mathbf{g}_k$ is the kth user's chip-matched filter response at the chip-rate sampling points, as shown in Fig. 3.4. If the chip-matched filter response is truncated to length PT_c, then the vector $\mathbf{g}_k$ will be of length P, and the signature waveform $\mathbf{d}_k(i)$ will have $N + P - 1$ non-zero elements. The mth element of $\mathbf{g}_k$ is given by

$$g_k(m) = \int_{-\infty}^{\infty} \psi(\tau - \delta_k T_c) \psi^*(mT_c - \tau) d\tau \ , \qquad \text{m} \ \in \{1, 2, \ldots, P\} \tag{3.64}$$

The error vector $\Delta\mathbf{d}_k(i)$ for the band-limited chip pulse shape is the convolution of the user spreading codes with the first derivative vector $\mathbf{f}_k$ of the kth user's chip-matched filter response at the sampling points, i.e.,

$$\Delta\mathbf{d}_k(i) = \mathbf{c}_k(p_k, i) * \mathbf{f}_k \tag{3.65}$$

with elements

$$f_k(m) = \frac{\partial}{\partial t} \int_{-\infty}^{\infty} \psi(\tau - \delta_k T_c)\psi^*(t-\tau)d\tau \mid_{t=mT_c} \quad , \qquad \mathrm{m} \in \{1, 2, \ldots, P\} \quad (3.66)$$

The kth user's signature waveform for the ith interval $\mathbf{d}_k(i)$ is first-order Taylor expanded as

$$\mathbf{d}_k(i) \approx \hat{\mathbf{d}}_k(i) + (\delta_k - \hat{\delta}_k)\Delta\mathbf{d}_k(i) \quad (3.67)$$

The expansion is not exact unlike the expression (3.14) derived for the case of rectangular chip pulse shapes. Actually the case of rectangular chip pulse shapes can be viewed as a special case of the band-limited chip pulse, with $P = 2$, $\mathbf{g}_k = [(1 - \hat{\delta}_k)\ \hat{\delta}_k]$ and $\mathbf{f}_k = [-1\ 1]$.

After we obtain (3.65) and (3.67), the delay-robust SIC detector of Section 3.3 can be applied by substitution into (3.14). Since the Taylor expansion of (3.67) is not exact, there will be some residual interference. As will be shown in Section 3.7, this interference is not large as long as the timing error is small enough so that first-order Taylor expansion is a good approximation.

3.7 Numerical and Simulation Results

In this section, through simulation we compare the performance of the delay-robust SIC multiuser detector to that of the decorrelating detector with and without perfect time delay estimates. Performance results for large delay error and for band-limited chip pulse shapes are also included.

Throughout the simulations, we will assume as in [85] that the delay estimation errors are independent zero-mean Gaussian random variables with equal standard deviation $\sigma_\tau = 0.1T_c$ for all users if not otherwise stated. Gold code sequences of length 31 and a block size of $M = 9$ are used. The power of the first user is fixed at unity, and different near-far ratios P_k/P_1 are obtained by varying the power of other users, where $P_k = a_k^2$. The signal-to-noise ratio (SNR) is defined for the first user as $SNR = P_1/\sigma_n^2$. Unless otherwise stated, the estimated time delays have only

fractional chip uncertainty and rectangular chip-pulse shapes are used. Although a Gaussian delay error distribution is used for the simulations, we note the delay-robust SIC detector operation does not depend on the delay error distribution.

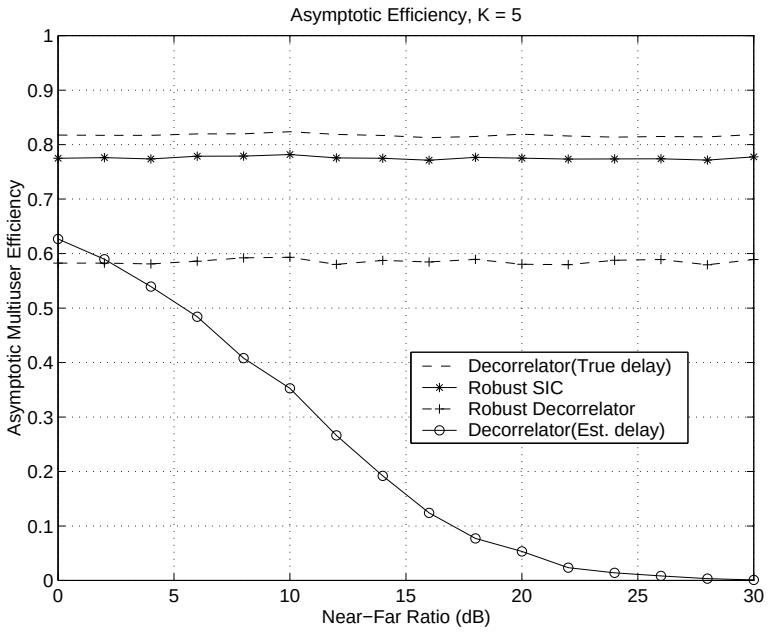

Figure 3.5: Asymptotic multiuser efficiency (AME) as a function of near-far ratio for $\sigma_\tau = 0.1T_c$. $K = 5$ users.

In Figures 3.5-3.15, the *Decorrelator(True Delay)* curves refer to the decorrelating detector with true time delays, Eq. (3.13). *Decorrelator(Est. Delay)* refers to the decorrelating detector with estimated time delays, Eq. (3.24), *Robust SIC* refers to the delay-robust SIC detector of Eqs. (3.14), (3.26)-(3.30), *Robust Decorrelator* refers to the delay-robust decorrelating detector with $2K$ virtual users of Eq. (3.19). As expected, the delay-robust decorrelators employing virtual users as in (3.14) have almost identical BERs compared to that using (3.15). In all figures, therefore, only the curves of the delay-robust decorrelator using (3.14) will be shown. The *Decorrelator(True Delay, Analytical)*, *Robust SIC(Analytical)* and *Robust Decorrelator(Analytical)* curves refer to the analytical bit error rate (BER) calculated using the Q-function, with the SNR adjusted by a factor of 2/3, to account for the chip-asynchronous loss for rectangular chip pulses [70]. These analytical curves serve to

confirm the accuracy of the BER simulation curves.

The asymptotic multiuser efficiency (AME) simulations in Figs. 3.5 and 3.6 are calculated for user 1. The power of other users are equal and the near-far ratio is defined as P_k/P_1. The result is obtained through 500 Monte Carlo runs with an independent realization of delay at each run.

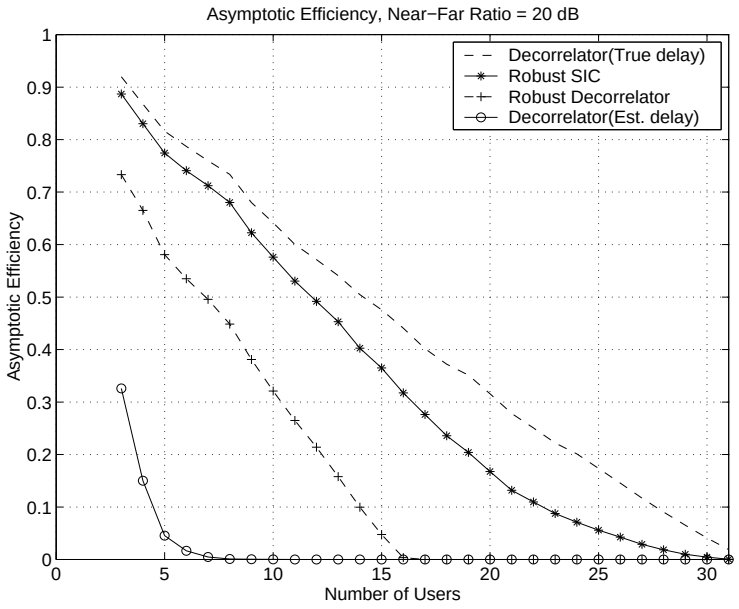

Figure 3.6: Asymptotic multiuser efficiency (AME) as a function of number of users for $\sigma_\tau = 0.1T_c$. Near-far ratio 20 dB.

In Fig. 3.5, the number of users is $K = 5$ and the near-far ratio is increased from 0 to 30 dB. The multistage delay-robust decorrelating detector with correct data bit decisions serves as the upper bound for the delay-robust SIC detector. As shown, the AME of the proposed delay-robust SIC detector is between the AME value of decorrelating detector with true delays and the delay-robust decorrelating detector, and stays constant as the near-far ratio increases. Therefore this delay-robust SIC detector exhibits near-far resistance under delay mismatch. As the near-far ratio increases, the AME of the decorrelating detector with estimated time delays decreases toward zero.

Fig. 3.6 compares the AME performance as the number of users is increased from

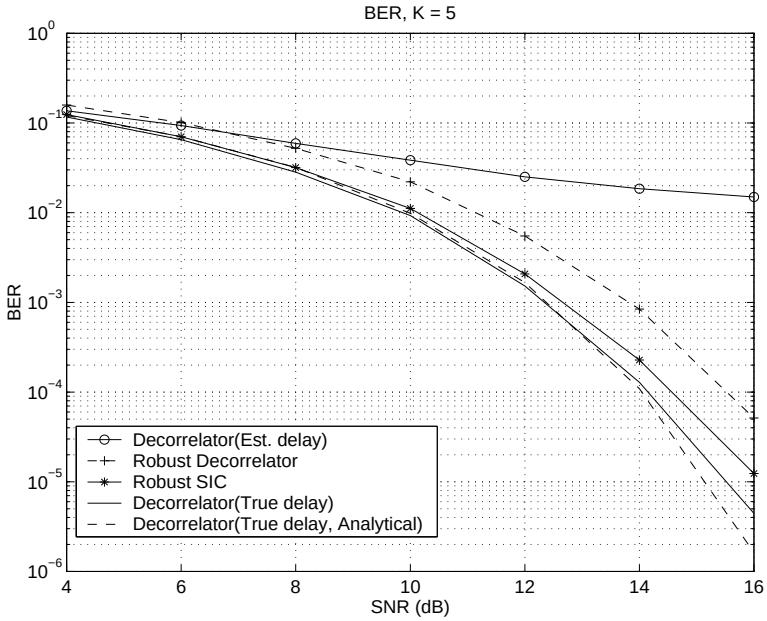

Figure 3.7: Bit Error rate (BER) of user 1 for $\sigma_\tau = 0.1T_c$. Proposed delay-robust SIC detector with $K = 5$ users. Near-far ratio 20 dB.

3 to 31. The near-far ratio is fixed at 20 dB. As expected from Section 3.4.1, the delay-robust SIC can support $\frac{M}{M+1}N = \frac{9}{10} \times 31 \simeq 28$ users (AME is greater than zero). The decorrelator with estimated delays can only support 5 or 6 users while the delay-robust decorrelator can support 16 users, about half the spreading factor, N/2. It can also be observed that as the number of users increases, the AME of the delay-robust decorrelator approaches zero at twice the rate compared to the decorrelator with true delays, while the delay-robust SIC decrease is close to that of the decorrelator with true delays.

For the BER and AME simulations in Figures 3.7-3.15, the near-far ratio is defined as the power ratio of the second user to the first user, P_2/P_1. The second user is the strongest user, and the user of interest, the first user, has the lowest received power. The near-far ratio is 20 dB and all other users have unequal power ratio uniformly distributed between 20 dB and 0 dB. The BER is averaged over 500 different delay realizations. For each delay realization, a large number (i.e., 500) of Monte Carlo simulations are run, with the transmitted data bits generated independently for each

run.

In Fig. 3.7, the results show that with 5 users the BER of the delay-robust SIC detector (Section 3.3.1) is lower than that of the delay-robust decorrelator and is close to the BER of the ideal decorrelator with known time delays. At a BER of 10^{-3}, the loss compared to the ideal decorrelator is about 0.2 dB. The BER of the decorrelator with estimated delays is larger than 10^{-2} in large SNR, which makes it completely unusable in this severe near-far condition. We find that the proposed delay-robust SIC detector converges in 15 iterations, where we define convergence of the robust SIC detector to occur when the difference in estimated value of signal amplitude between two consecutive iterations is less than 0.1%.

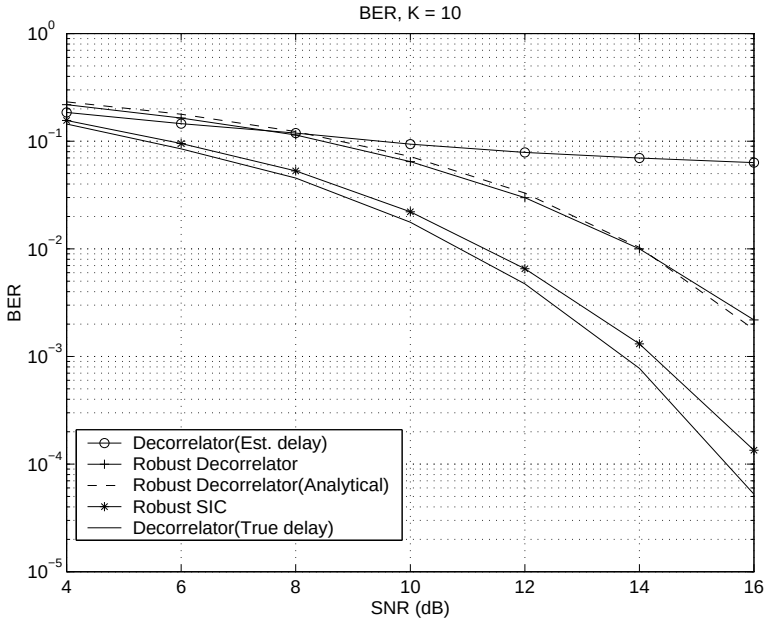

Figure 3.8: Bit Error rate (BER) of user 1 for $\sigma_\tau = 0.1T_c$. Proposed delay-robust SIC detector with $K = 10$ users. Near-far ratio 20 dB.

While in Fig. 3.7, the performance improvement of the delay-robust SIC detector over the delay-robust decorrelator is not large for 5 users, in Fig. 3.8 we increase the number of users to $K = 10$. The BER improvement is now obvious.

We have claimed that the delay-robust SIC detector has a capacity of over 50% of the spreading factor. To show this, a system with 20 users is simulated in Fig.

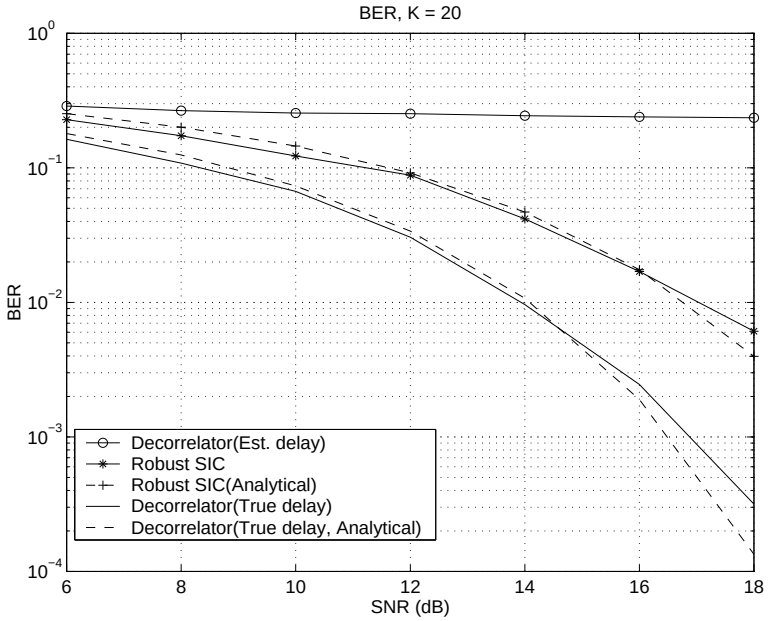

Figure 3.9: Bit Error rate (BER) of user 1 for $\sigma_\tau = 0.1T_c$. Proposed delay-robust SIC detector with $K = 20$ users. Near-far ratio 20 dB.

3.9. The difference between the delay-robust SIC detector and the decorrelator with true delays is significant. This can be explained by the AME values of Fig. 3.6, in which the AME of the delay-robust SIC detector is about half of that of the ideal decorrelator.

In Fig. 3.10, we compare the standard deviations of the time delay error estimation of the weakest (first) user by the delay-robust SIC detector and the multistage delay-robust decorrelating detector with correct data bit decisions to the Cramér-Rao lower bound (CRLB). The near-far ratio is 20 dB. The number of users is $K = 5$. The result is obtained through 500 Monte Carlo simulations. The root mean square error (RMSE) of the delay-robust SIC detector and the multistage delay-robust decorrelating detector with correct data bit decisions are almost identical. Since the decorrealting detector output is an unbiased estimate, this means that the delay-robust SIC detector output is approximately unbiased. Their standard deviations have a constant gap compared to the CRLB as the SNR changes. This performance gap is the result of the noise enhancement in the decorrelating detector.

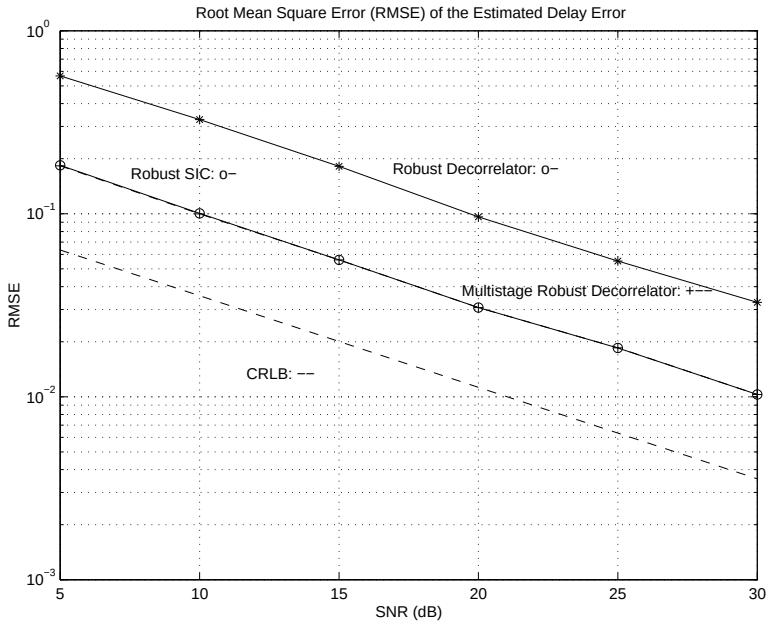

Figure 3.10: RMSE and Cramér-Rao lower bound (CRLB) of user 1's delay error estimate for $\sigma_\tau = 0.1T_c$ and $K = 5$ users. Near-far ratio = 20 dB.

In Fig. 3.11, performance of the two proposed approaches are compared for $\sigma_\tau = 0.1T_c$. *Robust SIC(Guard Vector)* refers to the delay-robust SIC detector using (3.16) of Section 3.3.3, *Robust SIC(No Guard Vector)* refers to the delay-robust SIC detector using (3.14) of Section 3.3.1 in both integer and fractional uncertainty delay conditions where the fractional delay error may across integer chip boundary. From Fig. 3.11, as the SNR gets larger, the delay-robust SIC detector (Guard Vector) of Eq. (3.16) outperforms the delay-robust SIC detector (No Guard Vector) of Eq. (3.14) and as expected since there is little noise enhancement, but at a cost of reduced capacity, which is now reduced to $\frac{M}{M+2}N$. In Fig. 3.12, we increase the delay error standard deviation σ_τ from $0.1T_c$ to $0.15T_c$ to make the error floor of the delay-robust SIC detector (No Guard Vector) more obvious.

In Figs. 3.13 and 3.14, we simulated the AME and BER of the delay-robust SIC. When $\sigma_\tau \geq 0.2T_c$, $\hat{\mathbf{d}}_{k-dec}(i)$ (defined in Section 3.5) is used in (3.27) and (3.28). When $\sigma_\tau < 0.2T_c$, $\hat{\mathbf{d}}_k(i)$ is used in (3.27) and (3.28). From the results, our delay-robust SIC is usable as long as the estimated time delay is within $\pm 0.5T_c$ of the true delay (under

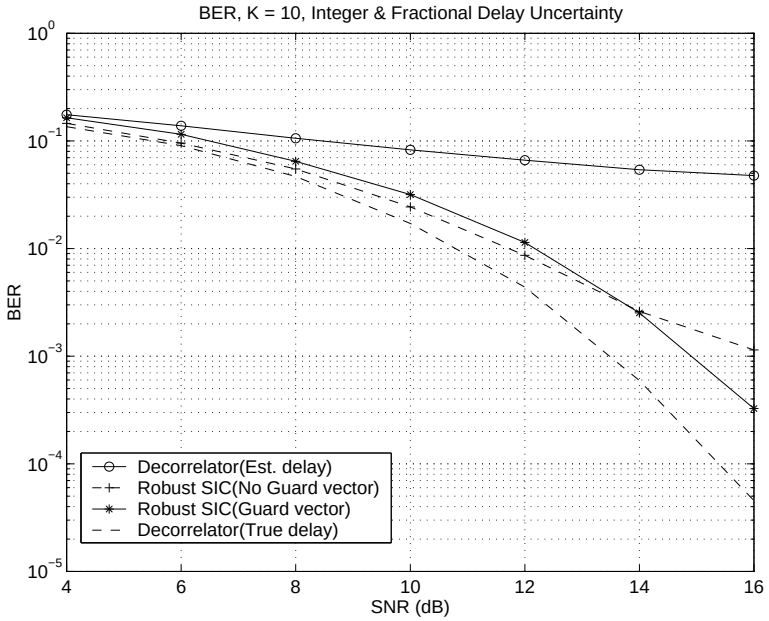

Figure 3.11: Integer and fractional uncertainty delay estimates. Bit Error rate (BER) of user 1 for $\sigma_\tau = 0.1T_c$ and $K = 10$ users. Near-far ratio 20 dB.

acquisition), although its performance is best when $\sigma_\tau \leq 0.1T_c$.

Fig. 3.15 shows simulation results of the delay-robust SIC detector for band-limited chip-pulse shapes with $K = 5$ users and the $SNR = a_1^2 \int_{-\infty}^{\infty} \psi(t)^2 dt/\sigma^2 T_c$. From Fig. 3.15, the delay-robust SIC detector has a lower BER than the delay-robust decorrelating detector. Although both the BERs of the delay-robust SIC detector and the delay-robust decorrelating detector show significant improvement over the decorrelating detector with estimated delays, there is a larger performance gap compared to the ideal decorrelator, due to the residual error in the first-order Taylor expansion in (3.67).

3.8 Conclusion

In this chapter, we have proposed a delay-robust SIC detector that is robust to time delay estimation errors under near-far conditions. The BER and AME performance

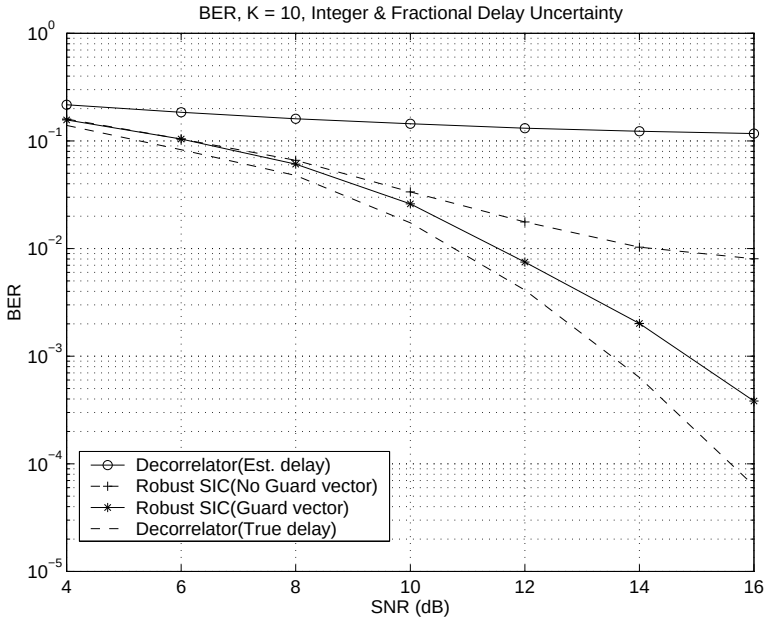

Figure 3.12: Integer and fractional uncertainty delay estimates. Bit Error rate (BER) of user 1 for $\sigma_\tau = 0.15T_c$ and $K = 10$ users. Near-far ratio 20 dB.

measures are derived and simulated. The receiver is near-far resistant when the estimated delay is close to that of the true delay. Performance is only slightly inferior to a decorrelating detector with perfect delay estimates, but better than a decorrelating detector with estimated delays. User capacity is greater than the 50% capacity limit of the synchronous delay-robust decorrelating detector [40] [46], and the AME is improved as well. This delay-robust SIC detector is also equivalent to iterative maximization of the log-likelihood function using the SAGE algorithm, so convergence to at least a fixed point is guaranteed. The delay-robust SIC can also be used as a delay error estimator, and its root mean square error (RMSE) performance is compared to the CRLB. For large delay errors and rectangular chip pulses, a local decorrelation step is incorporated into the delay-robust SIC to improve performance. Finally, this delay-robust SIC detector, when generalized to band-limited chip pulse shapes, exhibits some performance degradation due to incomplete interference cancellation.

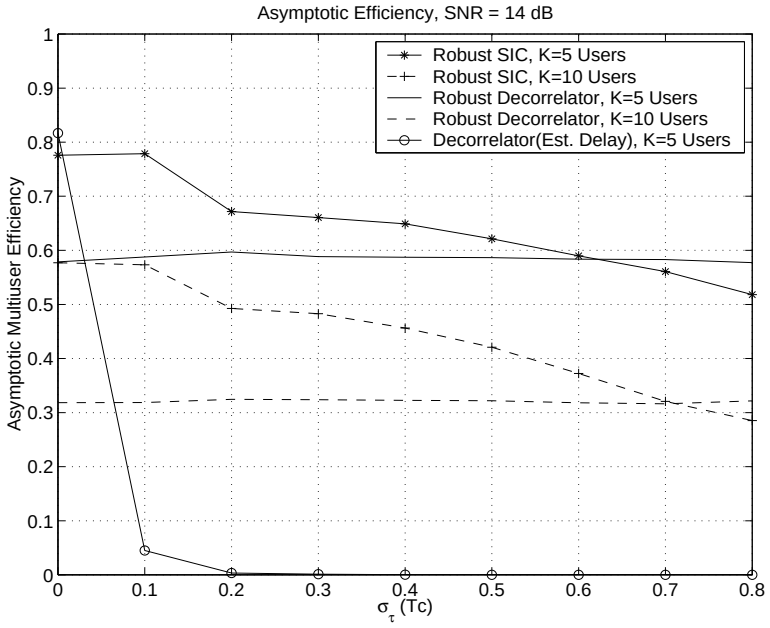

Figure 3.13: Asymptotic multiuser efficiency (AME) as a function of the delay error standard deviation σ_τ. Near-far ratio 20 dB.

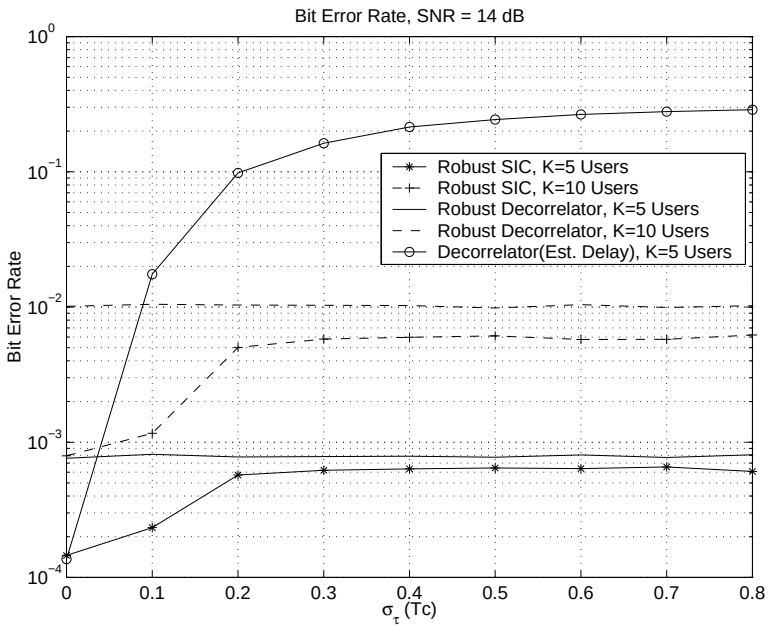

Figure 3.14: Bit Error rate (BER) of user 1 as a function of the delay error standard deviation σ_τ. Near-far ratio 20 dB.

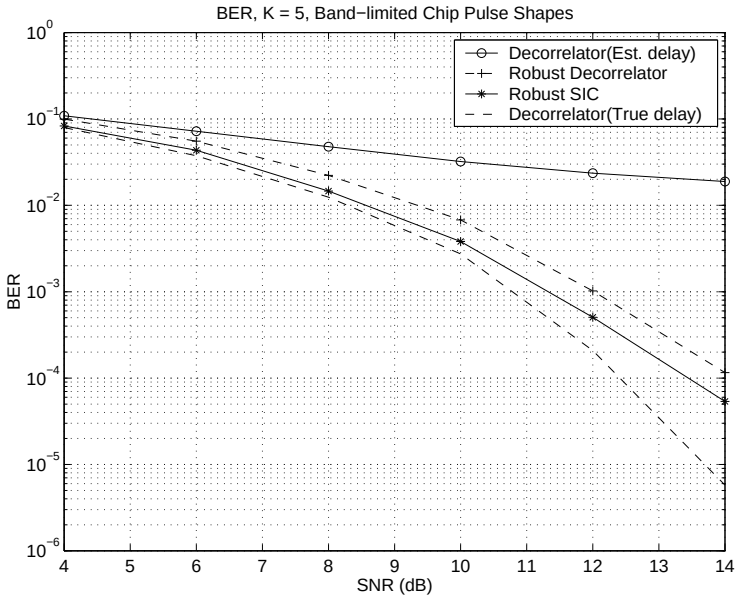

Figure 3.15: Band-limited chip pulse shapes. Bit Error rate (BER) of user 1 for $\sigma_\tau = 0.1T_c$ and $K = 5$ users. Near-far ratio 20 dB.

Chapter 4

Soft-Decision Interference Cancellation and Multiuser Delay Tracking

Both the successive interference canceller (SIC) and the parallel interference canceller (PIC) belong to a family of low complexity multiuser detection methods for DS-CDMA systems. In Chapter 3, we have investigated a proposed delay-robust multistage SIC that employs a linear decision function (linear SIC) for the estimated virtual users. However, the performance of a multistage SIC, in general, depends on the decision function used in the interference cancellation iterations, e.g. hard decision, soft decision or linear decision may be employed. Due to error propagation, the multistage SIC with hard data bit decisions may perform more poorly than a multistage SIC with linear or soft decision functions. We propose and analyze a family of generalized unit-clipper bit decision functions that are a mixture of linear and hard decisions. Performance within 0.4 dB of the single-user bound can be obtained. We then employ results in Chapter 3 to robustify the new soft-decision SIC to time delay errors as large as half a PN chip, and evaluate performance. We also consider a sliding window version of the delay-robust SIC as a multi-user delay tracking receiver. Tracking performance is simulated for both rectangular chip and square-root raised cosine chip pulses, in both AWGN and multipath fading channels.

4.1 Introduction

The SIC and PIC regenerate and cancel interference from other users before data detection of the desired user. The decision function used in the SIC may be hard, soft, or linear. If the regeneration and cancellation of other users' signals use a hard decision function, the interference could actually double from error propagation of incorrect hard decisions [45]. Methods including soft or linear interference cancellation and partial interference cancellation have been proposed to mitigate this error propagation [19]. However, the linear SIC reduces to the decorrelating detector, which is inferior to the upper bound performance that SIC can achieve with an ideal decision function [93]. The performance of partial interference cancellation methods depend on the cancellation weights at each stage and the decision functions used. The selection of the optimum weights for the multiple stages can therefore be complex [130].

The SIC with hard or soft decision functions requires signal amplitude to perform interference cancellation. Since the true amplitude information is not available, it needs to be estimated at the receiver. When the channel changes slowly, it is shown in [84] that an SIC receiver incorporating amplitude estimation by averaging over several bits can potentially result in a significant bit error rate (BER) performance improvement. In fact, the single-user BER lower bound may be reached if perfect amplitude information is available. Although amplitude averaging is a known technique, its performance depends on the decision function used in multistage SIC. For example, if hard decisions are used, error propagation may dominate over amplitude estimation errors.

Since linear (soft) decision interference cancellation has no error propagation and will converge to the decorrelating detector, hard decision interference cancellation can completely cancel interference when the hard decisions are correct. We seek to combine the advantages of hard and soft decision functions. In our proposed decision function, when the instantaneous signal amplitude estimation is small compared to the averaged amplitude, linear decision cancellation is used. Otherwise hard decision cancellation is employed. We therefore take advantage of amplitude averaging and

achieve performance close to that of the single user bound.

Our proposed detector is similar in principle to the two-stage decorrelating detector of [131], where hard decisions made from the first stage decorrelator are used only when highly reliable. While [131] uses either multi-dimensional search or decorrelation in the second stage, we propose to incorporate the two stages into the SIC iterations to gain a computational advantage, i.e., the two-stage decorrelator [131] has computational complexity proportional to the third power of the number of users [67] while the proposed multistage SIC has computational complexity linear in the number of users [93]. Moreover, the two-stage decorrelator performance is affected by time delay estimation errors [85], while the soft-decision multistage SIC can be made robust to time delay errors as described in Section 4.6.

We consider the proposed decision function in the context of SIC with amplitude averaging. We note that this technique may also be applied to PIC as well, but will not be discussed further. In the following sections we describe the system model, propose a new decision function with amplitude averaging in the SIC receiver, analyze performance and provide comparisons through bit simulations.

Since the delay-robust SIC proposed in Chapter 3 is based on improving the linear decision SIC implementation of decorrelator, the amplitude averaging is not utilized. In this chapter, the SIC with amplitude averaging is robustified as in Chapter 3 to operate under time delay estimation errors.

We also propose using the delay-robust SIC with soft-decision and amplitude averaging for multiuser delay tracking, since the delay error information can be estimated by the delay-robust SIC and thus be used to improve the current delay estimate for the next detection. The tracking ability is shown for both rectangular and band-limited chip pulses. For multipath fading CDMA channels, since the multipath decorrelating detector can eliminate MAI completely before channel estimation [109], we extend the linear decision delay-robust SIC of Chapter 3 to tracking the multipath delays for all the users of the system.

4.2 System Model

We consider the basestation receiver for the asynchronous uplink CDMA channel with binary phase shift keying (BPSK) modulation. It is assumed that the user data are transmitted in blocks, with a block length M.

In Chapter 3, we assume that all users are carrier phase-synchronized which corresponding to the worst case MAI. In this chapter, we will consider the random user carrier phases. The equivalent baseband received signal for one block is similar to Eq. (3.1)

$$r(t) = \sum_{i=1}^{M} \sum_{k=1}^{K} a_k(i) e^{j\theta_k(i)} b_k(i) \tilde{s}_k(t - iT - \tau_k) + n(t) \tag{4.1}$$

except for the addition of the kth user's carrier phase shift for the ith time interval as $\theta_k(i) \in [0, 2\pi)$. Other parameters $a_k(i)$, $b_k(i)$, τ_k, T and K are the same as in Eq. (3.1). The white Gaussian noise $n(t)$ in Eq. (4.1) is complex valued, while $n(t)$ in Eq. (3.1) is real valued. The time delays, phase shifts and spreading codes of all users are assumed to be known at the basestation receiver.

In (4.1), the normalized signature waveform of user k, $\tilde{s}_k(t)$, is the same as in Eq. (3.2).

It is also assumed that the channel changes relatively slowly compared to observation length $(M+1)T$, so that the received signal amplitude and phase shift parameters can be modeled as constants, i.e., $a_k(i) = a_k$ and $\theta_k(i) = \theta_k$ for $i = 1, \ldots, M$. Due to asynchronism $\tau_k \in [0, T)$, we note that the observation interval must be $[0, (M+1)T)$.

After chip-matched filtering and chip-rate sampling, the received signal is discretized and the $(M+1)T$ observations can be organized into the vector

$$\mathbf{r} = \sum_{i=1}^{M} \sum_{k=1}^{K} a_k e^{j\theta_k} b_k(i) \mathbf{d}_k(i) + \mathbf{n} \tag{4.2}$$

Eq. (4.2) is similar to Eq. (3.3) except that here we also consider phase shifts $e^{j\theta_k}$. $\mathbf{d}_k(i)$, $\mathbf{r}$, $\mathbf{n}$ are defined in Section 3.2.

The received signal vectors $\mathbf{r}(i)$ over the $(M+1)T$ observation intervals, $i = 1, \ldots, M+1$, provides sufficient statistics for detecting the transmitted data bits from the K users.

4.3 SIC Multiuser Detector with Amplitude Averaging

Successive interference cancellation (SIC) is a low complexity suboptimal multiuser detector for CDMA systems. The signal corresponding to a particular user is first estimated by subtracting other users' regenerated signals from the original received signal. After data bit decisions are successively made based on these estimated signals, the estimated signals are regenerated and then the process repeats. To obtain accurate interference cancellation performance, the regenerated signal subtractions occur in decreasing order of signal power. We note that (1) this ordering can be approximated by only sorting in the first SIC stage, and (2) ordering with $O(Klog_2K)$ complexity/stage does not substantially increase the $O(KN)$/stage computational complexity of the SIC.

The SIC need users' amplitude information for data bit decisions and interference cancellation. Since the received signal amplitude is not known, it should be estimated. One approach is the *linear SIC receiver*, in which the ith signal's amplitude and data bits are estimated as the composite signal $\hat{b}_k(i)\hat{a}_k(i)$ [84] [93]. This is equivalent to estimating amplitude in bit-by-bit fashion. The MAI and noise will affect the accuracy of the amplitude estimate, where the error may be modeled as zero-mean Gaussian noise. In [84], it was shown in theory that amplitude estimation by averaging over M bits can reduce the noise variance by a factor of M, and results in a corresponding BER performance improvement. The single-user BER lower bound may also be approached for static channels if the number of bits used for averaging is large enough.

However, with averaged amplitudes, the multistage SIC receiver performance depends on the decision functions used in the interference cancellation iterations, as explained earlier. In the following, we will discuss some of the known decision functions and propose an improved decision function.

Suppose an SIC receiver with amplitude averaging starts interference cancellation

at stage $j = 1$. During the *(j+1)*st stage, the SIC first performs steps (1) to (3) on user $k = 1$, then repeats the same steps on users $k = 2$ until user $k = K$. Compared to the delay-robust SIC in Section 3.3.6, the steps (1) to (3) here incorporate the carrier phase shift θ_k, estimates the time-averaged amplitude over the block and uses a soft-decision function $f_{dec}(\cdot)$. However, the time delay is assumed exactly known here so delay-robust technique is not used.

Step (1): We estimate user k's received signal for bits $i = 1, \ldots, M$ in one block. For the ith bit, the k-th user's received signal is estimated by subtracting other users' regenerated signals from the received signal $\mathbf{r}(i)$ of (4.2):

$$\tilde{\mathbf{r}}_k^{j+1} = \mathbf{r} - \sum_{l=1}^{k-1} \sum_{i=1}^{M} e^{j\theta_l} \bar{a}_l^{j+1} \hat{b}_l^{j+1}(i) \mathbf{d}_l(i) - \sum_{l=k+1}^{K} \sum_{i=1}^{M} e^{j\theta_l} \bar{a}_l^{j} \hat{b}_l^{j}(i) \mathbf{d}_l(i)$$

Step (2): Obtain the averaged amplitude estimate by averaging the instantaneous estimate of user k's amplitudes over the M-bit block after despreading with PN sequence $\mathbf{d}_k(i)$:

$$\bar{a}_k^{j+1} = \frac{1}{M} \sum_{i=1}^{M} abs\ (Re\ (e^{-j\theta_k} (\mathbf{d}_k(i))^H\ \tilde{\mathbf{r}}_k^{j+1}))$$

where $abs(\ )$ and $Re(\ )$ denote the absolute value and the real part, respectively.

Step (3): For each bit in the block, $i = 1, \ldots, M$, obtain the normalized soft data bit estimate and make a data bit decision. For the ith bit, the soft data bit estimate is normalized with respect to the averaged amplitude $\bar{a}_k^{j+1}$:

$$\tilde{b}_k^{j+1}(i) = \mathrm{Re}\ (e^{-j\theta_k} (\mathbf{d}_k(i))^H\ \tilde{\mathbf{r}}_k^{j+1}) / \bar{a}_k^{j+1}$$

The data bit decision is made by the decision function $f_{dec}(\cdot)$:

$$\hat{b}_k^{j+1}(i) = f_{dec}(\tilde{b}_k^{j+1}(i)) \tag{4.3}$$

The interference canceller for user k is depicted in Figure 4.1. The above multistage SIC is performed either for a desired number of cancellation stages, or is

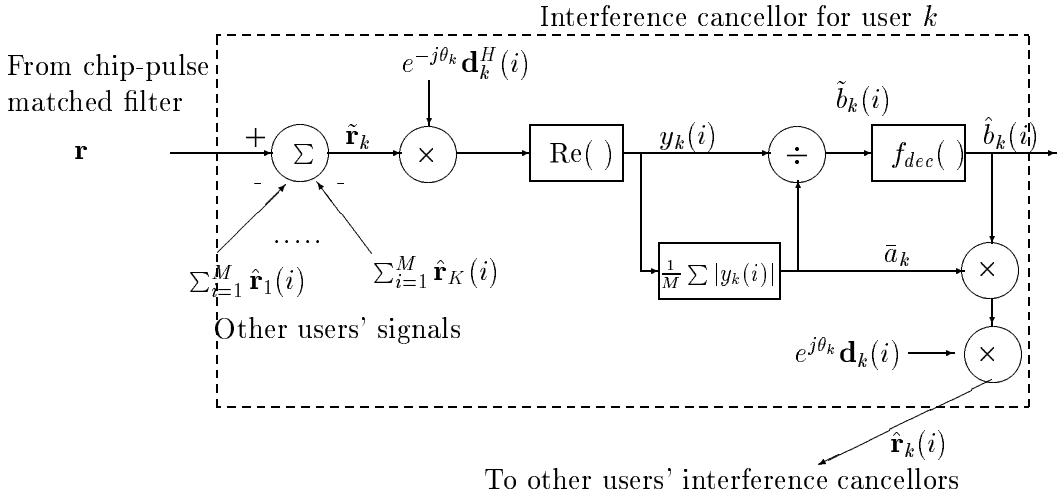

Figure 4.1: The interference cancellation unit for user k.

terminated when there is no significant change from the previous stage. Note if the perfect amplitude information were available, step (2) may be omitted.

Several possible decision functions $f_{dec}(\cdot)$ are depicted in Fig. 4.2. The hard-limiter decision function [78] of Fig. 4.2(a) utilizes only the sign of the soft data bit estimate, $\hat{b}_k^{j+1}(i) = sign(\tilde{b}_k^{j+1}(i))$. Assume for example that the correct data bit is $+1$. If its soft estimate is a small negative number close to zero due to MAI and noise, i.e., -0.1, the hard decision will be -1. From this example, we can observe that interference may actually be amplified by the hard-limiter. This may cause error propagation, which could result in the SIC to converge to a local maximum. Partial interference cancellation [19] has been proposed to mitigate this error propagation, but its parameters can be difficult to optimize.

The hyperbolic tangent (tanh) [78] decision function of Fig. 4.2(c) has been shown to be optimum in the single-user case when the interference and noise are Gaussian, which may not accurately model MAI of CDMA systems. In any case, hyperbolic tangent performance is only slightly better than that of the hard-limiter [78].

The null-zone decision function [45] of Fig. 4.2(d) improves the hard-limiter by using sign information only when the soft bit estimate has a large enough amplitude.

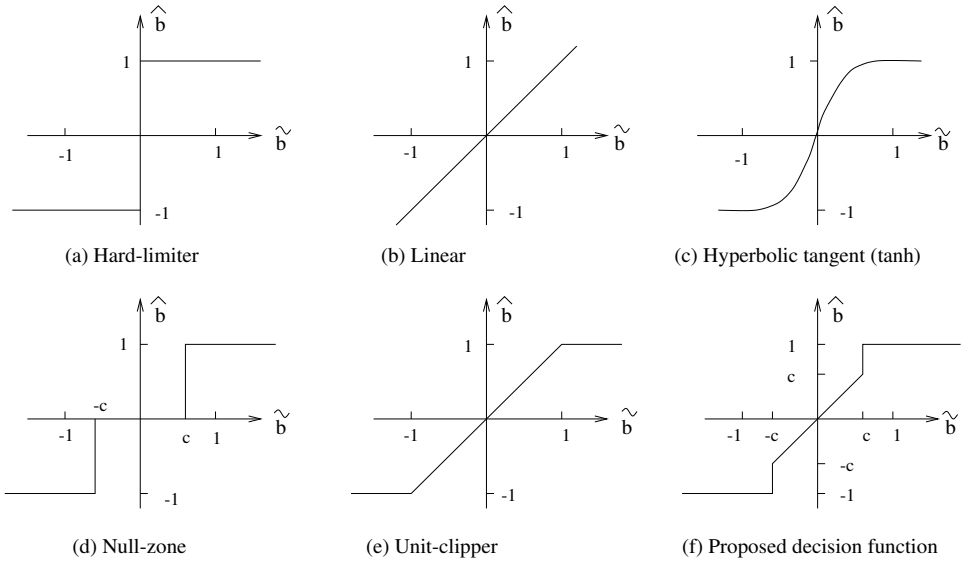

Figure 4.2: The decision functions for interference cancellation multiuser detectors (SIC and PIC).

The linear decision function [84] [93] of Fig. 4.2(b) does not make hard bit decisions. This *linear SIC* converges to the decorrelating detector as the number of interference cancellation stages goes to infinity [93]. Linear SIC performance is therefore limited by decorrelating detector noise enhancement [67].

The limiter in the unit-clipper decision function [78] [133] of Fig. 4.2(e) improves performance over the linear SIC. However, the unit-clipper cancels only the part of the noise above the amplitude limit. It has been shown in [113] that a multistage interference cancellation receiver with a unit-clipper function is equivalent to the (0,1)-constrained maximum-likelihood (ML) solution of the optimum multiuser detection, subject to a box-constraint.

To improve the tradeoff between linear SIC noise enhancement and error propagation from hard limiting, we propose to generalize the unit-clipper to the following

function depicted in Fig. 4.2(f):

$$\hat{b} = f_{dec}(\tilde{b}) = \begin{cases} 1, & \tilde{b} > c \\ \tilde{b}, & \tilde{b} \in [-c, c] \\ -1, & \tilde{b} < -c \end{cases} \tag{4.4}$$

where the threshold $0 \leq c \leq 1$. The effect of the choice of c on the performance of the SIC using the above proposed decision function will be analyzed in Section 4.4 and simulated in Section 4.9.

The decision function (4.4) makes a linear bit decision when the value of the normalized soft bit estimate is small, and so will exhibit desirable convergence similar to that of the linear SIC. Otherwise, it makes a hard bit decision, which will be correct with high probability.

The performance of the proposed SIC in (4.4) can also be compared to an SIC using a Gibbs sampler [98]. The Gibbs sampler introduces randomness into the SIC cancellation, where the hard data bit decision is made by choosing a sample from a conditional probability density function (pdf) of the soft data bit estimate. For example, if the soft bit estimate is $\tilde{b} = 0.5$, the Gibbs sampler draws a sample which will be $+1$ with probability 88%. With perfect power control and perfect amplitude information, the SIC using a Gibbs sampler achieves BER performance within 0.5 dB of the single user bound [98]. While our SIC uses deterministic soft decisions, it may reach a fixed point faster than [98], although [98] may convergence to a lower steady-state error. Under a 10 dB near-far ratio and with imperfect amplitude information, the soft-decision SIC achieves a BER performance within 0.4 dB of the single-user bound as will be described in Section 4.9. While the number of iterations may not be identical, the Gibbs sampler has the same order of computation as that of the proposed SIC.

4.4 A Steady-State Performance Analysis

In this section, we analyze the steady-state performance of the proposed SIC detector after convergence. It has been shown by simulation [9] [45] that convergence is approximately achieved after about five iterations for multistage SIC with null-zone and hard-limiter decision functions. The multistage SIC with the proposed soft-decision function also converges in about five iterations, as will be described in Section 4.9.

After convergence, the residual interference can be assumed to be Gaussian-distributed, and the interference introduced by individual users can be assumed to be mutually independent [9]. Let the interference variance from one bit of user k be σ_k^2. The total interference and noise variance σ^2, is the sum of the K users' interference variances and the channel noise variance σ_N^2, i.e., $\sigma^2 = \sum_{k=1}^{K} \sigma_k^2 + \sigma_N^2$.

For the multistage linear SIC detector, denote the interference and noise variance of the estimated received signal of user k at the input of the correlator be σ^2 at convergence. After correlation, the variance of the reconstructed signal $e^{j\theta_k}\bar{a}_k\hat{b}_k(i)\mathbf{d}_k(i)$ will be $\sigma_k^2 = \sigma^2/N$ due to spreading gain N. Therefore it can be shown [9] that σ^2 is the solution to:

$$\sigma^2 = K\frac{\sigma^2}{N} + \sigma_N^2 \tag{4.5}$$

That is, $\sigma^2 = \frac{1}{1-\frac{K}{N}}\sigma_N^2$. For a spreading factor $N = 31$ and $K = 20$ users, the performance loss of the linear soft-decision SIC detector relative to the single-user lower bound is 4.5 dB.

For the proposed decision function Fig. 4.2(f), let user k's amplitude be a_k. Without loss of generality, let user k's transmitted data bit be $b_k(i) = +1$. Its unnormalized correlator output $y_k(i) = \text{Re}\ (e^{-j\theta_k}(\mathbf{d}_k(i))^H\ \hat{\mathbf{r}}_k(i)) = \bar{a}_k\tilde{b}_k(i)$ can be modelled as a Gaussian random variable with mean a_k and variance σ^2. User k's decision region for the unnormalized correlator output $y_k(i)$ can be partitioned into (1) a hard-decision region$(ca_k, +\infty)$, (2) a linear decorrelator region $[-ca_k, ca_k]$ and (3) a bit-error region $(-\infty, -ca_k)$. The reconstructed signal of user k for interference cancellation is $e^{j\theta_k}\bar{a}_k\hat{b}_k(i)\mathbf{d}_k(i)$. This leads to three cases:

Case (1): The unnormalized correlator output $y_k(i)$ falls in hard-decision region $(ca_k, +\infty)$ with probability $\left[1 - Q\left(\frac{(1-c)a_k}{\sigma}\right)\right]$, where $\mathcal{Q}(x) = \int_x^\infty \frac{1}{\sqrt{2\pi}} e^{-\frac{y^2}{2}} dy$. The data bit decision is correct, i.e, $\hat{b}_k(i) = b_k(i)$. Its regenerated signal for interference cancellation is $e^{j\theta_k}\bar{a}_k b_k(i)\mathbf{d}_k(i)$, which uses the averaged amplitude for all $i = 1, 2, \ldots, M$. The introduced interference variance can be calculated as the second moment of the difference between the reconstructed signal and the true signal $e^{j\theta_k}a_k b_k(i)\mathbf{d}_k(i)$, i.e.,

$$Var_1 = \frac{1}{N} E\left[(\bar{a}_k b_k(i) - a_k b_k(i))^2\right] = \frac{\sigma^2}{MN} \tag{4.6}$$

where N is due to spreading gain and M is due to averaging gain.

Case(2): The unnormalized correlator output $y_k(i)$ falls in the linear decorrelator region $[-ca_k, ca_k]$ with probability $\left[Q\left(\frac{(1-c)a_k}{\sigma}\right) - Q\left(\frac{(1+c)a_k}{\sigma}\right)\right]$. The regenerated signal $e^{j\theta_k}y_k(i)\mathbf{d}_k(i)$ uses the instantaneous amplitude estimate $abs(y_k(i))$, which has a variance $Var_2 = \sigma^2/\mathrm{N}$ due to spreading gain only.

Case (3): The unnormalized correlator output $y_k(i)$ falls in bit-error region $(-\infty, -ca_k)$ with probability $Q\left(\frac{(1+c)a_k}{\sigma}\right)$. Since a wrong hard bit decision is made, $\hat{b}_k(i) = -b_k(i)$. The regenerated signal for interference cancellation is $e^{j\theta_k}\bar{a}_k(-b_k(i))\mathbf{d}_k(i)$. Assuming that the data bit error and the amplitude estimation error are independent, the introduced interference variance can be calculated as

$$\begin{aligned} Var_3 &= \frac{1}{N} E\left[(\bar{a}_k(-b_k(i)) - a_k b_k(i))^2\right] \\ &= \frac{1}{N}\left\{E\left[(2a_k b_k(i))^2\right] + E\left[(\bar{a}_k b_k(i) - a_k b_k(i))^2\right]\right\} \\ &= \frac{(2a_k)^2}{N} + \frac{\sigma^2}{MN} \approx \frac{(2a_k)^2}{N} \end{aligned} \tag{4.7}$$

Combining the above cases, the average interference variance contribution from one bit of user k conditioned on its amplitude a_k is:

$$\begin{aligned} \sigma_k^2(a_k) &= \left[1 - Q\left(\frac{(1-c)a_k}{\sigma}\right)\right]\frac{\sigma^2}{MN} + \left[Q\left(\frac{(1-c)a_k}{\sigma}\right) - Q\left(\frac{(1+c)a_k}{\sigma}\right)\right]\frac{\sigma^2}{N} \\ &\quad + Q\left(\frac{(1+c)a_k}{\sigma}\right)\frac{(2a_k)^2}{N} \end{aligned} \tag{4.8}$$

If the received user signals have unequal powers, we assume that the received amplitudes a_k are uniformly distributed between a_{min} and $a_{min}X$, where $a_{min} =$

$\min\{a_1, \ldots, a_K\}$ is the amplitude of the weakest user, and $X > 1$ is the ratio of $\max\{a_1, \ldots, a_K\}/a_{min}$. The average interference variance contribution from user k can be calculated by averaging (4.8) over the distribution of a_k, which is uniform in $[a_{min}, a_{min}X]$.

Denote the expectation

$$\begin{aligned} f(b) &= E_{a_k}\left[Q\left(\frac{ba_k}{\sigma}\right)\right] = \frac{1}{a_{min}(X-1)}\left[a_{min}XQ\left(\frac{ba_{min}X}{\sigma}\right) - a_{min}Q\left(\frac{ba_{min}}{\sigma}\right)\right] \\ &\quad + \frac{\sigma}{\sqrt{2\pi}b}\left[e^{-\frac{b^2a_{min}^2}{2\sigma^2}} - e^{-\frac{b^2(a_{min}X)^2}{2\sigma^2}}\right] \end{aligned} \tag{4.9}$$

and by using the approximation $Q(t) \approx \frac{1}{\sqrt{2\pi}t}e^{-t^2}$

$$\begin{aligned} g(b) &= E_{a_k}\left[a_k^2Q\left(\frac{ba_k}{\sigma}\right)\right] = \frac{1}{a_{min}(X-1)}\int_{a_{min}}^{a_{min}X} a_k^2Q\left(\frac{ba_k}{\sigma}\right)da_k \\ &\approx \frac{\sigma^3}{\sqrt{2\pi}b^3}\frac{1}{a_{min}(X-1)}\left(e^{-\frac{b^2a_{min}^2}{2\sigma^2}} - e^{-\frac{b^2(a_{min}X)^2}{2\sigma^2}}\right) \end{aligned} \tag{4.10}$$

Substituting (4.9) and (4.10) into (4.8), the total interference σ^2 for all K users including the channel noise variance σ_N^2 is the solution to

$$\begin{aligned} \sigma^2 &= \sum_{k=1}^{K} E_{a_k}[\sigma_k^2(a_k)] + \sigma_N^2 \\ &\approx \left\{(1 - f(1-c))\frac{\sigma^2}{MN} + (f(1-c) - f(1+c))\frac{\sigma^2}{N} + \frac{4}{N}g(1+c)\right\}K \\ &\quad + \sigma_N^2 \end{aligned} \tag{4.11}$$

For example, for an amplitude averaging length of $M = 9$ bits, SNR of 10 dB, near-far ratio of 10 dB, spreading factor of $N = 31$ and number of users $K = 20$, the loss to the single-user bound is about 0.35 dB for threshold $c = 0.5$, 0.68 dB for $c = 0.8$, and 1.93 dB for $c = 1.0$. The value $c = 1.0$ is a special case where our proposed decision function reduces to the unit-clipper decision function.

Alternatively, if the received user powers are all equal under ideal power control, i.e., $a_k = a$ for $k = 1, \ldots, K$, then (4.8) need not be averaged. Instead of (4.11), the total interference and noise variance is given as

$$\sigma^2 = \sum_{k=1}^{K} \sigma_k(a_k)^2 + \sigma_N^2 = \left\{\left[1 - Q\left(\frac{(1-c)a}{\sigma}\right)\right]\frac{\sigma^2}{MN}\right.$$

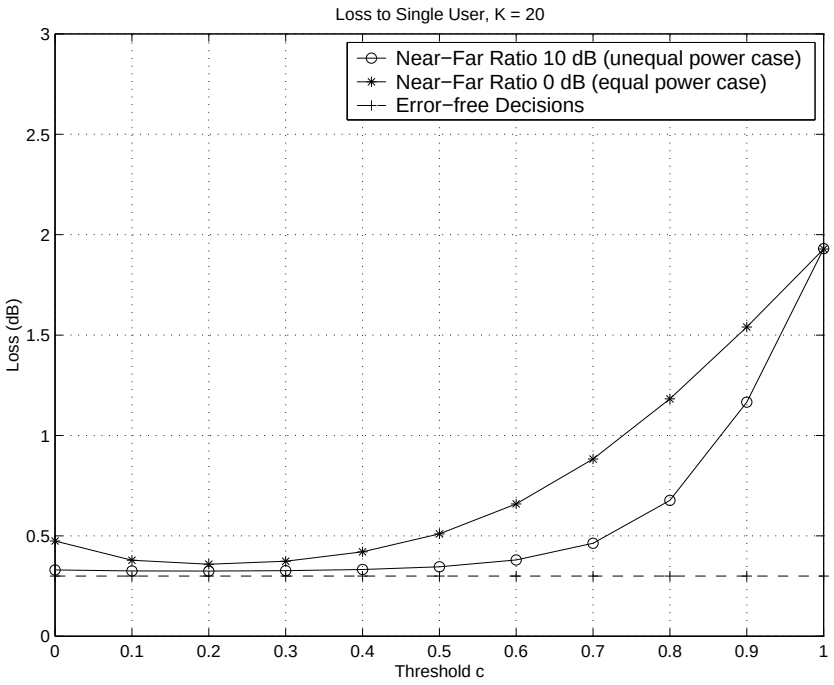

Figure 4.3: The SNR loss for the proposed SIC detector compared to the single user detector as a function of the thresholds $0 \leq c \leq 1$. $K = 20$ users. SNR = 10 dB. $c = 1$ represents the unit-clipper.

$$+\left[Q\left(\frac{(1-c)a}{\sigma}\right) - Q\left(\frac{(1+c)a}{\sigma}\right)\right]\frac{\sigma^2}{N} + Q\left(\frac{(1+c)a}{\sigma}\right)\frac{(2a)^2}{N}\Bigg\}K$$
$$+\sigma_N^2 \tag{4.12}$$

Modifying the above example to a near-far ratio of 0 dB corresponding to equal user powers, the loss to the single user bound is about 0.51 dB for $c = 0.5$, 1.18 dB for $c = 0.8$, and 1.93 dB for $c = 1.0$. Comparing to the previous example, the proposed SIC detector performs worse under equal received power conditions.

It is also interesting to calculate the performance loss to the single-user bound when the decision function used is ideal, i.e., decision error free, with the amplitude be averaged. Similar to the decorrelator, after correlation, the variance of the reconstructed signal $e^{j\theta_k}\bar{a}_k\hat{b}_k(i)\mathbf{d}_k(i)$ will be $\sigma_k^2 = \sigma^2/(MN)$ due to spreading gain N and

averaging gain M. Therefore σ^2 is the solution to:

$$\sigma^2 = K\frac{\sigma^2}{MN} + \sigma_N^2 \tag{4.13}$$

That is, $\sigma^2 = \frac{1}{1-\frac{K}{MN}}\sigma_N^2$. For a spreading factor $N = 31$ and $K = 20$ users, the performance loss of the error-free decision SIC detector relative to the single-user bound is 0.3 dB. This loss is due to the noise term in the averaged amplitude compared to the noise-free true amplitude information.

It is possible to analytically solve (4.11) and (4.12), but they are nonlinear equations, so we resort to numerical solutions. In Fig. 4.3, the SNR loss to the single user lower bound as a function of the thresholds at SNR = 10 dB is calculated by solving the corresponding equations. The curve for the near-far ratio 10 dB case is calculated using (4.11), while the curve for the near-far ratio 0 dB case is calculated using (4.12). Since our analysis may underestimate the SNR loss when c is close to zero, we should choose c as large as possible when the performance loss is roughly the same. From Fig. 4.3, a suitable choice of the threshold c is near 0.5 for near-far ratio 10 dB case. Under a near-far ratio of 10 dB, the analyzed SNR loss compared to the single user bound is 0.35 dB and 1.93 dB for thresholds $c = 0.5$ and 1.0, respectively. Thus, the generalized unit-clipper results in a 1.6 dB improvement.

Note that the SNR loss at $c = 0.5$ for near-far ratio 10 dB, compared to the error-free decision SIC is only 0.1dB, which means that the proposed soft-decision function is quite insensitive to the value of c and there will be no significant gain in further optimization.

4.5 Modification for Phase Error

In Section 4.3, the multistage soft-decision SIC algorithm is developed based-on the assumption that the carrier phase shifts are exactly known at the receiver. In practice, the phase shift will also have an estimation error. However, the multiuser detector performance is not sensitive to the small phase shift errors as it is to the timing delay estimation errors [14].

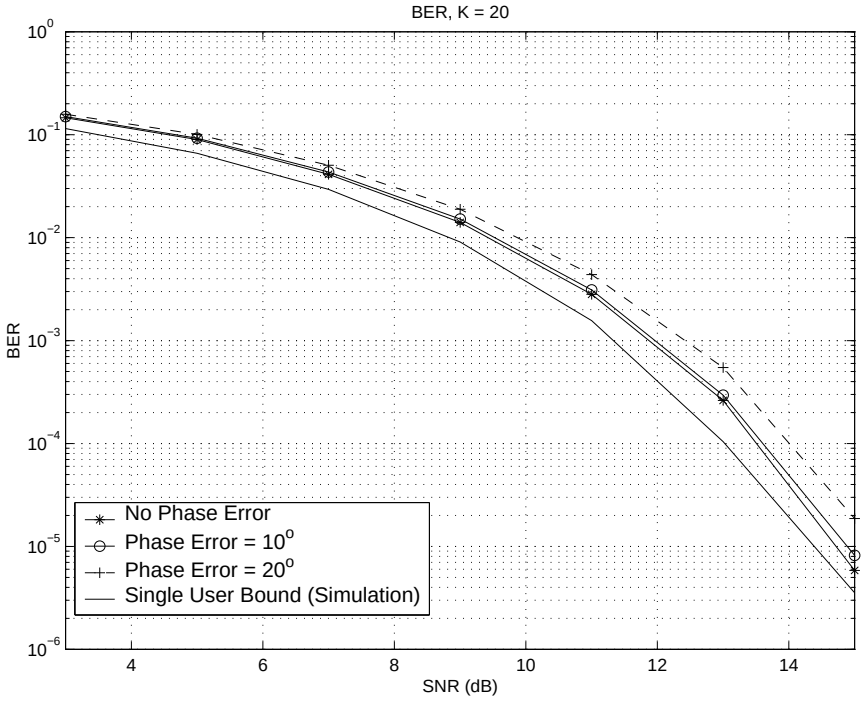

Figure 4.4: Bit error rate (BER) of user 1 for proposed SIC detector with phase errors. $K = 20$ users. Near-far ratio = 10 dB. The threshold is $c = 0.5$.

Let the estimated phase shifts for the users be $\hat{\theta}_k$, $k = 1, \ldots, K$. In this section, we modify the algorithm in Section 4.3 for the estimated phase shifts:

Step (1): We estimate user k's received signal for bits $i = 1, \ldots, M$ in one block. For the ith bit, the k-th user's received signal is estimated by subtracting other users' regenerated signals from the received signal $\mathbf{r}(i)$ of (4.2):

$$\tilde{\mathbf{r}}_k^{j+1} = \mathbf{r} - \sum_{l=1}^{k-1} \sum_{i=1}^{M} \overline{e^{j\theta_l} a_l}^{j+1} \hat{b}_l^{j+1}(i) \mathbf{d}_l(i) - \sum_{l=k+1}^{K} \sum_{i=1}^{M} \overline{e^{j\theta_l} a_l}^{j} \hat{b}_l^{j}(i) \mathbf{d}_l(i)$$

Step (2): Obtain the averaged amplitude estimate by averaging the instantaneous estimate of user k's amplitudes over the M-bit block after despreading with PN sequence $\mathbf{d}_k(i)$:

$$\overline{e^{j\theta_k} a_k}^{j+1} = \frac{1}{M} \sum_{i=1}^{M} sign\ (Re(e^{-j\hat{\theta}_k} (\mathbf{d}_k(i))^H\ \tilde{\mathbf{r}}_k^{j+1}))(\mathbf{d}_k(i))^H\ \tilde{\mathbf{r}}_k^{j+1}$$

where $Re(\ )$ denote the real part.

Step (3): For each bit in the block, $i = 1, \ldots, M$, obtain the normalized soft data bit estimate and make a data bit decision. For the ith bit, the soft data bit estimate is normalized with respect to the averaged amplitude $\bar{a}_k^{j+1}$:

$$\tilde{b}_k^{j+1}(i) = \text{Re}\ (e^{-j\hat{\theta}_k}(\mathbf{d}_k(i))^H\ \tilde{\mathbf{r}}_k^{j+1})/\text{Re}\ (e^{-j\hat{\theta}_k}\overline{e^{j\theta_k}a_k}^{j+1})$$

The data bit decision is made by the decision function $f_{dec}(\cdot)$:

$$\hat{b}_k^{j+1}(i) = f_{dec}(\tilde{b}_k^{j+1}(i))$$

In the simulation results, we will show that the multistage soft-decision SIC using the estimated phase shifts has almost the same BER performance as using the true phase shifts. We assume a given constant phase error as in [81]. In Fig. 4.4, the phase shift estimation errors are set to $\pm 10^o$ and $\pm 20^o$, where the single user lower bound corresponds to the no-phase-error case. We can see that phase error has little impact on the performance of the multistage SIC multiuser receiver: the BER curves are almost identical for no phase error and a phase error of 10^o, and even for phase errors as large as 20^o, the degradation is small. Similar results were observed in [8].

Although we have assumed that an initial phase shift estimate is available, this assumption can be relaxed in practice. Since the receiver has the knowledge of the modulation, i.e., BPSK or QPSK is used, by using one or several short training bits, the phase shifts can be easily estimated given the time delay information as in [74].

4.6 Soft-Decision Delay-Robust SIC

In the previous sections, we have assumed that users' time delay information is known exactly by the soft-decision multistage SIC receiver with amplitude averaging. When there are time delay estimation errors, the delay-robust multiuser detection method presented in Chapter 3 based on linear SIC can be improved by the proposed soft-decision framework in Section 4.5.

We first briefly review robustness to time delay error results in Chapter 3. Following this, we incorporate the proposed soft-decision function.

Denote the estimated time delay of the kth user as $\hat{\tau}_k = (\hat{p}_k + \hat{\delta}_k)T_c$. It is assumed that all users are acquired so that the estimated time delays are within $\pm 0.5T_c$ of the true time delays, i.e., $|\hat{\tau}_k - \tau_k| \leq 0.5T_c$.

Since the chip-rate sampling time instants are chosen arbitrarily at the receiver, the relative position of the estimated and true time delays can be divided two cases: in the same sampling interval and in two adjacent sampling intervals.

If the true delay and the estimated delay are in the same chip sampling interval, then they have the same integer part, i.e, $p_k = \hat{p}_k$ for $1 \leq k \leq K$. The kth user's discretized signature waveform for the ith interval $\mathbf{d}_k(i)$ in (3.9) can be expressed in a *prediction error form* as the weighted sum of two signals $\hat{\mathbf{d}}_k(i)$ and $\Delta\mathbf{d}_k(i)$ as in Eq. (3.14):

$$\mathbf{d}_k(i) = \hat{\mathbf{d}}_k(i) + (\delta_k - \hat{\delta}_k)\Delta\mathbf{d}_k(i) \tag{4.14}$$

where the $(M+1)N$-dimensional vector $\Delta\mathbf{d}_k(i)$ is denoted as the *error vector*. Note that MN entries of (4.14) have zero value.

If the true delay and the estimated delay happen to fall in adjacent sampling intervals, without loss of generality, we may assume that we have the situation where $\hat{p}_k = p_k - 1$. $\mathbf{d}_k(i)$ can instead be expressed as the weighted sum of three signals $\hat{\mathbf{d}}_k(i)$, $\Delta\mathbf{d}_k(i)$ and $\mathbf{c}_k(p_k + 1, i)$ as in Eq. (3.16):

$$\mathbf{d}_k(i) = (1 - \delta_k)\left[\hat{\mathbf{d}}_k(i) + (1 - \hat{\delta}_k)\Delta\mathbf{d}_k(i)\right] + \delta_k\mathbf{c}_k(\hat{p}_k + 2, i) \tag{4.15}$$

where the vector $\mathbf{c}_k(\hat{p}_k + 2, i)$ is denoted as the *guard vector*.

Since the receiver cannot know whether the estimated and true time delays are in the same sampling interval, the delay-robust SIC detector uses (4.15) to cancel two residual MAI terms for each user, corresponding to the error vector and the guard vector. If the estimated and true time delays are in the same sampling interval, then the estimated signal corresponding to the guard vector will contribution noise terms only, i.e., the negative effect of using (4.15) instead of (4.14) is the noise enhancement.

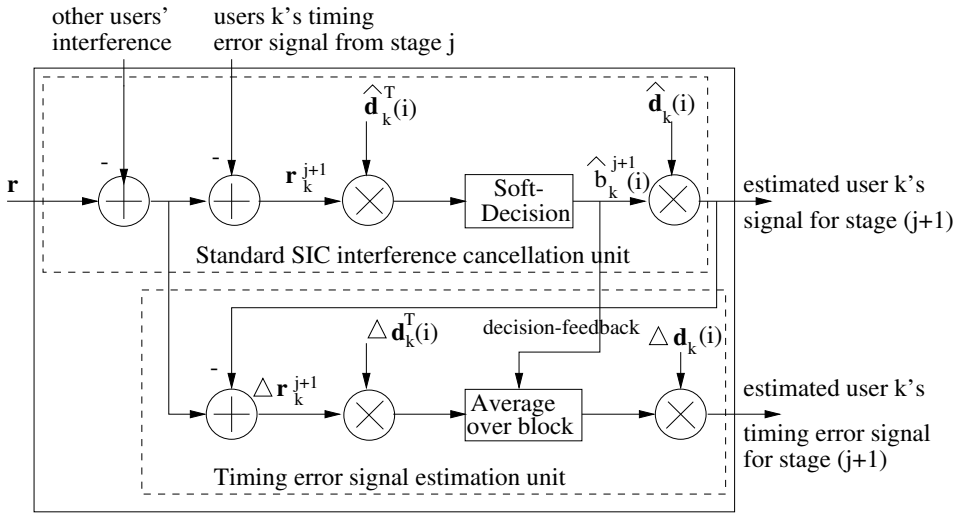

Figure 4.5: Interference cancellation unit of delay-robust SIC for user k at the $(j+1)$st stage.

At the jth SIC stage, the non-zero terms of error vectors of each user in (4.14) are concatenated into an $\mathcal{R}^{(M+1)N}$ *long* error vector based on the tentative data bit decisions, $\hat{b}_k(i)$, as in Eq. (3.21):

$$\mathbf{e}_k^j = \sum_{i=1}^{M} \Delta\mathbf{d}_k(i)\hat{b}_k^j(i) \tag{4.16}$$

Similarly the M guard vectors in (4.15) are combined into a *long* guard vector as:

$$\mathbf{u}_k^j = \sum_{i=1}^{M} \mathbf{c}_k(\hat{p}_k + 2, i)\hat{b}_k^j(i) \tag{4.17}$$

Denote the amplitude estimate of $\mathbf{e}_k^j$ as $\hat{f}_k^j$, and the amplitude estimate of $\mathbf{u}_k^j$ as $\hat{h}_k^j$. The soft-decision SIC in Section 3.3 can be robustified by subtracting the estimated signals due to timing errors in step (1). Step (1) can be replaced by:

Step (1R):

$$\hat{f}_k^{j+1} = \frac{1}{M}(\mathbf{e}_k^{j+1})^H(\breve{\mathbf{r}}_k^{j+1})$$

$$\hat{h}_k^{j+1} = \frac{1}{M}(\mathbf{u}_k^{j+1})^H(\breve{\mathbf{r}}_k^{j+1})$$

$$\breve{\mathbf{r}}_k^{j+1} = \mathbf{r} - \sum_{l=1}^{k-1}(\hat{f}_l^{j+1}\mathbf{e}_l^{j+1} + \hat{h}_l^{j+1}\mathbf{u}_l^{j+1} + \sum_{i=1}^{M} e^{j\theta_l}\bar{a}_l^{j+1}\hat{b}_l^{j+1}(i)\mathbf{d}_l(i))$$

$$- \sum_{l=k+1}^{K} (\hat{f}_l^j \mathbf{e}_l^j + \hat{h}_l^j \mathbf{u}_l^j + \sum_{i=1}^{M} e^{j\theta_l} \bar{a}_l^j \hat{b}_l^j(i) \mathbf{d}_l(i)) \tag{4.18}$$

The interference cancellation unit for the kth user at stage $(j+1)$ is as shown in Fig. 4.5. It can be shown from Fig. 4.5 that through the added timing error estimation and cancellation, the proposed delay-robust SIC approximately doubles both computational complexity and processing delay, compared to the standard SIC algorithm [84]. As a function of the number of users, the complexity and processing delay are of the same order of magnitude as the standard SIC.

4.7 Multiuser Delay Tracking Based on Delay-Robust SIC

In this section, we proposed a sliding window version of the delay-robust SIC as a delay tracking mode multiuser detector.

Existing multiuser delay tracking receivers can be categorized into two types: those based on extended Kalman filter (EKF) [10] [47] [62] and those based on delay-locked loops (DLL) combined with interference cancellation [55] [56]. Both types of delay trackers require accurate initialization or they will not converge.

The EKF-based delay tracker of [10] [62] can track both complex channel gain and timing delay variations. However, in simulation results, only the ability to track two users is demonstrated. The largest number of users that can be tracked simultaneously has not been investigated. The minimum mean squared error EKF (MMSE-EKF) delay tracker of [47] uses K disjoint (separate) EKFs for the K users, which lowers complexity compared to [10] [62] which track the users' parameters jointly. The MAI is modeled as colored Gaussian noise and suppressed by a whitening filter. The MMSE-EKF's performance closely matches that of the ideal MMSE detector, and also demonstrates a tracking capability of a large number of users. However, the MMSE-EKF is a one-shot detector, which is inherently suboptimal [49]. The EKF-based delay tracker also has high computational complexity since it needs to update

the inverse of its innovation matrix every symbol.

The parallel interference cancellation (PIC) based delay tracker combines PIC with delay-locked loops (DLL) [51] [55] [56] [57]. Based on a finite memory length approximation [101], the PIC-based delay tracker can track a large number of users under ideal power power control conditions. However, when the near-far ratio increases to 10 dB, performance breaks down since the delay error introduced residual interference from strong users results in the weak users making wrong bit decisions.

This motivates using a delay-robust SIC for delay tracking. The early-late delay locked loop is widely used in single-user receivers for tracking time delay variations [89]. Since the error vector used in the robust SIC is equivalent to a single-branch implementation of the early-late delay-locked-loop, the delay-robust SIC implicitly combines the DLL into the SIC iterations. Due to robustness to delay errors even under severe near-far conditions, the tracking ability of the weak users is greatly improved.

If the channel is constant or slowly varying, the channel can be accurately estimated. A soft-decision function can be used in the delay-robust SIC to deliver close to single-user lower bound bit error rates (BER). For fast fading channels, we may use a linear decision function combined with a delay-robust SIC to achieve robustness to both fading and time delay errors.

Related research appears recently in [35] and [129]. However, [129] assumes a fixed global timing error identical for all users and rectangular pulses. The method in [129] does not utilize the error vector combined with decision-feedback to estimate different users' random timing error. In [129] performance is evaluated under ideal power control conditions. Here, we consider drifting timing errors that differ among users and arbitrary bandlimited pulses. We evaluated performance under severe near-far conditions. Although the local reference adjustment (Scheme 3) in [129] appears to be somewhat similar to our proposed method in updating the user signature sequence according to the estimated timing error, this updating is not used in the random timing error estimation procedure. Thus, the two algorithms are quite different and

[129] cannot be generalized to the proposed method in this paper. In [35], it is assumed that the data is known, while we consider that the data symbols are unknown and to be estimated iteratively in the timing error estimation procedure. Although [35] can also be used in a decision-directed fashion as in [36], we emphasize that data detection and timing error estimation must be performed jointly for best performance.

We note that since $\widehat{\Delta a}_k = a_k(\delta_k - \hat{\delta}_k)$ from (4.14), $\widehat{\Delta a}_k$ can be used to improve the delay estimate. When there are large delay errors, we can always use $\hat{\mathbf{d}}_{k-dec}(i)$ in (3.27) and (4.3) first to bring the delay error within $0.2T_c$ and apply the delay-robust SIC again using $\hat{\mathbf{d}}_k(i)$ for a second pass. Almost all current CDMA delay estimation methods can provide delay error less than $0.2T_c$ [4] [5] [87] [110] [134], so the first step is usually not needed.

We propose using a sliding window version of the delay-robust SIC as a multiuser delay tracker. The values computed during the previous window can be used as an initial guess for the current window computation so the complexity can be reduced [50]. It is required that all users are initially under acquisition, i.e., within $\pm 0.5T_c$ of the true delay. This initial acquisition can be obtained by using other delay estimation algorithms [4] [5] [87] [110] [134].

The delay-robust SIC based multiuser delay tracker can be implemented in two steps:

step(1): The delay-robust SIC using the local decorrelator $\hat{\mathbf{d}}_{k-dec}(i)$ to estimate the delay error, and refine the delay error with in $0.2T_c$ of the true delay.

step(2): The delay-robust SIC with no local decorrelator $\hat{\mathbf{d}}_k(i)$ to track the time varying user delays. The delay update is performed in $0.05T_c$ steps. When the delay error estimate is larger than $\pm 0.05T_c$, the user time delay is updated by $\pm 0.05T_c$ and slide to the next window and the step(2) repeats.

We note that there are implementation advantages when the time delays are updated in small steps, i.e., $0.05T_c$: the re-calculation of the user signature sequence according to (4.14) is avoided if the time change is small. It also avoids the suddenly large change due to impulse noise or interference. When using sliding window version,

we assume that the user data bits are transmitted continuously and no blank bits are inserted in the data stream. The change from the blank bit insertion mode to the continuous transmission mode will have little performance degradation, as [49] has shown that when the observation window is larger than 8 symbols, the edge effect is not obvious. This will also be shown by BER simulation results between the dynamic tracking and static mode in Section 4.9.3.

4.8 Multiuser Channel and Delay Tracking for Unknown Multipath Fading CDMA Channels

In Section 4.7, we have assumed that the complex channel gain (amplitude and phase) remains constant while the user time delays are varying. However, in practical wideband CDMA mobile channels, the user time delays vary relatively slowly compared to the variation of the complex channel gains. The system model in Eq. (4.1) can be modified for the multipath fading channel to be:

$$\mathbf{r} = \sum_{i=1}^{M} \sum_{k=1}^{K} \sum_{l=1}^{L} \alpha_{k,l}(i) b_k(i) \mathbf{d}_{k,l}(i) + \mathbf{n} \tag{4.19}$$

where the amplitude and carrier phase shift are absorbed into the complex channel gain for the lth path of the kth user, $\alpha_{k,l}(i)$. The channel is assumed to remain constant for the duration of a bit interval, and varies from bit to bit. For simplicity, the number of multipaths are assumed to be the same for all users, L.

However, channel estimation for a fast fading multiuser CDMA channel is a difficult problem, since the effect of MAI must be suppressed or eliminated to obtain an accurate channel estimate for the desired user.

One sub-optimum solution is the multipath decorrelating detector pre-filter. The multipath decorrlating detector can be used first to decorrelate each path of each user before channel estimation. The channel estimator works on these MAI-free decorrelator outputs [108] [109]. The price paid for this MAI-free decorrelation is the noise enhancement and reduced system capacity, since each user is detected as L

users.

The proposed delay-robust SIC based multiuser delay tracking receiver can also be applied to the multipath fading channel, under the condition that the fading channel gains for all the users are already known. The long error vector $\mathbf{e}_k$ in delay-robust SIC in Eq. (4.16) is now modified for the lth path as:

$$\mathbf{e}_{k,l} = \sum_{i=1}^{M} \Delta\mathbf{d}_{k,l}(i)\hat{b}_k(i)\alpha_{k,l}(i) \tag{4.20}$$

As we have pointed out in Section 4.3, the linear decision multistage SIC is an iterative implementation of the decorrelator. The data bit $b_k(i)$ and complex channel gain $\alpha_{k,l}(i)$ are estimated as a composite signal $o_{k,l}(i)$ at stage $(j+1)$:

$$\tilde{o}_{k,l}^{j+1}(i) = (\mathbf{d}_{k,l}(i))^H \ \tilde{\mathbf{r}}_{k,l}^{j+1} \tag{4.21}$$

and $\mathbf{e}_{k,l}$ at stage $(j+1)$ is:

$$\mathbf{e}_k^{j+1} = \sum_{i=1}^{M} \Delta\mathbf{d}_{k,l}(i)\tilde{o}_{k,l}^{j+1}(i) \tag{4.22}$$

Therefore, for fading channels, the delay-robust SIC using a linear decision function can also be used to track the time delays of all users. The tracking results are shown in Section 4.9.4.

4.9 Numerical and Simulation Results

Throughout the simulations, Gold code sequences of length $N = 31$ are used. The signal-to-noise ratio (SNR) is defined with respect to the user of interest, user 1. The near-far ratio is defined as the power ratio between the strongest user and user 1, which is fixed at 10 dB. All other users have an amplitude uniformly distributed between that of the strongest user and the weakest user.

4.9.1 Soft-Decision Multistage SIC

In this subsection, we compare the different decision functions described in Section 4.3. In this simulation, a block size of $M = 9$ bits is used. An additive white Gaussian

noise (AWGN) channel is simulated. The number of users is $K = 20$ to account for a highly-loaded system.

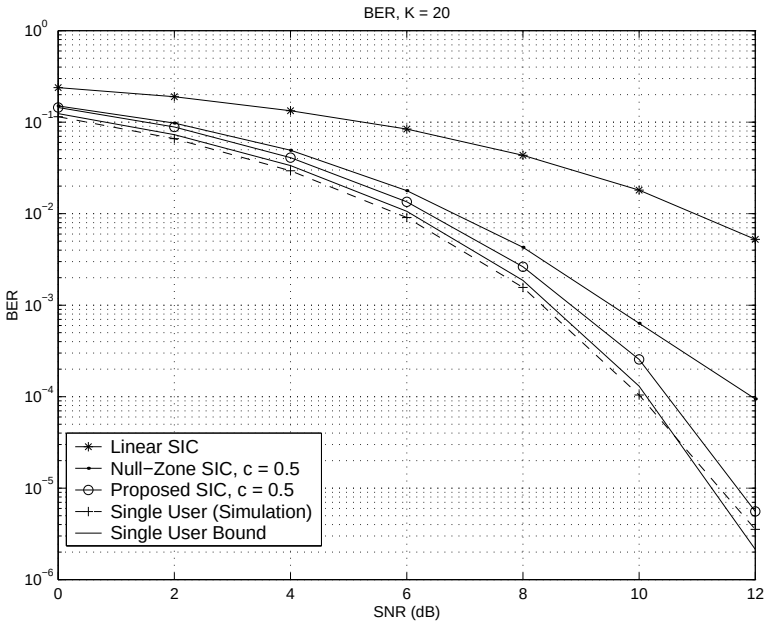

Figure 4.6: Bit error rate (BER) of user 1 for proposed SIC detector and other SIC detectors. $K = 20$ users. Near-far ratio = 10 dB. The threshold is $c = 0.5$.

Fig. 4.6 compares the bit error rate (BER) performance of the linear SIC, null-zone SIC and the proposed SIC detector with threshold $c = 0.5$. At a BER of 10^{-3}, the proposed SIC with $c = 0.5$ has a performance loss of about 0.4 dB compared to the single-user BER curve. The BER curve of the SIC using the null-zone decision function with fixed threshold $c = 0.5$ exhibits an error floor due to the error propagation effects. Adaptive adjustment of c for each user at each stage is required to improve null-zone performance [45].

In Fig. 4.7, the BER of the multistage SIC with proposed soft-decision function is compared with that with linear-clipper and hyperbolic tangent ($tanh(\cdot)$) decision functions. The linear-clipper is defined as:

$$\hat{b} = f_{dec}(\tilde{b}) = \begin{cases} 1, & \tilde{b} > c \\ \tilde{b}/c, & \tilde{b} \in [-c, c] \\ -1, & \tilde{b} < -c \end{cases} \tag{4.23}$$

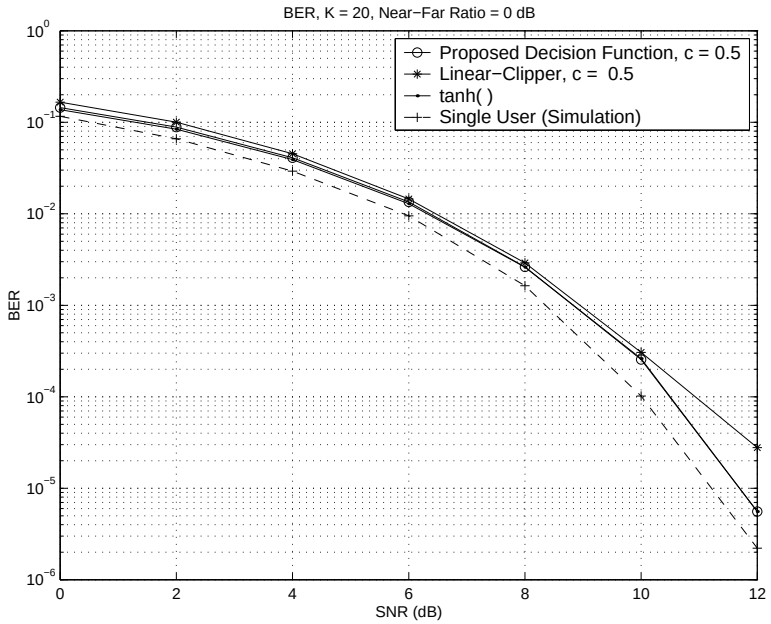

Figure 4.7: Bit error rate (BER) of user 1 for proposed decision function compared with linear-clipper and $tanh(\cdot)$. $K = 20$ users. Near-far ratio = 10 dB.

which is a pair-wise linear approximation of the log-likelihood ratio based hyperbolic tangent decision function [111]. From the figure, our proposed decision function results a better approximation to the $tanh(\cdot)$ function, where their BER curves are almost identical. However, our proposed decision function has implementation advantages compared to the $tanh(\cdot)$ function: the SIC with the proposed decision function either keeps the estimated signal amplitude (linear decision region) or uses the average amplitude (hard decision region) for interference cancellation, which has minimum computational complexity; the SIC with $tanh(\cdot)$ function needs to either calculate the hyperbolic tangent function values or use a look-up table for these values, then multiply them by the average amplitude.

In Fig. 4.8, the proposed SIC detector with various threshold values $c = 0.0$ (hard-limiter), 0.5, 0.8, 1.0 (unit-clipper) are shown. The BER curve of the hard-limiter also exhibits an error floor due to error propagation. At a BER of 10^{-3}, the losses relative to the single-user bound are 0.40 dB for $c = 0.5$ and 2.1 dB for $c = 1.0$, which are very close to the analytically derived results of 0.35 dB and 1.93 dB, as shown in

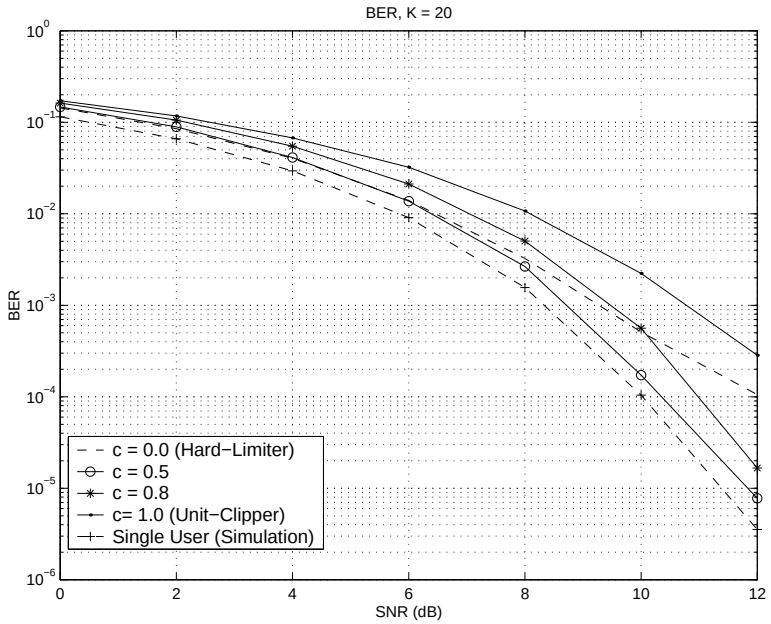

Figure 4.8: Bit error rate (BER) of user 1 for proposed SIC detector with $K = 20$ users. Near-far ratio = 10 dB. The thresholds are $c = 0.0$, 0.5, 0.8 and 1.0 respectively. $c = 0.0$ represents the hard-limiter. $c = 1.0$ represents the unit-clipper.

Fig. 4.3.

In Fig. 4.9, we compared the BER for $c = 0.2$ and $c = 0.5$ at near-far ratios of 0 dB and 10 dB, respectively. For the 10 dB near-far ratio, the BERs for $c = 0.2$ and $c = 0.5$ are almost identical, which agrees with Fig. 4.3. However, for 0 dB near-far ratio, the analysis results of Fig. 4.3 underestimate SNR loss for small c, at large SNR. So, in the following simulations, we select $c = 0.5$.

Fig. 4.10 shows the BER curves of the proposed SIC detector with threshold value $c = 0.5$ from stages 1 to 5. The largest improvements are in early stages, while the BER curves of stages 4 and 5 are almost identical, showing that convergence is approximated after five stages.

In Fig. 4.11, the BER of the different SIC receivers are compared as a function of the number of users at 10 dB SNR. The thresholds for both the null-zone and the proposed decision functions are $c = 0.5$.

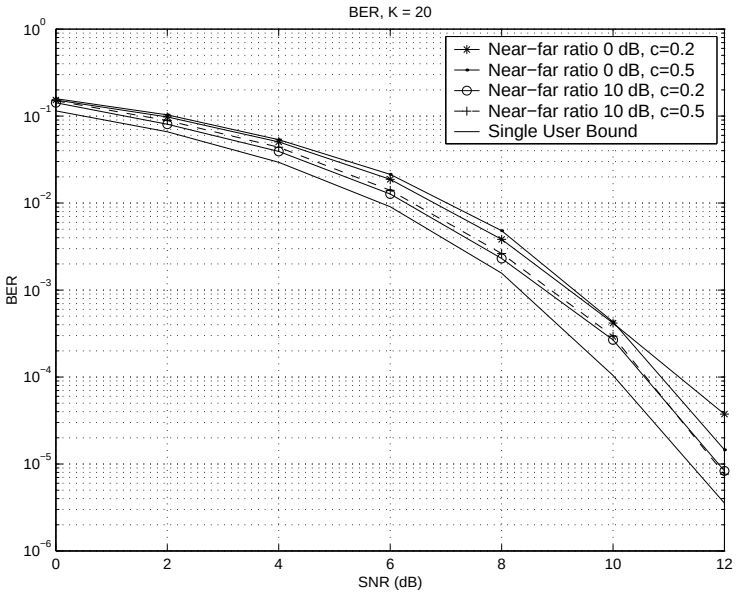

Figure 4.9: Bit error rate (BER) of user 1 for proposed SIC detector with $K = 20$ users. Near-far ratio = 10 dB and 0 dB. The thresholds are $c = 0.2$ and 0.5, respectively.

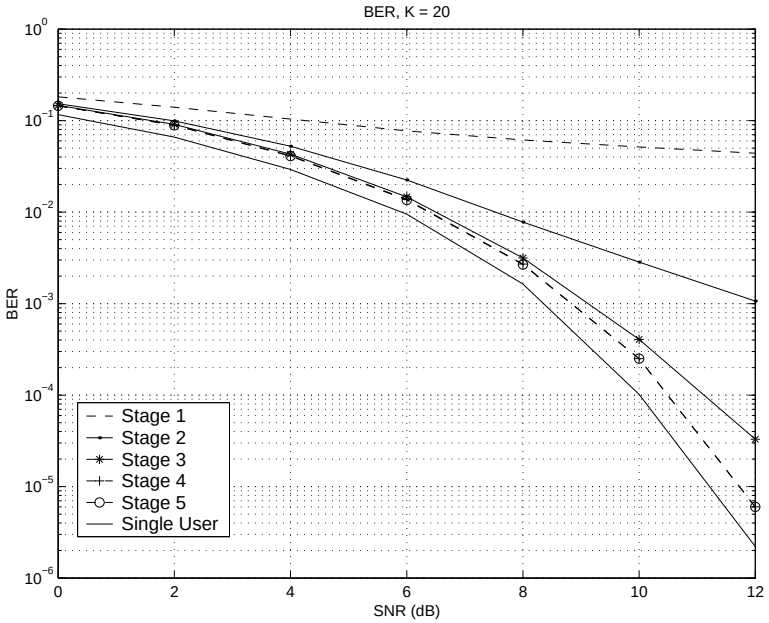

Figure 4.10: Bit error rate (BER) of user 1 for proposed SIC detector as a function of the number of SIC stages. $K = 20$ users. Near-far ratio = 10 dB. The threshold is $c = 0.5$.

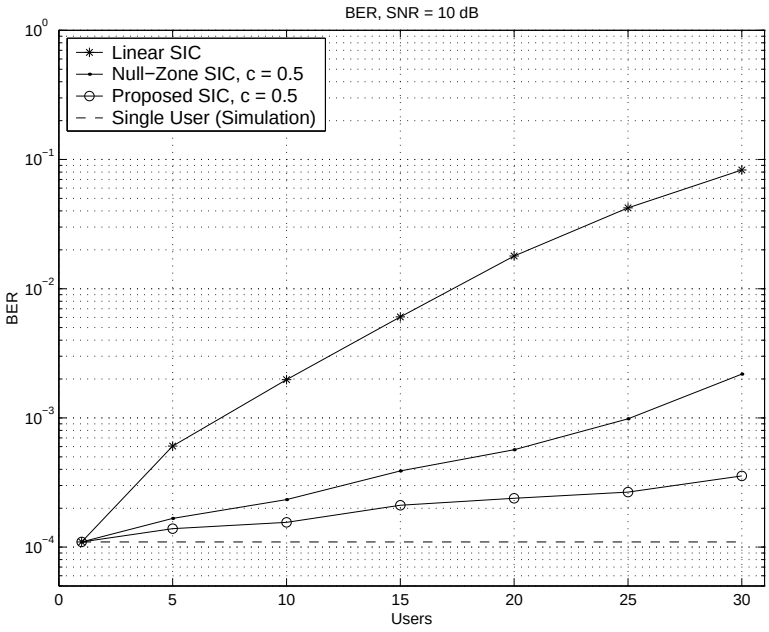

Figure 4.11: Bit error rate (BER) of user 1 for proposed SIC detector and other SIC detectors as a function of the number of users. SNR = 10 dB. Near-far ratio = 10 dB. The threshold is $c = 0.5$.

4.9.2 Soft-Decision Multistage Delay-Robust SIC

In this subsection, we assess the performance of the proposed detector in Section 4.6. In this simulation, the conditions are the same as that described in Section 4.9.1 except that estimated time delays are used at the receiver. The time delay errors are modeled as zero-mean Gaussian random variables truncated to be within the interval $\pm 0.5T_c$.

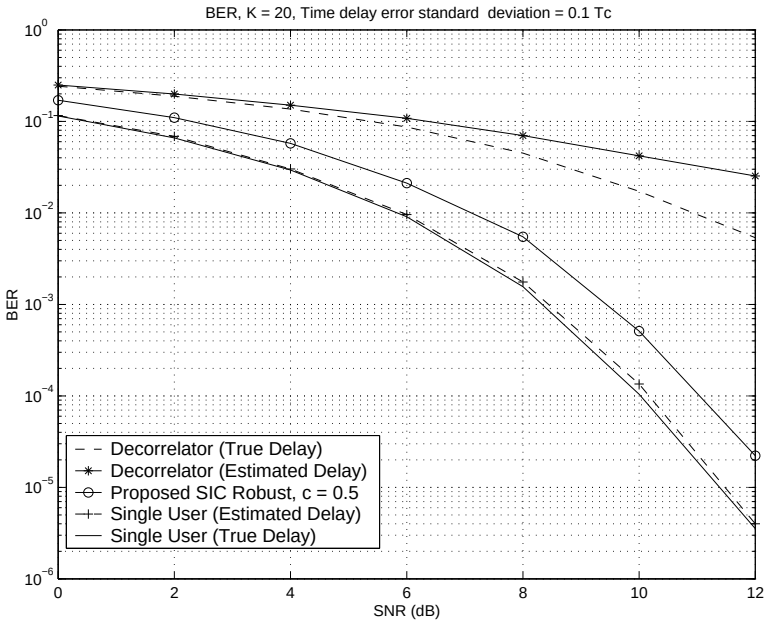

Figure 4.12: Bit error rate (BER) of user 1 for robustified SIC detector. $K = 20$ users. Near-far ratio = 10 dB. The threshold is $c = 0.5$. The time delay has an error of $\sigma_\tau = 0.1T_c$.

In Fig. 4.12, the standard deviation of the time error is $\sigma_\tau = 0.1T_c$, which is typical of current timing estimation methods for CDMA. Our robustified soft-decision SIC (that employs (4.18)) performs within 1.2 dB of the single user case.

In Fig. 4.13, the extreme case of $\sigma_\tau = 0.5T_c$ is shown. Usually the estimated time delay will have an error much smaller than in this case. However, our robustified soft-decision SIC performs almost the same as a decorrelating detector containing true time delay information, although it exhibits an error floor as the SNR gets larger.

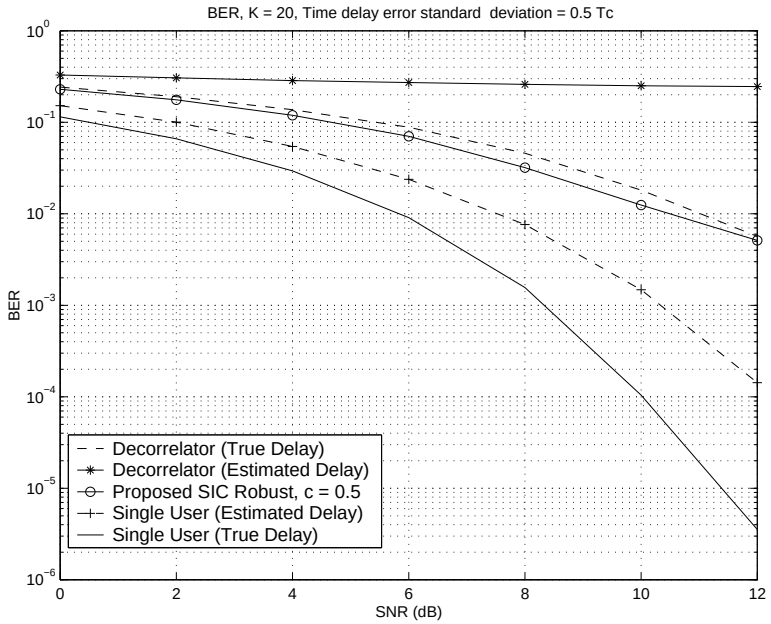

Figure 4.13: Bit error rate (BER) of user 1 for robustified SIC detector. $K = 20$ users. Near-far ratio = 10 dB. The threshold is $c = 0.5$. The time delay has an error of $\sigma_\tau = 0.5T_c$.

In Fig. 4.14, we compare the BER performance of the delay-robust SIC and the standard SIC detectors [84] under two different delay error conditions of $\sigma_\tau = 0.1T_c$ and $\sigma_\tau = 0.2T_c$, respectively. As shown, the delay-robust SIC is much more insensitive to the σ_τ increase. This indicates that it is advantageous to jointly estimate delay errors and detect data symbols.

In Fig. 4.15, we compared the root mean square error (RMSE) of the delay error estimation by the delay-robust SIC to the CRLB derived in Section 3.4.2 for $\sigma_\tau = 0.1T_c$ and $0.5T_c$. The delay error estimator is approximately unbiased, so it is meaningful to compare its RMSE to the CRLB. The CRLB is conditioned on the user amplitudes, data bits and delays, and is averaged over different runs to get the average curve. For comparison, we also show the RMSE of the unbiased estimator assuming ideal decision-feedback. The CRLB and the RMSE of the unbiased estimator are not affected by the value of σ_τ. When SNR is larger than 15 dB, the RMSEs of the delay-robust SIC and the unbiased estimator are almost identical for $\sigma_\tau = 0.1T_c$, so

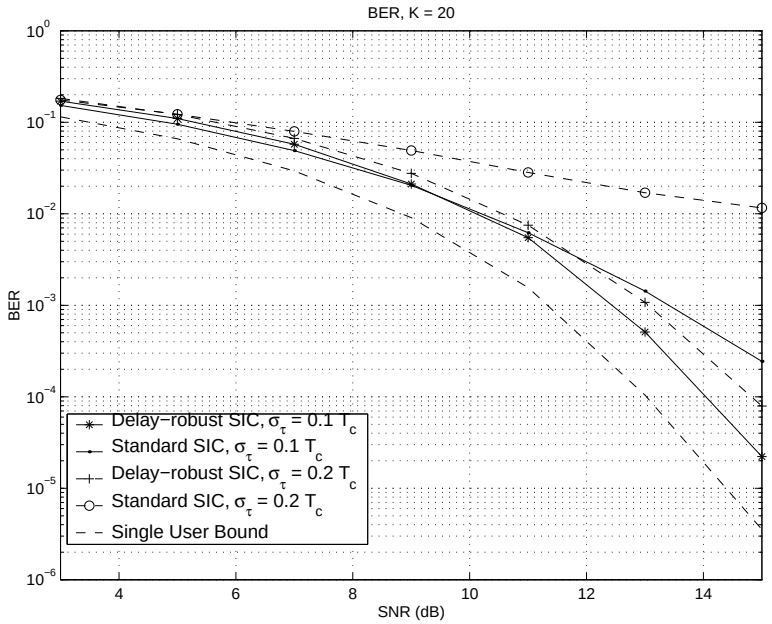

Figure 4.14: Bit error rate (BER) of user 1 for delay-robust SIC and standard SIC detectors. $K = 20$ users. Near-far ratio = 10 dB. Soft decision function is used with threshold $c = 0.5$.

the delay-robust SIC based estimator is approximately unbiased, and it is meaningful to compare its RMSE to the CRLB. As we can see, there is a gap between the RMSE curve and the CRLB. This gap is due to decorrelator noise enhancement. The robustness of the delay-robust SIC is justified by its decreased RMSE as the SNR increases, since the time delay error introduced interference is increased as we increase the SNR while keeping the near-far ratio fixed. Even with $\sigma_\tau = 0.5T_c$, the RMSE also decreases as the SNR increase, so robustness is achieved.

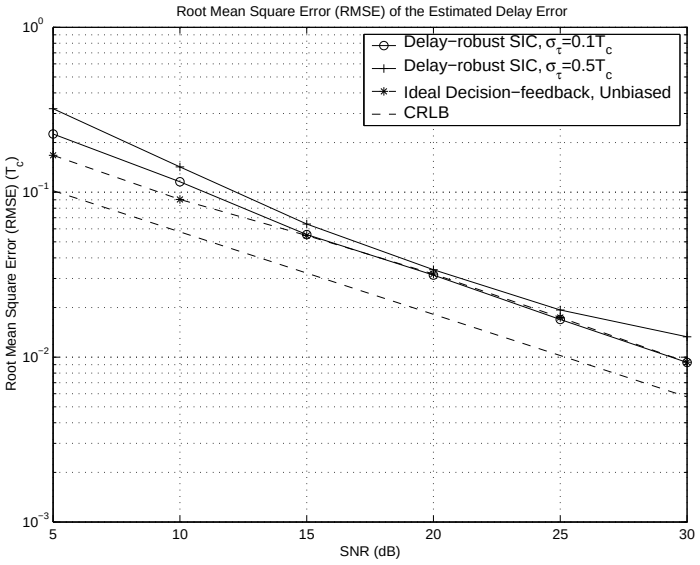

Figure 4.15: Root Mean Square Error (RMSE) of user 1 for proposed SIC detector compared to the Cramér-Rao Lower Bound (CRLB). $K = 20$ users. Near-far ratio = 10 dB. The threshold is $c = 0.5$.

4.9.3 Delay Tracking Based on Delay-Robust SIC

In this subsection, we evaluate the tracking performance of the proposed delay tracker based on delay-robust SIC as described in Section 4.7. For simulating the tracking of multiuser time delays, data symbols are assumed to be transmitted continuously. We let sliding window length be $M = 9$ symbols.

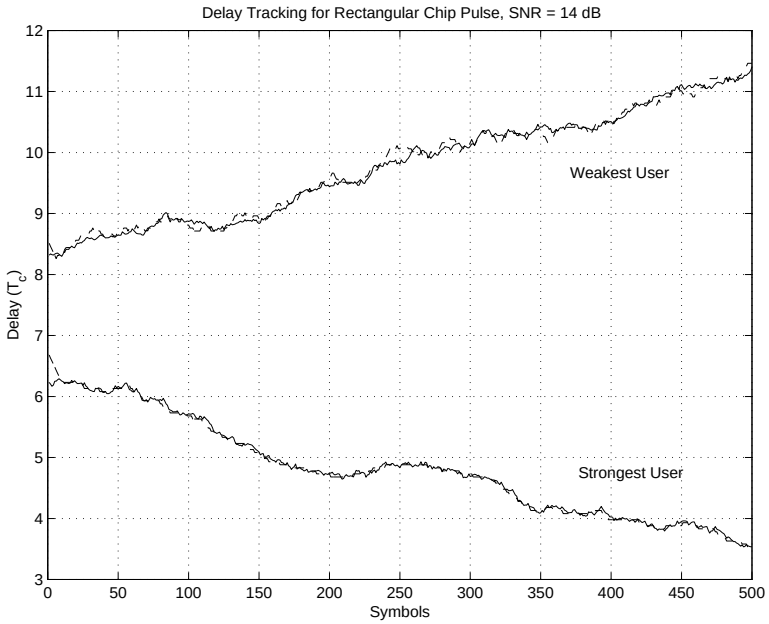

Figure 4.16: Delay tracking curves of delay-robust SIC. $K = 20$ users. Near-far ratio = 10 dB. The weakest user has $SNR = 14$ dB. Soft decision function is used with threshold $c = 0.5$.

In this simulation, rectangular chip pulses are used for Figs. 4.16 to 4.18. We tracked a total of $K = 20$ users' delays. The SNR of the weakest user is 14 dB. Both the weakest and strongest users' delay tracking curves are shown in Fig. 4.16, where the solid line and the dashed line represent actual and estimated delay trajectories, respectively. The initial acquisition has a delay error standard deviation of $0.5T_c$. The spreading factor is $N = 31$. The time update step of the delay tracking is $0.05T_c$.

We assume the delay varies with time as a first-order Gauss-Markov process as in [62]:

$$\tau(m+1) = \tau(m) + w(m) + u(m) \tag{4.24}$$

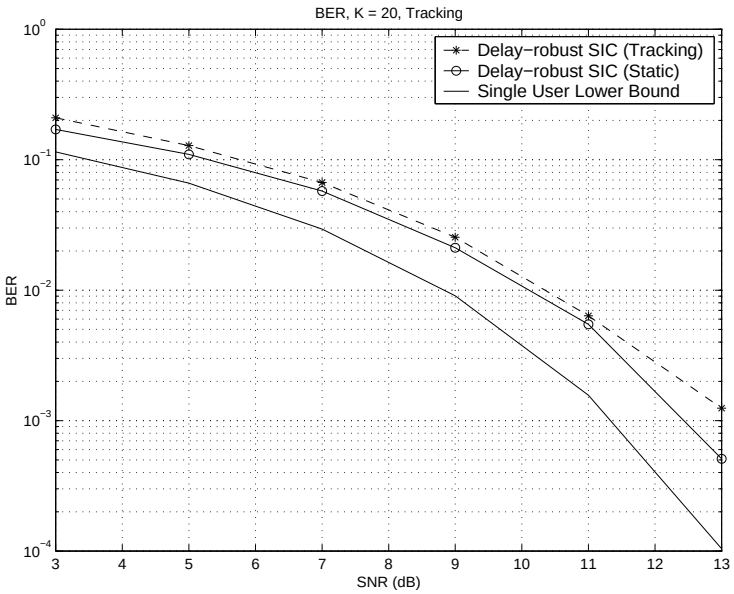

Figure 4.17: Bit error rate (BER) of user 1 for delay-robust SIC detector in tracking time delays. $K = 20$ users. Near-far ratio = 10 dB. Soft decision function is used with threshold $c = 0.5$.

where $w(m)$ is a zero-mean noise process with variance σ_w^2, and $u(m)$ is a deterministic scalar that models global drift. We use $\sigma_w^2 = 0.01\sigma^2$. The global time variation $u(m)$ is selected to change at a rate of $0.005T_c$ per symbol. Assuming a propagation speed of 3.0×10^8 m/s, this is equivalent to $\frac{0.005}{31} \times 3.0 \times 10^8 \approx 5 \times 10^4$ m/s, or 1.8×10^5 km/h [10].

As we can see, the delay-robust SIC based delay tracking receiver can track the time delays for both strongest and weakest users. In Fig. 4.17, the BER of the delay-robust SIC using dynamic tracking is compared to the BER of the delay-robust SIC in the static model of 4.9.2. The time delay variation in the tracking model adds only a small amount of noise, and the BER error floor is not obvious.

From Fig. 4.17, the delay tracking multiuser receiver has a BER of approximately 20% for the weakest user at an SNR of 3 dB. Even for such high BER, the delay-robust SIC based delay tracker can still follow the delay variation as shown in Fig. 4.18.

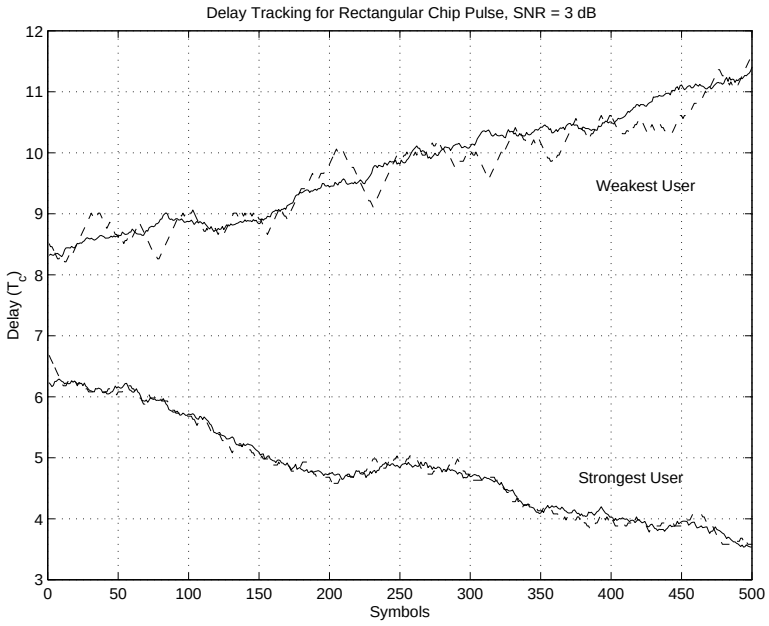

Figure 4.18: Delay tracking curves of delay-robust SIC. $K = 20$ users. Near-far ratio = 10 dB. The weakest user has $SNR = 3$ dB. Soft decision function is used with threshold $c = 0.5$.

In Fig. 4.19, a square-root raised cosine chip pulse with roll-off factor 0.35 is used. The SNR of the weakest user is 14 dB. Since band-limited chip pulse is more sensitive to the time delay errors, the initial acquisition delay error standard deviation is reduced to $0.1T_c$, and the update step is smaller, $0.01T_c$. We found that for band-limited chip pulses, the delay tracking algorithm cannot track the time variations of Section 4.9.3, so we used more mild conditions, i.e., we set σ_w^2 10 dB lower and reduce the global drift to $0.001T_c$ per symbol.

Figure 4.19: Delay tracking curves of delay-robust SIC for band-limited chip pulses. $K = 20$ users. Near-far ratio = 10 dB. The weakest user has $SNR = 14$ dB. Soft decision function is used with threshold $c = 0.5$.

4.9.4 Delay Tracking for Unknown Fading Channels

In this subsection, we evaluate the tracking performance of the proposed delay tracker described in Section 4.8 for a fast fading channel. It is assumed that the user time delays vary relatively slowly compared to the variation of the complex channel gains.

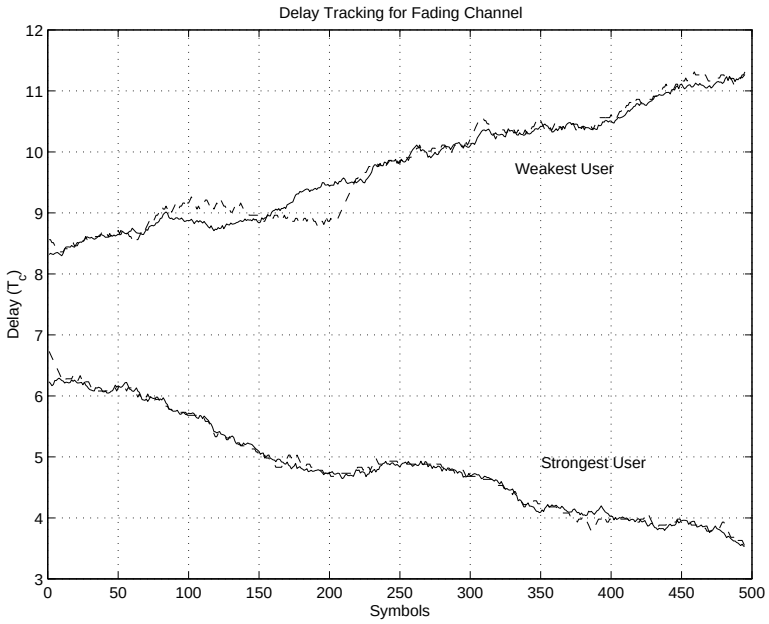

Figure 4.20: Delay tracking curves of delay-robust SIC for Rayleigh fading channels. Normalized Doppler fading rate is $f_D T = 0.01$. $K = 20$ users. Near-far ratio = 5 dB. The weakest user has $SNR = 14$ dB. A linear decision function is used.

The delay-robust SIC with a linear decision function is used to track the delay variations. Since the data symbol $b_k(i)$ and complex channel gain $\alpha_{k,l}(i)$ are estimated as a composite signal $\hat{o}_{k,l}(i)$, data detection is not possible before knowing $\alpha_{k,l}(i)$. The tracking results are shown in Fig. 4.20 for the weakest and strongest users. The SNR of the weakest user is 14 dB. The time variation is the same as in Section 4.9.3. Time-correlated Rayleigh fading channel gains are generated using the fading simulator of [132] with normalized Doppler fading rate of $f_D T = 0.01$. Because of the noisy estimate $\hat{o}_{k,l}(i)$, the tracking performance of the weakest user is reduced. Note that this simulation is approximately equivalent to a $K = 10$ user system with $L = 2$ paths for each user.

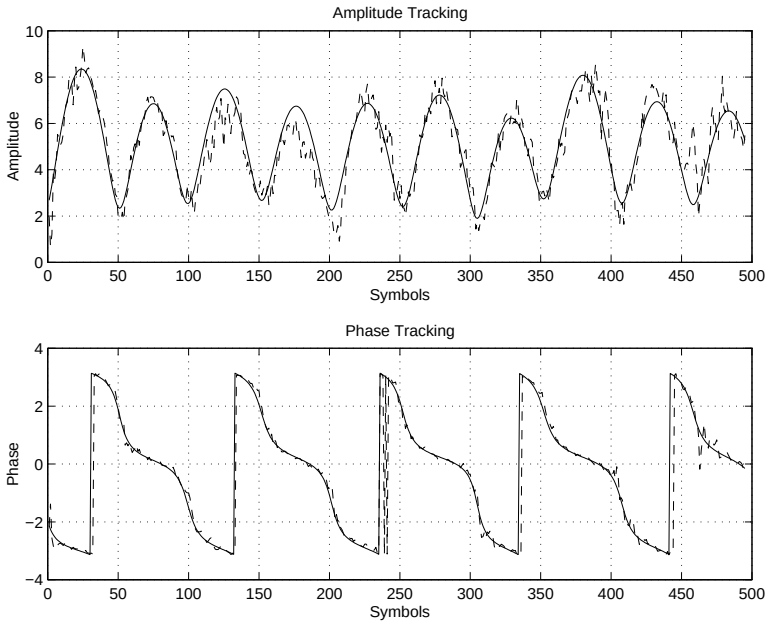

Figure 4.21: Channel amplitude and phase tracking curves of delay-robust SIC for Rayleigh fading channels for the weakest user. Normalized Doppler fading rate is $f_D T = 0.01$. $K = 20$ users. Near-far ratio = 5 dB. The weakest user has $SNR = 14$ dB. Linear decision function is used. The solid line is the true delay and the dashed line is the delay tracking results.

By assuming exact knowledge of the transmitted data symbol $b_k(i)$, the complex channel gain is tracked in Fig. 4.21 for user 1. The delay-robust SIC decorrelates the fading signal for different users, and can be used to track both delay and channel variations. The decorrelated multiuser signals can be used for channel estimation and data detection by the methods in [127].

4.10 Discussion

Although we have demonstrated delay tracking using noisy estimates of the composite signal, it is desirable to have smoothed estimates. In addition, for multipath fading channels, it is advantages to coherently combine the multipath signals before data detection. Coherent diversity combining requires the channel estimates $\alpha_{k,l}(i)$, not

just the composite signal $o_{k,l}(i)$ [107] [109].

In [109], the multipath decorrelator is followed by KL adaptive channel estimators using the least mean square (LMS) algorithm assuming the channel fading follows the Gauss-Markov model. In [127], disjoint Kalman filtering channel estimation is applied where each user uses a Kalman filter to estimate its channel coefficients based also on the MAI-free decorrelator outputs. However, the use of the multipath decorrelator or multipath linear MMSE receiver as the front-end for the channel estimator can only be applied to the case of relatively few users because the loss of degrees of freedom in the signal subspace as the number of users gets large [52] [58].

Multiuser channel estimation that does not use a multipath decorrelator front-end may have less noise enhancement and larger capacity for relatively slow fading where there is no severe tracking problem. In [107], pilot symbols are periodically inserted for channel estimation using a Hamming windowed finite impulse response (FIR) low-pass filter to approximate the optimal Wiener filter. Interpolation is used to obtain the channel estimate for other symbols for the multistage SIC receiver [107]. The performance of a pilot symbol aided channel estimator with interpolation for a single user channel was analyzed in [12]. In [55] [56], a PIC-based channel estimator uses a decision-directed linear predictor and a linear smoother. The decision-directed linear predictor and linear smoother was previously proposed for a single user channel estimation [64].

As seen from Section 4.9.3, the user delay variation in a practical system is far less than that used in our simulations. In our simulations, we have averaged the time delay error over a block of $M = 9$ symbols to filter out the noise. Although the delay-robust SIC based multiuser delay tracker does track the multiuser delay variations, it sometimes loses tracking because of the small block length used. In practice, the delay error can be averaged over a larger block, i.e., $M = 70$ symbols, to have better tracking performance. In practical implementations, the block averaging may be replaced by exponential weighting with a forgetting factor less than unity.

The channel estimation and delay tracking can be separated by using different

block lengths for prediction and smoothing by using our delay-robust SIC technique, in a similar manner to the PIC-based delay tracker [55] [56]. This provides an alternative to the extended Kalman filter (EKF) based channel and delay trackers [10] [47] [62]. The extended Kalman filter was introduced since the time delay is a nonlinear function of the user signature sequence. When channel and delay estimation are separated, the simpler Kalman filter can be used for the channel estimation, while the delay tracking can be handled by the delay-robust SIC using a longer smoothing length.

4.11 Conclusion

We have proposed and analyzed a family of improved bit decision procedures for the SIC. These new decision functions combine the advantages of the unit-clipper and the hard-limiter decision functions. By using time-averaged amplitude estimation, the noise in the amplitude estimate can be greatly reduced. BER performance within 0.4 dB of the single-user bound has been shown both by simulation and analysis. The previously proposed unit-clipper (c=1) [78] [133] can incur a performance loss of more than 2 dB. Our analysis enables optimization of the threshold parameter in the decision function. This new SIC with amplitude averaging was then made robust to time delay estimation errors up to half a PN chip. The delay-robust SIC is also used for multiuser delay tracking in both known and unknown fading channels.

Chapter 5

Application of Multiuser Receiver Structures to Multi-Antenna Systems

In previous chapters, we have considered CDMA multiuser detection for systems with a single antenna at the receiver. In this chapter, we consider the application of multiuser detection to multiple antenna systems. A straightforward extension of single antenna CDMA to multiple antenna CDMA requires that the users' array response vectors are known or estimated. This was considered in [122] - [124]. Alternatively, we may exploit certain similarities between multiple input multiple output (MIMO) systems and the synchronous CDMA system, and modify previously developed CDMA multiuser detection methods to MIMO systems. We consider the latter case here in this chapter. In particular, we consider the Bell Labs Layered Space-Time (BLAST) system, which is a linear MIMO system. We propose a stable reduced-complexity detection method for BLAST by modifying the CDMA decorrelating decision-feedback multiuser detection to obtain optimal detection ordering.

5.1 Introduction

The CDMA multiuser receiver structures we have investigated so far are for the single receiver antenna system. To improve performance or to increase throughput, the receiver is usually equipped with multiple antennas. It is therefore important

to apply the multiuser detection methods to multiple antenna systems. One type of multiple antenna system employs closely spaced antennas, with one half a wavelength spacing. The second kind of multiple antenna system is the multiple input multiple output (MIMO) system, where the transmitter sends multiple streams of data through the multiple transmitting antennas, spaced several wavelengths apart to ensure low inter-element correlation. The receiver also utilizes multiple receiving antennas for data detection.

5.1.1 Application to Antenna Array CDMA Systems

Although the application of multiuser detection to antenna array CDMA systems is straightforward, the main difficulty is in the parameter estimation, i.e., the array response vector estimation for each signal path of each user. The "spatial" dimension can increase the received signal-to-noise (SNR) ratio and thus improve the multiuser receiver performance. The spatial-temporal detector proposed in [73] first passes the received signal vector through a K dimensional beamformer. The outputs of the K beamformers are then input into a bank of K matched filters. The symbol-rate sampled matched filter outputs are sufficient statistics to detect the block of bits $\mathbf{b}$.

Another approach [122] - [124] uses an iterative method to estimate the channel attenuation and array response vectors. The estimated parameters are used in a maximum-SNR beamformer followed by a multistage detector. The iterative method used is either the EM or SAGE algorithm. The effect of time delay errors on this iterative spatial-temporal multiuser detector is investigated in [123], where it is found that performance is sensitive to time delay errors as small as $\frac{1}{8}$ chip.

Since the delay-robust SIC investigated in the previous chapters is also based on iterative computation, it is possible to apply delay-robust techniques to an antenna array CDMA multiuser detector. We will not elaborate on the extension of delay robust to antenna array CDMA system in this chapter. Rather we focus on applying CDMA multiuser detection for the emerging MIMO systems, which promise significant capacity increases for future generation wireless systems [65] [77].

5.1.2 Application to MIMO Systems

Multiple input multiple output (MIMO) systems that use multiple transmit and receive antennas to transmit a high data rate over the wireless channel form an active research area [65] [77]. MIMO systems for flat fading channels may be categorized as those involving: space-time trellis coding [114] [115], space-time block coding [116] [117], space-time differential coding [41] [44], and linear space-time coding (or mapping) [25] [26] [32].

The Bell Labs Layered Space-Time (BLAST) is linear space-time coding architecture well-suited for high-rate wireless communications [25]. We denote an (M_T, M_R) BLAST system as having M_T antennas at the transmitter and M_R antennas at the receiver. When $M_T \leq M_R$, there exists an ordered SIC algorithm to detect the transmitted information symbols from each transmit antenna [26] [32], instead of the exponentially complex maximum-likelihood search over all possible transmitted symbol combinations. Th ordered SIC is not the same as the SIC CDMA detector [84] in the previous chapters. The ordered SIC uses iterative zero-forcing or MMSE nulling and cancellation of interference, while the CDMA SIC uses only interference cancellation.

The main computation in using the ordered SIC algorithm for BLAST symbol detection is the determination of the optimal ordering of the nulling and cancellation steps, and the computation of the corresponding nulling vectors. This method will be reviewed in Section 5.2.1. These steps have computational complexity of order $O(M_T^4)$. When the number of transmit and receive antennas is large, i.e, $M_T \geq 18$, the repeated use of the pseudo-inverse to calculate the nulling vectors may lead to numerical instability [38].

Since BLAST is a linear space-time coding system, there exist efficient detection algorithms and recently there has been much research activity in extending and improving BLAST [11] [39] [79] [128]. In [11], adaptive modulation for each transmit antenna was proposed to increase the multiple-input multiple-output (MIMO) system's spectral efficiency. The detection method used for this adaptive modulation

BLAST is also an ordered SIC. A high-rate linear space-time code of [39] is an extension of BLAST to the case where the number of receive antennas, M_R, is less than the number of transmit antennas, M_T. The detection algorithms of BLAST are the same as those of its extensions [39] [79] and [128], so it is important to develop an efficient and stable detection algorithm.

A square-root algorithm based on QR decomposition of the channel matrix and unitary transformations is used in [38] to avoid the repeated computation of the nulling vectors. Instead, the QR decomposition is computed only once. Not only is computation complexity reduced, but also the numerical robustness is improved by this square-root algorithm.

In this chapter, we propose to further reduce the complexity of the algorithm in [38]. Motivated by the decorrelating decision-feedback multiuser detection algorithm originally proposed for synchronous code division multiple access (CDMA) systems [20], we interpret an (M_T, M_R) BLAST system as an M_T-user CDMA system with spreading factor M_R, as first suggested in [26].

5.2 System Model

In the following, we assume that $M_T \leq M_R$ to facilitate simple ordered SIC at the receiver.

At the transmitter, the incoming information stream is serial-to-parallel converted to M_T sub-streams. Each sub-stream is associated with a transmit antenna. At each time instant, one symbol from each sub-stream is transmitted from its corresponding transmit antenna, resulting in M_T symbols transmitted simultaneously. The system model for BLAST is shown in Fig. 5.1.

The wireless channel is assumed to be rich-scattering and flat-fading. The fading between each transmit and receive antenna pair are assumed independent. The channel is also assumed quasi-static, and the channel parameters are assumed to have been estimated at the receiver by transmitting a short training sequence before the

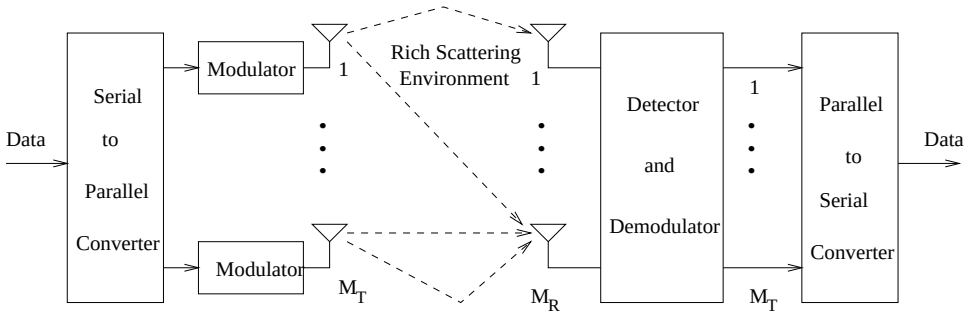

Figure 5.1: Model of BLAST space-time systems. $M_T \leq M_R$.

detection procedure [72].

The received signal at the M_R receive antennas can be organized into a vector after matched filtering and symbol rate sampling:

$$\mathbf{x} = [x_1 \dots x_{M_R}]^T \tag{5.1}$$

The transmitted signal from the M_T transmit antennas can also be organized in vector form:

$$\mathbf{s} = [s_1 \dots s_{M_T}]^T \tag{5.2}$$

The received signal $\mathbf{x}$ can be expressed as a linear combination of the transmitted signal $\mathbf{s}$:

$$\mathbf{x} = \mathbf{H}\mathbf{s} + \mathbf{v} \tag{5.3}$$

where $\mathbf{H} \in \mathcal{C}^{M_R \times M_T}$ is the complex channel matrix, and $\mathbf{v} \in \mathcal{C}^{M_R}$ is the spatially and temporarily white zero-mean Gaussian noise vector collected from the M_R receive antennas, with auto-correlation $\sigma^2\mathbf{I}$.

The elements of $\mathbf{H}$ are independent of one other due to the rich-scattering environment. The channel matrix $\mathbf{H}$ can be partitioned into its columns corresponding to the M_T transmitted signals, and it is denoted as $\mathbf{H}^{M_T}$:

$$\mathbf{H}^{M_T} = [\mathbf{h}_1 \dots \mathbf{h}_{M_T}] \tag{5.4}$$

5.2.1 Ordered SIC Method

We first briefly describe the ordered SIC method for symbol detection in BLAST [32]. The ordered SIC uses an iterative nulling and cancellation procedure in the decreasing signal-to-noise (SNR) ordering. In this chapter, we only consider the zero-forcing (ZF) criterion for nulling to simplify the algorithm description. The formulation using minimum mean-squared error (MMSE) criterion for nulling vector computation would be a straightforward extension.

The algorithm consists of the following steps repeated M_T times:

For $K = M_T$ to 1:

Step 1 Calculate the inverse of the correlation matrix as $(\mathbf{R}^K)^{-1} = (\mathbf{H}^{K*}\mathbf{H}^K)^{-1}$.

Step 2 Since the users' signal-to-noise ratios (SNR) are inversely proportional to their respective diagonal entries of $(\mathbf{R}^K)^{-1}$, find the smallest diagonal entry. Let α be the index of the smallest diagonal entry. Reorder $\mathbf{H}^K$ such that the α-th column and the last (K-th) column are interchanged:

$$\mathbf{H}^{K'} = [\mathbf{h}_1 \dots \mathbf{h}_K \dots \mathbf{h}_{K-1}\mathbf{h}_\alpha] \stackrel{\text{def}}{=} \left[\mathbf{H}^{(K-1)}\mathbf{h}_\alpha\right] \tag{5.5}$$

where the deflated channel matrix $\mathbf{H}^{(K-1)}$ is the same as $\mathbf{H}^{K'}$ with the last column $\mathbf{h}_\alpha$ deleted.

Step 3 Calculate the pseudo-inverse matrix $(\mathbf{H}^{K'})^\dagger$. Let the nulling vector $\mathbf{w}$ be the last row of $(\mathbf{H}^{K'})^\dagger$. The transmitted signal is detected as the closest point in the signal constellation

$$\hat{s}_K = dec(\mathbf{wx})$$

where $dec(\cdot)$ is the slice function, which depends on the modulation used.

Step 4 Perform interference cancellation by subtracting the detected signal from the received signal:

$$\mathbf{x} \leftarrow \mathbf{x} - \hat{s}_K \mathbf{h}_K$$

It has been proved in [26] that choosing the signal with the largest SNR at each step for nulling and cancellation achieves the global optimization that minimizes the probability of symbol errors. So the optimal ordering is the ordering of decreasing SNR .

Since at each step of the above algorithm, a pseudo-inverse of the deflated channel matrix is computed which is of order $O(M_T^3)$, the total complexity of the algorithm is $\frac{27}{4}M_T^4$ for the case of $M_T = M_R$.

5.2.2 Other Detection Algorithms

A sphere decoding algorithm based on the lattice sphere packing representation of the BLAST system can achieve maximum-likelihood performance [18]. However, this algorithm has complexity approximately proportional to $(2M_T)^6$, which limits its application.

An efficient square-root algorithm avoids the repeated computation of nulling vectors by QR decomposition [38]. The optimal ordering and the nulling vectors are all computed by unitary transformations on the QR decomposed matrices. This method has computational complexity $\frac{29}{3}M_T^3$ for the case of $M_T = M_R$.

5.3 Decorrelating Decision-feedback Methods

5.3.1 Original Decorrelating Decision-Feedback Method

The original decorrelating decision-feedback multiuser detector was used for detecting multiple user signals of a synchronous CDMA system [20]. By making a connection between a BLAST system and a synchronous CDMA system, decorrelating decision-feedback methods can be applied to the BLAST systems as well. The CDMA decorrelating decision-feedback method is similar to a generalized decision feedback equalizer (GDFE) which is applied to the BLAST system [31]. The GDFE is equivalent to the ordered SIC method when the optimal detection ordering is known in advance.

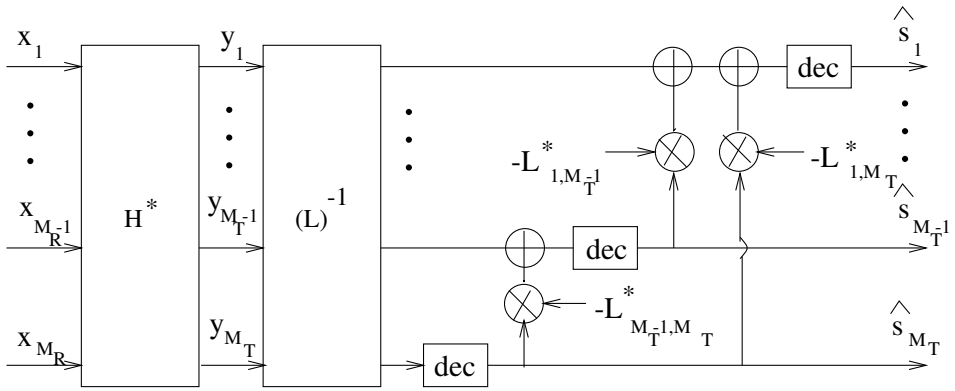

Figure 5.2: Correlator and the decision-feedback detector.

The received signal vector $\mathbf{x}$ is correlated with the conjugate transpose of the channel matrix. This correlation is analogous to the matched filter bank front-end of a CDMA multiuser receiver. The correlator output $\mathbf{y} \in \mathcal{C}^{M_T}$ is:

$$\mathbf{y} = \mathbf{H}^*\mathbf{x} = \mathbf{R}\mathbf{s} + \mathbf{z} \tag{5.6}$$

where $\mathbf{R} = \mathbf{H}^*\mathbf{H}$ is a $M_T \times M_T$ cross-correlation matrix, and $\mathbf{z}$ is a zero-mean Gaussian noise vector with auto-correlation $\sigma^2\mathbf{R}$.

The cross-correlation matrix can be Cholesky decomposed as $\mathbf{R} = \mathbf{L}\mathbf{L}^*$, where $\mathbf{L}$ is a lower triangular matrix and $\mathbf{L}^*$ is its conjugate transpose. A filter with impulse response $\mathbf{L}^{-1}$ is applied to the correlator outputs $\mathbf{y}$ of (5.6) to whiten the noise:

$$\check{\mathbf{y}} = \mathbf{L}^{-1}\mathbf{y} = \mathbf{L}^*\mathbf{s} + \mathbf{n} \tag{5.7}$$

Since $\mathbf{L}^*$ is upper triangular, the k-th component of $\check{\mathbf{y}}$ can be expressed as:

$$\check{y}_k = L^*_{k,k}s_k + \sum_{i=k+1}^{M_T} L^*_{k,i}s_i + n_k \tag{5.8}$$

which contains only interference from $(M_T - k)$ signals.

The last component $\check{y}_{M_T}$ contains no interference, so a decision for this transmitted signal can be made first: $\hat{s}_{M_T} = dec(\check{y}_{M_T})$. The next signal can be detected by subtracting the interference contribution from the M_T-th signal using the previous decision, i.e., $\hat{s}_{M_T-1} = dec(\check{y}_{M_T-1} - L^*_{M_T-1,M_T}\hat{s}_{M_T})$. This procedure is repeated until all signals are detected. Its structure is depicted in Fig. 5.2.

The above decorrelating decision-feedback method first cancels the interference using the feedback of previous decisions, and then makes a decision on the current signal. The detection and decision-feedback are performed in decreasing ordering of received signal energies in the original decorrelating decision-feedback CDMA multiuser detector in [20]. The Cholesky decomposition is calculated only once, so repeated calculation of the pseudo-inverse is avoided. A question that needs to be asked is whether the decreasing energy ordering for decorrelating decision-feedback the same as that of BLAST, i.e., the decreasing SNR ordering.

In the BLAST system, the received energies correspond to the column norms of the channel matrix $\mathbf{H}$. In a CDMA system, the cross-correlation between the different user codes can be designed to be equal, so decreasing energy ordering is the same as decreasing SNR ordering. However, in the BLAST system, the "spreading codes" values are actually channel gains, which are random and generally do not have equal cross-correlations. We therefore propose a modification to the original decorrelating decision-feedback method to obtain the optimal ordering.

5.3.2 Modified Decorrelating Decision-Feedback Method

The original cross-correlation matrix $\mathbf{R}$, or its corresponding Cholesky decomposition matrices $\mathbf{L}$ and $\mathbf{L}^*$, have to be reordered for optimal detection ordering. In this subsection, we propose a modified decorrelating decision-feedback detector where the detected signal has the largest SNR at every step.

The inverse of the cross-correlation matrix is $\mathbf{R}^{-1} = \mathbf{L}^{-*}\mathbf{L}^{-1}$, where $\mathbf{L}^{-1}$ can be easily calculated from the lower triangular matrix $\mathbf{L}$ by back-substitution, and $\mathbf{L}^{-*}$ is the conjugate transpose of $\mathbf{L}^{-1}$. The signal to be detected with the largest SNR corresponds to the signal with the smallest diagonal entry of $\mathbf{R}^{-1}$. Note that we do not need to calculate $\mathbf{R}^{-1}$ to find the smallest diagonal entry, since the diagonal entries of $\mathbf{R}^{-1}$ are equal to the column norms of $\mathbf{L}^{-1}$ using the property hat $\mathbf{R}^{-1} = \mathbf{L}^{-*}\mathbf{L}^{-1}$.

We find the smallest column norm of $\mathbf{L}^{-1}$, and then reorder the columns of $\mathbf{L}^{-1}$ by interchanging the smallest column-norm column with the last (M_T-th) column. The

rows of $\mathbf{L}$, corresponding to columns of $\mathbf{L}^{-1}$, as well as both the corresponding rows and columns of $\mathbf{R}$ are interchanged in the same way. Interchanging two columns of a matrix can be performed by post-multiplication by a unitary permutation matrix $\mathbf{P}$, and interchanging two rows of a matrix can be performed by pre-multiplication by a unitary permutation matrix $\mathbf{P}^*$, so the matrices after reordering are:

$$\mathbf{P}^*\mathbf{R}\mathbf{P} = (\mathbf{P}^*\mathbf{L})(\mathbf{L}^*\mathbf{P}) \tag{5.9}$$

In the following, we exploit the fact that there exists a unitary matrix $\mathbf{\Sigma}$ that transforms $\mathbf{L}^*\mathbf{P}$ into upper triangular form [33]. Similarly, its conjugate transpose $\mathbf{\Sigma}^*$ transforms $\mathbf{P}^*\mathbf{L}$ into lower triangular form:

$$\mathbf{P}^*\mathbf{R}\mathbf{P} = (\mathbf{P}^*\mathbf{L}\mathbf{\Sigma}^*)(\mathbf{\Sigma}\mathbf{L}^*\mathbf{P}) \tag{5.10}$$

The following symmetry property (Claim 1) is very useful to lower triangularize the reordered inverse matrix $\mathbf{L}^{-1}\mathbf{P}$.

Claim 1: *Let $\mathbf{\Sigma}$ be the unitary matrix that transforms $\mathbf{L}^*\mathbf{P}$ to upper triangular form, then the reordered inverse matrix $\mathbf{L}^{-1}\mathbf{P}$ is transformed to lower triangular form by the same $\mathbf{\Sigma}$.*

Proof:

$$\mathbf{I} = \mathbf{P}^*\mathbf{P} = (\mathbf{P}^*\mathbf{L})(\mathbf{L}^{-1}\mathbf{P}) = (\mathbf{P}^*\mathbf{L}\mathbf{\Sigma}^*)(\mathbf{\Sigma}\mathbf{L}^{-1}\mathbf{P}) \tag{5.11}$$

where we have used the property that for unitary matrix: $\mathbf{\Sigma}^*\mathbf{\Sigma} = \mathbf{I}$. Since $\mathbf{\Sigma}\mathbf{L}^*\mathbf{P}$ is upper triangular, its conjugate transpose $\mathbf{P}^*\mathbf{L}\mathbf{\Sigma}^*$ is in lower triangular form. Since $\mathbf{\Sigma}\mathbf{L}^{-1}\mathbf{P}$ is the inverse of $\mathbf{P}^*\mathbf{L}\mathbf{\Sigma}^*$, it also must be lower triangular.□

Instead of finding the unitary transformation based on the $\mathbf{L}^{-1}\mathbf{P}$ directly, we may use $\mathbf{L}^*\mathbf{P}$ to find $\mathbf{\Sigma}$ to increase numerical stability.

In addition to finding the smallest norm, reordering and triangularization using (5.9), (5.10) and (5.11) for the first step, the following Claims 2 and 3 ensure that it is sufficient to use deflated Cholesky factors $\mathbf{L}^{(M_T-1)}$ and $(\mathbf{L}^{(M_T-1)})^{-1}$ for the next step.

Claim 2: *We can reduce* $\mathbf{P}^*\mathbf{L}\mathbf{\Sigma}^*$ *to matrix* $\mathbf{L}^{(M_T-1)}$ *as*

$$\begin{bmatrix} \mathbf{L}^{(M_T-1)} & \mathbf{0} \\ \times & \times \end{bmatrix} = \mathbf{P}^*\mathbf{L}\mathbf{\Sigma}^* \tag{5.12}$$

where $\times$ *represents entries that are irrelevant,* $\mathbf{L}^{(M_T-1)}\mathbf{L}^{(M_T-1)*} = \mathbf{R}^{(M_T-1)}$*, and* $\mathbf{R}^{(M_T-1)} = \mathbf{H}^{(M_T-1)*}\mathbf{H}^{(M_T-1)}$ *is the cross-correlation matrix for the reordered and deflated channel matrix* $\mathbf{H}^{(M_T-1)}$ *using the notation in (5.5).*

Proof: This proof is similar to that of [38]. By substituting (5.12) into (5.10), we obtain:

$$\begin{aligned} \mathbf{P}^*\mathbf{R}\mathbf{P} &= \begin{bmatrix} \mathbf{L}^{(M_T-1)} & \mathbf{0} \\ \times & \times \end{bmatrix} \begin{bmatrix} \mathbf{L}^{(M_T-1)*} & \times \\ \mathbf{0} & \times \end{bmatrix} \\ &= \begin{bmatrix} \mathbf{L}^{(M_T-1)}\mathbf{L}^{(M_T-1)*} & \times \\ \times & \times \end{bmatrix} \end{aligned} \tag{5.13}$$

By (5.5), it is also true that:

$$\begin{aligned} \mathbf{P}^*\mathbf{R}\mathbf{P} &= \begin{bmatrix} \mathbf{H}^{(M_T-1)*} \\ \mathbf{h}_\alpha^* \end{bmatrix} \begin{bmatrix} \mathbf{H}^{(M_T-1)} & \mathbf{h}_\alpha \end{bmatrix} \\ &= \begin{bmatrix} \mathbf{H}^{(M_T-1)*}\mathbf{H}^{(M_T-1)} & \times \\ \times & \times \end{bmatrix} \end{aligned} \tag{5.14}$$

Thus, the upper triangular matrix $\mathbf{L}^{(M_T-1)*}$ retains all the information contained in the deflated channel matrix $\mathbf{H}^{(M_T-1)}$. □

Claim 3: *The inverse lower triangular matrix* $\mathbf{\Sigma}\mathbf{L}^{-1}\mathbf{P}$ *can be expressed in reduced form as*

$$\mathbf{\Sigma}\mathbf{L}^{-1}\mathbf{P} = \begin{bmatrix} (\mathbf{L}^{(M_T-1)})^{-1} & \mathbf{0} \\ \times & \times \end{bmatrix} \tag{5.15}$$

where $(\mathbf{L}^{(M_T-1)})^{-*}(\mathbf{L}^{(M_T-1)})^{-1} = (\mathbf{R}^{(M_T-1)})^{-1}$.

Proof: Let

$$\begin{bmatrix} \mathbf{B} & \mathbf{0} \\ \times & \times \end{bmatrix} = \mathbf{\Sigma}\mathbf{L}^{-1}\mathbf{P}$$

Then by (5.11):

$$\begin{aligned}
\mathbf{I} &= (\mathbf{P}^*\mathbf{L}\mathbf{\Sigma}^*)(\mathbf{\Sigma}\mathbf{L}^{-1}\mathbf{P}) \\
&= \begin{bmatrix} \mathbf{L}^{(M_T-1)} & \mathbf{0} \\ \times & \times \end{bmatrix} \begin{bmatrix} \mathbf{B} & \times \\ \mathbf{0} & \times \end{bmatrix} \\
&= \begin{bmatrix} \mathbf{L}^{(M_T-1)}\mathbf{B} & \mathbf{0} \\ \mathbf{0} & \mathbf{1} \end{bmatrix}
\end{aligned} \tag{5.16}$$

From the above equation

$$\mathbf{L}^{(M_T-1)}\mathbf{B} = \mathbf{I}^{(M_T-1)} \tag{5.17}$$

Thus, $\mathbf{B} = (\mathbf{L}^{(M_T-1)})^{-1}$. Since $(\mathbf{R}^{(M_T-1)})^{-1} = (\mathbf{L}^{(M_T-1)})^{-*}(\mathbf{L}^{(M_T-1)})^{-1}$, $\mathbf{B}$ retains all the information to calculate $(\mathbf{R}^{(M_T-1)})^{-1}$ and to find the largest SNR for the next step. □

The complete algorithm of the modified decorrelating decision-feedback detection for BLAST systems can be described by the following steps:

Initialization:

Cholesky decompose $\mathbf{R} = \mathbf{L}\mathbf{L}^*$ and invert matrix $\mathbf{L}$ by back-substitution. Let $\mathbf{L}^{M_T} = \mathbf{L}$.

Iterations:

For $K = M_T$ to 1

1. Find the column of $(\mathbf{L}^K)^{-1}$ with the smallest column norm, and reorder it to the last column via the transformation $(\mathbf{L}^K)^{-1}\mathbf{P}$. Similarly reorder the columns of $\mathbf{L}^{K*}$ by $\mathbf{L}^{K*}\mathbf{P}$.

2. Find a unitary matrix $\mathbf{\Sigma}$ that transforms $\mathbf{L}^{K*}\mathbf{P}$ to upper triangular form $\mathbf{\Sigma}\mathbf{L}^{K*}\mathbf{P}$. Similarly compute lower triangular matrix $\mathbf{\Sigma}(\mathbf{L}^K)^{-1}\mathbf{P}$. $\mathbf{\Sigma}$ can be realized by a series of Givens rotations [33].

Detection:

Perform decorrelating decision-feedback detection in Eq. (5.7) with the reordered matrices [20].

5.3.3 Implementation Issues

In a practical implementation, we do not need to calculate the cross-correlation matrix $\mathbf{R}$ first to get its Cholesky decomposition matrix $\mathbf{L}$. Rather we can perform a QR decomposition on the channel matrix $\mathbf{H}$ directly to get $\mathbf{L}$. Let the QR decomposition be $\mathbf{H} = \mathbf{QF}$, where $\mathbf{Q}$ is orthonormal and $\mathbf{F}$ is upper triangular. Since $\mathbf{Q}^*\mathbf{Q} = \mathbf{I}$, we have $\mathbf{H}^*\mathbf{H} = (\mathbf{F}^*\mathbf{Q}^*)(\mathbf{QF}) = \mathbf{F}^*\mathbf{F}$. Then we can conclude that $\mathbf{L} = \mathbf{F}^*$.

Although both algorithms utilize a QR decomposition, and our research was partially inspired by [38], our modified decorrelating decision-feedback method is different from the square-root algorithm in [38]. The square-root algorithm uses both the matrix $\mathbf{Q}$ for nulling vector calculation and the inverse matrix $\mathbf{F}^{-1}$ for optimal ordering. The square-root algorithm performs repeated triangularization on the inverse matrix $\mathbf{F}^{-1}$. Even with back-substitution, this may lead to instability, so [38] adopts a computationally complex series of transformations to avoid computing $\mathbf{F}^{-1}$ directly by inverting $\mathbf{F}$.

Our method utilizes symmetry properties, so we can perform repeated triangularization on the conjugate transpose matrix $\mathbf{L}^*$, while the inverse matrix $\mathbf{L}^{-1}$ is triangularized by symmetry by the same transformation. As the accuracy requirement on $\mathbf{L}^{-1}$ is relaxed, it can be computed by simple back-substitution. Another possible advantage of the proposed method is that there should be less rounding error effects in a fixed-point implementation, since normally $\mathbf{L}$ has larger entry values than $\mathbf{L}^{-1}$.

The dominant computation of the modified decorrelating decision-feedback receiver is in the QR decomposition, the matrix inversion and the reordering and triangularization of matrices $\mathbf{L}^*$ and $\mathbf{L}^{-1}$.

The computation complexity for QR decomposition is $2M_T^2(M_R - M_T/3)$ [33]. The computational complexity to calculate $\mathbf{L}^{-1}$ by back-substitution is $M_T^3/3$. At the i-th step, finding the smallest column norm takes $i^2/2$ operations, and triangularization

of the two matrices takes $2M_T i$. So the total complexity for the M_T steps is

$$\sum_{i=1}^{M_T}(\frac{1}{2}i^2 + 2M_T i) = \frac{1}{6}M_T^3 + M_T^3 = \frac{7}{6}M_T^3 \tag{5.18}$$

Thus, the total complexity for the algorithm is:

$$\frac{5}{6}M_T^3 + 2M_T^2 M_R \tag{5.19}$$

When $M_T = M_R$, it is $\frac{17}{6}M_T^3$, which is less than $\frac{29}{3}M_T^3$ of the square-root algorithm [38] and $\frac{27}{4}M_T^4$ of the ordered SIC algorithm [32].

As an example, for an $M_T = M_R = 14$ antenna BLAST system, 1 Mbit/sec data rate can be transmitted over a 30 kHz channel. The transmission symbol rate is 24.34 ksymbol/sec for each transmit antenna, and 16-QAM modulation is used. The training sequence length is $L_T = 32$ symbols, and the payload sequence length is $L_P = 100$ symbols. The channel estimation requires $2M_T M_R log_2 L_T$ computations, when the training sequence is taken as columns of an $L_T \times L_T$ fast Fourier transform (FFT) matrix. The payload processing complexity is $2M_T M_R L_P$.

The computational complexity for the different steps of the ordered SIC algorithm is given in Table 5.1 [38].

	Flops/burst	MegaFlops/s	%
channel estimation	7,840	1.44	0.65
nulling vectors and ordering	1,036,000	190.8	86.3
payload processing	156,800	28.9	13.1
TOTAL	1,200,000	221.2	100

Table 5.1: Complexity of Ordered SIC Algorithm

From Table 5.1, the nulling vector and optimum ordering calculation is the dominant calculation, 190 MFlops/sec, nearly 90% of the total 221 MFlops/sec complexity. For the square-root algorithm, the optimum ordering calculation complexity reduces to 19 MFlops/sec, and the total complexity is reduced to 50 MFlops/sec, as shown in Table 5.2 [38].

	Flops/burst	MegaFlops/s	%
channel estimation	7,840	1.44	2.9
nulling vectors and ordering	106,100	19.5	39.1
payload processing	156,800	28.9	58.0
TOTAL	270,400	49.8	100

Table 5.2: Complexity of Square-Root Algorithm

The relative complexity of our modified decorrelating decision-feedback algorithm is shown in Table 5.3. The optimum ordering calculation complexity reduces to 5.72 MFlops/sec and the total complexity is further reduced to 36.1 MFlops/sec. Note that the payload processing dominates the computation, occupies more than 80%, which is a desirable result.

	Flops/burst	MegaFlops/s	%
channel estimation	7,840	1.44	4.0
nulling vectors and ordering	31,100	5.72	15.9
payload processing	156,800	28.9	80.1
TOTAL	195,740	36.1	100

Table 5.3: Complexity of Modified Decorrelating Decision-Feedback Algorithm

If instead of zero-forcing nulling, MMSE-nulling is required, then the decorrelating decision-feedback receiver can be modified to a MMSE decision-feedback receiver either by Cholesky decomposition on matrix $(\mathbf{R} + \alpha\mathbf{I})$, where $\alpha > 0$, or by QR decomposition on the augmented channel matrix directly as in [38].

The application of turbo processing to the space-time coding system has received significant recent interest. This system uses a simple convolutional or turbo code combined with simple space-time mapping to achieve the large capacity of the MIMO Rayleigh fading channels with a large number of antennas. Linear space-time coding

such as that of BLAST is used as the component code for turbo space-time coding systems due to its simplicity [3]. In symbol detection using turbo processing, the optimal ordering according to the SNR is still required [3]. Therefore our simplified algorithm to find the optimal ordering can also be applied to the turbo space-time coding systems.

5.4 Simulation Results

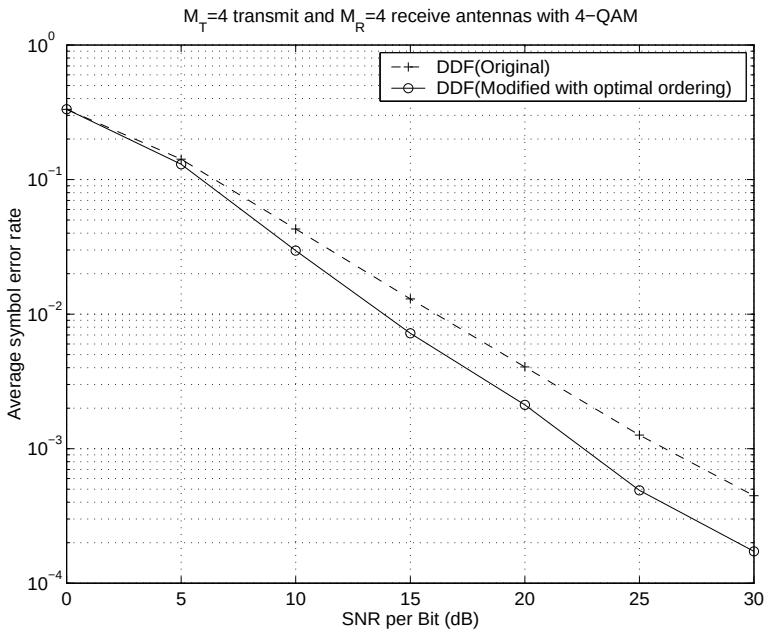

Figure 5.3: Average symbol error rate of the original and modified decorrelating decision-feedback (DDF) detectors for BLAST system with $M_T = 4$ transmit antennas, $M_R = 4$ receive antennas and 4-QAM modulation.

Throughout the simulations, q-QAM constellations are used. The average energy per bit is fixed to unity, so the average energy per symbol is $\bar{E}_s = 2(q-1)/3$ as in [18]. The channel matrix is simulated as zero-mean complex Gaussian with variance 0.5 per dimension. The additive zero-mean white Gaussian noise (AWGN) is complex-valued, with variance σ^2 per dimension, where σ^2 is subject to the following equation

[18]:

$$\sigma^2 = \frac{M_T \bar{E}_s}{2 \log_2 q} 10^{-\frac{SNR}{10}} \tag{5.20}$$

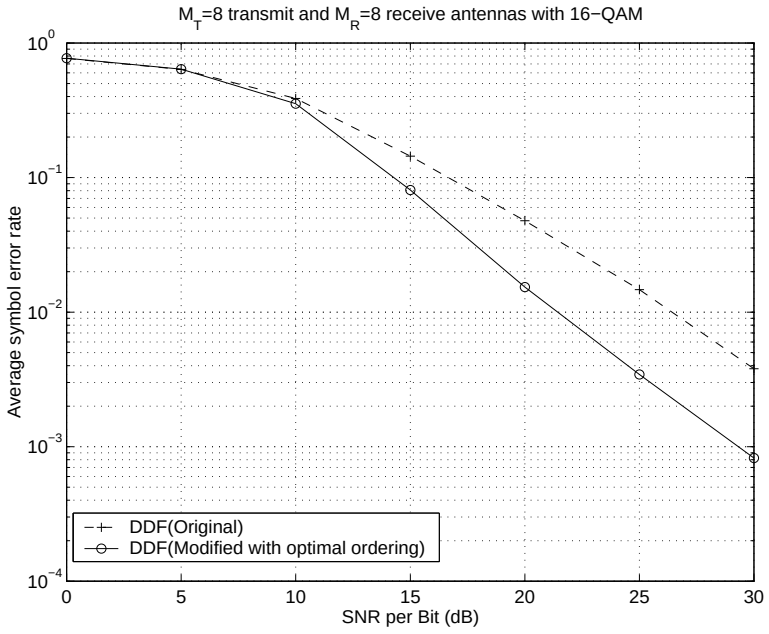

Figure 5.4: Average symbol error rate of the original and modified decorrelating decision-feedback (DDF) detectors for BLAST system with $M_T = 8$ transmit antennas, $M_R = 8$ receive antennas and 16-QAM modulation.

With optimal ordering, the symbol error rate (SER) performance of the ordered SIC detector, the square-root algorithm and the proposed modified decorrelating decision-feedback detector are identical under float-point simulation. However, the impact of the reordering on performance was not quantified in [32] and [38]. In Figs. 5.3 and 5.4, we compare the average symbol error rates (SER) of the original decorrelating decision-feedback (DDF) detector and the modified decorrelating decision-feedback detector with optimal ordering.

In Fig. 5.3, the number of transmit and receiver antennas are $M_T = M_R = 4$, and 4-QAM modulation is used. We observe that the SER of the optimal ordered DDF detector is lower than the original DDF without optimal ordering. In the simulations, the frequency of occurrence that the optimal ordering is the same as the original ordering is less than 30% of all channel realizations.

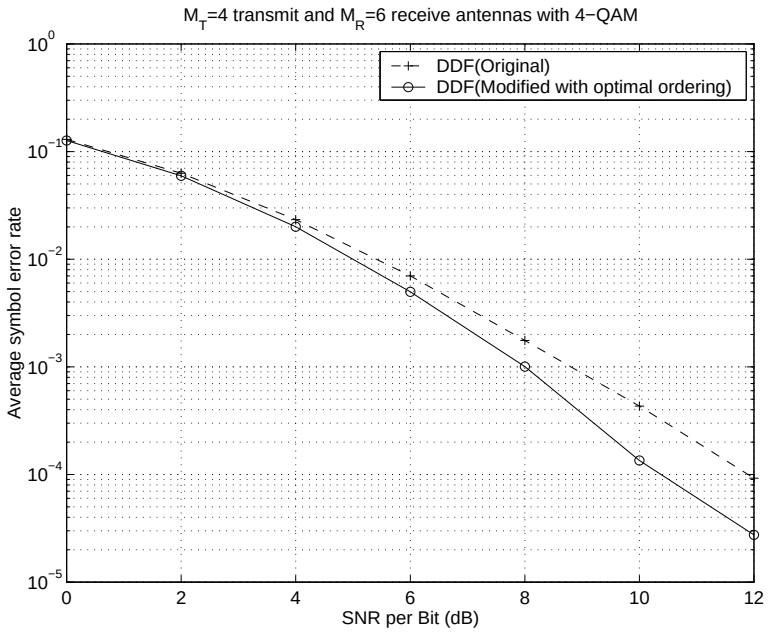

Figure 5.5: Average symbol error rate of the original and modified decorrelating decision-feedback (DDF) detectors for BLAST system with $M_T = 4$ transmit antennas, $M_R = 6$ receive antennas and 4-QAM modulation.

In Fig. 5.4, simulation results for $M_T = M_R = 8$ antennas, and 16-QAM modulation are shown. As the number of transmit and receive antennas increases, the frequency of occurrence that the optimal ordering is the same as the original ordering decreases to less than 1% of all channel realizations. This explains the larger performance improvement of the modified decorrelating decision-feedback detector over the original decorrelating decision-feedback detector in Fig. 5.4 versus that in Fig. 5.3.

The results for the case when there are more receive antennas than transmit antennas is simulated in Fig. 5.5 for $M_T = 4$, $M_R = 6$ and 4-QAM modulation, and in Fig. 5.6 for $M_T = 8$, $M_R = 12$ and 16-QAM modulation

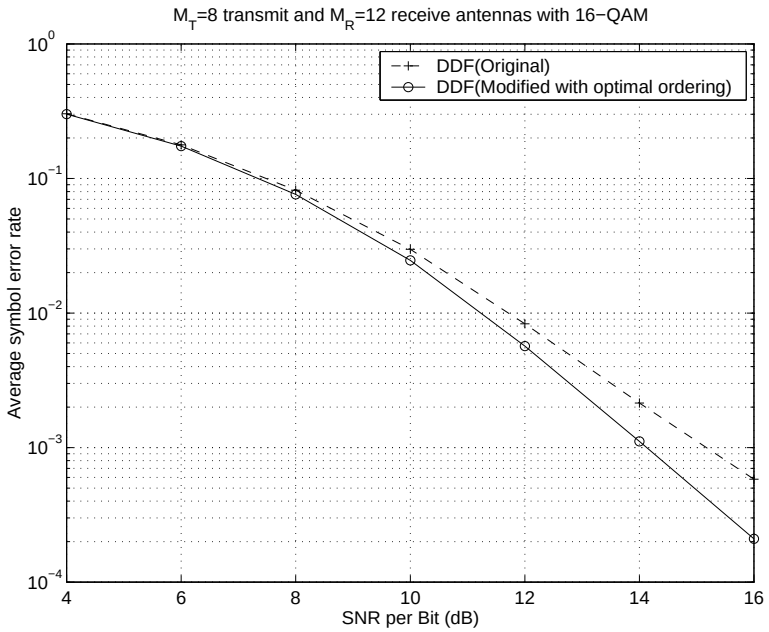

Figure 5.6: Average symbol error rate of the original and modified decorrelating decision-feedback (DDF) detectors for BLAST system with $M_T = 8$ transmit antennas, $M_R = 12$ receive antennas and 16-QAM modulation.

5.5 Conclusion

A modified decorrelating decision-feedback detection method is proposed and applied to the BLAST space-time system. The repeated computation of matrix pseudo-inverses is avoided by decorrelating decision-feedback detection. By exploiting the symmetry in triangularizing the conjugate transpose and the inverse matrix, increased numerical stability and decreased computational complexity are achieved. Although the proposed algorithm, the square-root algorithm and the ordered SIC algorithm have the same performance when the numerical precision is infinite, future research should be conducted to compare their performances in a fixed-point DSP implementation.

Chapter 6

Conclusions and Future Work

This chapter summarizes the major contributions in this thesis and presents possible future directions which could be extensions of the research presented in this thesis.

6.1 Thesis Summary

This thesis has investigated improvements to existing multiuser detection methods by using advanced signal processing. The multistage SIC detector was made robust to time delay errors, and a new soft-decision function was proposed to further enhance the delay-robust SIC detector performance. This new soft-decision function may also be applied to other SIC or PIC type CDMA multiuser detectors, e.g., the SAGE-based spatial-temporal decorrelator. An improvement was made to the CDMA multiuser decision-feedback method and this improved decision-feedback detection was applied to a high-rate linear space-time MIMO system, the BLAST system.

In Chapter 3, we considered enhancing the multistage SIC detector with an additional timing delay error signal estimation and cancellation procedure using a tentative decision-feedback. We found in Section 3.3 that the SIC can be robusitified to timing errors at the sacrifice of only a modest amount of system capacity. The asymptotic efficiency of the delay-robust SIC was analyzed in Section 3.4. It was shown that the delay-robust SIC is near-far resistant regardless the timing error distribution, whereas other multiuser detectors would be near-far limited with timing

errors present. The delay-robust SIC was first derived for rectangular chip pulse shapes, and later generalized to band-limited chip pulse shapes in Section 3.6. This delay-robust SIC can also be used for time delay error estimation since time delay error is implicitly estimated by this algorithm. The CRLB for the delay error estimation was calculated in Section 3.4, and time delay estimation accuracy was compared to the CRLB, where it was found that estimation accuracy exceeded the CRLB due to noise enhancement in decorrelation.

The delay-robust SIC of Chapter 3 is based on a multistage SIC implementation of the decorrelating detector using a linear decision function. The decorrelator's noise enhancement increased the BER of the delay-robust SIC to well above the single-user bound, and introduced time error variance well above the CRLB. This noise enhancement problem is more serious if the system is highly loaded. In Section 4.3, we compared several known decision functions and proposed a new soft-decision function to combine the advantages of different known decision functions. The SIC using the new proposed soft-decision function reduced both error propagation effects of the hard-limiter decision function as well as noise enhancement of the linear-soft decision function. Even when assuming that amplitude information must be estimated by time-averaging, the multistage SIC using the new soft-decision function still achieves performance within one dB of the single-user bound. This performance is both calculated by a steady-state analysis in Section 4.4 and confirmed by computer simulation in Section 4.9. In Section 4.6, the new soft-decision function is applied to the delay-robust SIC proposed in Chapter 3. It was found that the new soft-decision delay-robust SIC has improved performance when there are large numbers of users and larger delay errors.

We also applied the delay-robust SIC for multiuser delay tracking and data detection in a multipath fading channel. In Section 4.7, it is shown that for a slowly varying or constant channel, the soft-decision function can be effective to reduce noise enhancement. In Section 4.8, fast fading channels are considered, and a linear decision function is used in the delay-robust SIC based delay tracker to decorrelate the

multiuser fading signals. Both time delay variation and channel fading are tracked by this linear decision function. The tracking performance for both rectangular and band-limited chip pulse shapes are investigated in Section 4.9.

In Section 5.1, we make a connection between a linear space-time MIMO system, i.e., the BLAST system, and a synchronous CDMA system. In Section 5.3, we applied the decision-feedback multiuser detection method used in CDMA to the BLAST system, to reduce computation and increase numerical stability. To achieve the optimal signal power ordering, the decision-feedback matrix is permuted by a series numerically stable unitary transformations. It is proven that these transformations guarantee optimal ordering. Implementation complexity of several methods are compared in Section 5.3.3, and numerical results are provided in Section 5.4. It was found that the proposed improved decision-feedback detection uses the optimal ordering and achieves identical BER performance as that of the more complex ordered SIC method [26] [32], under the ideal float-point implementation.

6.2 Future Directions

Although this thesis has investigated the problem of improved multiuser detection for asynchronous CDMA system with time delay errors and with application to the space-time coding systems, there are several issues that remain to be explored. In this section, we discuss several important areas which require further study.

6.2.1 Time Delay Estimation for Time Varying Fading Channels

It is usually assumed that the relative time delays for all the users are known at the basestation receiver. However, in practical applications, we have to estimate these parameters. Previous studies show that the BER performance of multi-user receivers degrades significantly due to time delay estimation errors for single-antenna single-path systems

Current time delay estimation algorithms for multiuser CDMA systems require that the channel remains unchanged during the estimation period. However, the practical wireless channel is time-varying due to the movement of mobile terminals. Therefore, it is important to investigate efficient time delay estimation methods that operate under fading channels. It is observed that using multiple antennas at the basestation can increase the signal dimensionality and thus may be used to reduce the required estimation period. Using multiple antennas for delay estimation may also improve the delay estimation accuracy since the time delay and direction of arrival (DOA) are coupled and can thus be estimated jointly.

6.2.2 Multiuser Receivers in Multi-cell Systems

Most of the known multi-user detection methods considered only single-cell system, where the user spreading codes of the same cell (intra-cell users) are all known. However, one important advantage of CDMA systems is that no frequency planning is required so that the same frequency can be used in adjacent cells. In practical multi-cell environments, the multiple access interference (MAI) from the users in other cells (inter-cell users) is a fraction f of the MAIs from intra-cell users, typically is $f = 0.55$. Since the spreading codes of inter-cell users are unknown at the basestation, and joint multiuser detection of inter-cell users is complex even if all spreading codes were known, inter-cell MAI limits the capacity improvement of the multiuser detection to $(1 + f)/f = 2.8$ for $f = 0.55$.

Thus, it is important to suppress inter-cell MAI. Blind multiuser detection methods such as the minimum output energy (MOE) receiver, which is the blind equivalent to MMSE multiuser detection, can suppress strong inter-cell MAIs, since it treats intra-cell MAIs and inter-cell MAIs the same. However, MOE performance depends on the assumption that the signal subspace dimensionality of the strong MAIs are less than the spreading factor, and so is unlikely to perform satisfactorily in a multi-cell environment.

Another approach is to use an adaptive MMSE receiver as the front-end instead

of the matched-filter in current multiuser detectors [91] [92]. This adaptive MMSE front-end is followed by a multiuser detection stage. However, it will has the same drawback as the MOE.

Using an antenna array at the basestation provides another kind of signal subspace dimensionality, which can be used to better separate users' signals. The adaptive antenna array multiuser receivers of [28] [43] were proposed for a single-cell system. However, it may be possible to apply adaptive methods to multi-cell systems.

An adaptive antenna array feedforward/feedback multiuser detector based-on training can also suppress inter-cell MAIs [104]. This is the extension of the adaptive feedforward/feedback architecture of the single antenna case [103] to the multiple antenna case. However, in [104] it is assumed that the channel and MAIs remain unchanged during the training and the detection periods. Application is therefore limited to packet-based transmission at high rates.

In summary, for multi-cell CDMA systems, the use of adaptive antenna arrays with CDMA multiuser detection may be effective to suppress inter-cell interference. Future research needs to be performed in the development of adaptive array algorithms that can be combined with or incorporated into the multiuser detector.

6.2.3 Multiuser Detection for Fast Fading Channels

For fast fading CDMA channels, pilot symbols can be used to assist in channel estimation as in the single user channel case [12]. The effect of using decision-feedback of information symbols combined with pilot symbol estimation requires investigation for different Doppler fading conditions. Since 3G wireless standards propose to use pilot symbols to ease channel estimation and use turbo codes to lower the bit error probability and required transmission power level, combining pilot-assisted channel estimation and turbo decoding is worth investigation [60].

Mobile velocity estimation can be utilized in forming more accurate state equations for Kalman filtering. The performance compare of Kalman filtering and linear prediction and smoothing methods under multiuser detection needs investigation.

Long-range prediction of fading signals may be helpful for CDMA multiuser detection in fading channels [21]. A canonical time-frequency representation of the fast fading channel was proposed in [6] and [97] to exploit joint multipath-Doppler diversity for a single-user CDMA channels. This canonical time-frequency representation is similar to the basis expansion models and diversity techniques in [29]. The canonical time-frequency representation was also used for multiuser detection in fast fading multipath channels [96] and for multiuser timing estimation in multipath fading channels [95].

Appendix A

Derivation of the Cramér-Rao Lower Bound (CRLB)

The derivation of the CRLB follows the procedure of [110]. The log-likelihood function is

$$ln\Omega(\mathbf{r}) = -(M+1)Nln\sigma^2 - \frac{1}{\sigma^2}(\mathbf{r} - \mathbf{d}\,\mathbf{a} - \Delta\mathbf{d}\,\Delta\mathbf{a})^H(\mathbf{r} - \mathbf{d}\,\mathbf{a} - \Delta\mathbf{d}\,\Delta\mathbf{a}) \quad (A.1)$$

The gradients

$$\frac{\partial ln\Omega(\mathbf{r})}{\partial \psi} = \begin{bmatrix} \frac{\partial ln\Omega(\mathbf{r})}{\partial \sigma^2} \\ \frac{\partial ln\Omega(\mathbf{r})}{\partial \mathbf{a}} \\ \frac{\partial ln\Omega(\mathbf{r})}{\partial \Delta\mathbf{a}} \end{bmatrix} \quad (A.2)$$

are given as

$$\frac{\partial ln\Omega(\mathbf{r})}{\partial \sigma^2} = -\frac{(M+1)N}{\sigma^2} + \frac{1}{\sigma^4}\mathbf{n}^H\mathbf{n} \quad (A.3)$$

$$\frac{\partial ln\Omega(\mathbf{r})}{\partial \mathbf{a}} = \frac{2}{\sigma^2}\mathbf{a}^H\mathbf{d}^H\mathbf{n} \quad (A.4)$$

$$\frac{\partial ln\Omega(\mathbf{r})}{\partial \Delta\mathbf{a}} = \frac{2}{\sigma^2}\Delta\mathbf{a}^H\Delta\mathbf{d}^H\mathbf{n} \quad (A.5)$$

It can be shown that the (1,1) block of matrix $\mathbf{J}$ is

$$E\left[\left(\frac{\partial ln\Omega(\mathbf{r})}{\partial \sigma^2}\right)^2\right] = \frac{(M+1)N}{\sigma^4} \quad (A.6)$$

Since $\frac{\partial ln\Omega(\mathbf{r})}{\partial \sigma^2}$ is uncorrelated with all other gradients, the (1,2) and (1,3) blocks of matrix $\mathbf{J}$ are all zeros.

To calculate the other blocks in matrix $\mathbf{J}$, the general expression of the calculation is

$$E\left[\left(\frac{2}{\sigma^2}\mathbf{f}_1^H\mathbf{n}\right)\ (\frac{2}{\sigma^2}\mathbf{f}_2^H\mathbf{n})^H\right] = \frac{2}{\sigma^2}\mathbf{f}_1^H\mathbf{f}_2 \tag{A.7}$$

Appendix B

Calculation of Integer and Fractional Uncertainty Delay Estimate Probability

The conditional probability that $p_k \neq \hat{p}_k$ when the true fractional delay $\delta_k = x$ is

$$P(x) = \mathcal{Q}(\frac{x}{\sigma_\tau}) + \mathcal{Q}(\frac{1-x}{\sigma_\tau}) \tag{B.1}$$

Since x is uniformly distributed in $[0, 1)$, the average probability that $p_k \neq p'_k$ is

$$P = \int_0^1 \left[\mathcal{Q}(\frac{x}{\sigma_\tau}) + \mathcal{Q}(\frac{1-x}{\sigma_\tau})\right] dx = 2\int_0^1 \mathcal{Q}(\frac{x}{\sigma_\tau})\, dx \tag{B.2}$$

We note that through integration by parts

$$\int_0^1 \mathcal{Q}(\frac{x}{\sigma_\tau})dx = x \cdot \mathcal{Q}(\frac{x}{\sigma_\tau})|_0^1 + \int_0^1 x \cdot \frac{1}{\sqrt{2\pi}\sigma_\tau} e^{-\frac{x^2}{2\sigma_\tau^2}} dx \tag{B.3}$$

Substitute (B.3) into (B.2), we obtain

$$P = 2\left\{\mathcal{Q}(\frac{1}{\sigma_\tau}) + \frac{\sigma_\tau}{\sqrt{2\pi}}(1 - e^{-\frac{1}{2\sigma_\tau^2}})\right\} \tag{B.4}$$

Bibliography

[1] F. Adachi, M. Sawahashi and H. Suda, "Wideband DS-CDMA for next-generation mobile communications systems," *IEEE Commun. Mag.*, pp. 56-69, Sept. 1998.

[2] D. Agrawal, V. Tarokh, A. Naguib and N. Seshadri, "Space-time coded OFDM for high data-rate wireless communication over wideband channels," in *Proc. IEEE VTC*, Ottawa, 1998.

[3] S. L. Ariyavisitakul, "Turbo space-time processing to improve wireless channel capacity," *IEEE Trans. Commun.*, vol. 48, no. 8, pp. 1347-1359, Aug. 2000.

[4] S. E. Bensley and B. Aazhang, "Subspace-based channel estimation for code division multiple access communication systems," *IEEE Trans. Commun.*, vol. 44, no. 8, pp. 1009-1020, Aug. 1996.

[5] S. E. Bensley and B. Aazhang, "Maximum-likelihood synchronization of a single user for code-division multiple-access communication systems," *IEEE Trans. Commun.*, vol. 46, no. 3, pp. 392-399, Mar. 1998.

[6] S. Bhashyam, A. M. Sayeed and B. Aazhang, "Time-selective signaling and reception for communication over multipath fading channels," *IEEE Trans. Commun.*, vol. 48, no. 1, pp. 83-94, Jan. 2000.

[7] G. E. Bottomley, T. Ottosson and Y. E. Wang, "A generalized RAKE receiver for interference suppression," *IEEE J. Select. Areas Commun.*, vol. 18, no. 8, pp. 1536-1545, Aug. 2000.

[8] R. M. Buehrer, A. Kaul, S. Striglis and B. D. Woerner, "Analysis of DS-CDMA parallel interference cancellation with phase and timing errors," *IEEE J. Select. Areas Commun.*, vol. 14, no. 8, pp. 1522-1534, Oct. 1996.

[9] R. M. Buehrer and B. D. Woerner, "Analysis of adaptive multistage interference cancellation for CDMA using an improved Gaussian approximation," *IEEE Trans. Commun.*, vol. 44, no. 10, pp. 1308-1321, Oct. 1996.

[10] J. Caffery, Jr. and G. L. Stüber, "Nonlinear multiuser parameter estimation and tracking in CDMA systems," *IEEE Trans. Commun.*, vol. 48, no. 12, pp. 2053-2063, Dec. 2000.

[11] S. Catreux, P. F. Driessen and L. J. Greenstein, "Attainable throughput of an interference-limited multiple-input multiple-output (MIMO) cellular system," *IEEE Trans. Commun.*, vol. 49, no. 8, pp. 1307-1311, Aug. 2001.

[12] J. K. Cavers, "An analysis of pilot symbol assisted modulation for Rayleigh fading channels," *IEEE Trans. Vehicular Tech.*, vol. 40, no. 4, pp. 686-693, Nov. 1991.

[13] F. Cheng and J. M. Holtzman, "Effect of tracking error on DS/CDMA successive interference cancellation," in *Proc. GLOBECOM'94 Mini-Conference*, pp. 166-170.

[14] L. Chu and U. Mitra, "Performance analysis of an improved MMSE multi-user receiver for mismatched delay channels," *IEEE Trans. Commun.*, vol. 46, no. 10, pp. 1369-1380, Oct. 1998.

[15] L. Chu and U. Mitra, "Analysis of MUSIC-based delay estimators for DS-CDMA systems," *IEEE Trans. Commun.*, vol. 47, no. 1, pp. 133–138, Jan. 1999.

[16] L. Chu and U. Mitra, "Approximate maximum likelihood sequence detection for DS/CDMA systems with tracking errors," in *Proc. Thirty-third Annual Conference on Information Science and Systems (CISS'99)*, Baltimore, MD, Mar. 1999.

[17] E. Dahlman, B. Gudmundson, M. Nilsson and J. Sköld, "UMTS/IMT-2000 based on wideband CDMA," *IEEE Commun. Mag.*, pp. 70-79, Sept. 1998.

[18] O. Damen, A. Chkei and J.-C. Belfiore, "Lattice code decoder for space-time codes," *IEEE Commun. Let.*, vol. 4, no. 5, pp. 161-163, May 2000.

[19] D. Divsalar, M. K. Simon and D. Raphaeli, " Improved parallel interference cancellation for CDMA," *IEEE Trans. Commun.*, vol. 46, no. 6, pp. 258-268, Feb. 1998.

[20] A. Duel-Hallen, "Decorrelating decision-feedback multiuser detector for synchronous code-division multiple-access channel," *IEEE Trans. Commun.*, vol. 41, no. 2, pp. 285-290, Feb. 1993.

[21] A. Duel-Hallen, S. Hu and H. Hallen, "Long-range predection of fading signals enabling adaptive transmission for mobile radio channels," *IEEE Signal Process. Mag.*, pp. 62-75, May 2000.

[22] A. Duel-Hallen, J. Holtzman and Z. Zvonar, "Multiuser detection for CDMA systems," *IEEE Persoanl Commun.*, vol. 2, no. 2, pp. 46-58, Apr. 1995.

[23] M. Feder and E. Weinstein, "Parameter estimation of superimposed signals using the EM algorithm," , *IEEE Trans. Acoustics, Speech, and Signal Process.*, vol. 36, no.4, pp. 477-489, Apr. 1988.

[24] J. A. Fessler and A. O. Hero, "Space-alternating generalized expectation-maximization algorithm," , *IEEE Trans. Signal Process.*, vol. 42, no. 10, pp. 2664-2677, Oct. 1994.

[25] G. J. Foschini, "Layered space-time architecture for wireless communication in a fading enviroment when using multi-element antennas," *Bell Labs Technical Journal*, pp. 41-59, Autumn 1996.

[26] G. J. Foschini, G. D. Golden, R. A. Valenzuela and P. W. Wolniansky, "Simplified processing for high spectral efficiency wireless communication employing multi-element arrays," *IEEE J. Select. Areas Commun.*, vol. 17, no. 11, pp. 1841-1852, Nov. 1999.

[27] J. Geng, U. Mitra and M. P. Fitz, "Optimal space-time block codes for CDMA systems," in *Proc. Milcom 2000*, Los Angeles, CA, Oct. 2000.

[28] V. Ghazi-Moghadam and M. Kaveh, "A CDMA interference canceling receiver with an adaptive blind array," *IEEE J. Select. Areas Commun.*, vol. 16, no. 8, pp. 1542-1554, Oct. 1998.

[29] G. B. Giannakis and C. Tepedelenlioğlu, "Basis expansion models and diversitry techniques for blind identification and equalization of time-varying channels," *Proc. IEEE*, vol. 86, no. 10, pp. 1969-1986, Oct. 1998.

[30] K. S. Gilhousen, I. M. Jacobs, R. Padovani, A. J. Viterbi, L. A. Weaver, Jr. and C. E. Wheatley III, "On the capacity of a cellular CDMA system," *IEEE Trans. Vehicular Tech.*, vol.40, no.2, pp. 303-311, May 1991.

[31] G. Ginis and J. M. Cioffi, "On the relation between V-BLAST and the GDFE," *IEEE Commun. Let.*, vol. 5, no. 9, pp. 364-366, Sept. 2001.

[32] G. D. Golden, G. J. Foschini, R. A. Valenzuela and P. W. Wolniansky, "Detection algorithm and initial laboratory results using V-BLAST space-time communication architecture," *Electronics Letters*, vol. 35, no. 1, pp. 14-15, Jan. 1999.

[33] G. H. Golub, C. F. Van Loan, "*Matrix Computations*," Johns Hopkins University Press, Baltimore, MD, 3rd edition, 1996.

[34] S. D. Gray, M. Kocic and D. Brady, "Multiuser detection in mismatched multiple-access channels," *IEEE Trans. Commun.*, vol. 43, no. 12, pp. 3080-3089, Dec. 1995.

[35] M. Guenach and L. Vandendorpe, "Design and performance analysis of DA multiuser path trackers for long code DS-CDMA systems," in *Proc. IEEE GLOBECOM 2001 Conference*, San Antonio, Nov. 2001.

[36] M. Guenach and L. Vandendorpe, "Tracking performance of DA and DD multiuser timing synchronizers for short code DS-CDMA systems," *IEEE J. Select. Areas Commun.*, vol. 19, no. 12, pp. 2452-2461, Dec. 2001.

[37] D. Guo, L. K. Rasmussen, S. Sun and T. J. Lim, "A matrix-algebraic approach to linear parallel interference cancellation in CDMA," *IEEE Trans. Communications*, vol. 48, no. 1, pp. 152-161, Jan. 2000.

[38] B. Hassibi, "A fast square-root implementation for BLAST", in *Proc. 34th Asilomar Conference on Signal, Systems, and Computers*, Pacific Grove, California, Oct. 2000. Also submitted to *IEEE Trans. Signal Process.*, available online: http://mars.bell-labs.com.

[39] B. Hassibi and B. Hochwald, "High-rate linear space-time codes," in *Proc. IEEE Inter. Confer. ASSP*, Salt Lake City, May 2001.

[40] F. Heeswyk, D. D. Falconer and A. U. H. Sheikh, "A delay independent decorrelating detector for quasi-synchronous CDMA," *IEEE J. Select. Areas Commun.*, vol. 14, no. 8, pp. 1619-1626, Oct. 1996.

[41] B. M. Hochwald and W. Sweldens, "Differential unitary space-time modulation," *IEEE Trans. Commun.*, vol. 48, no. 12, pp. 2041-2052, Dec. 2000.

[42] K. Hooli, M. Latva-aho and M. Juntti, "Multiple access interference suppression with linear chip equalizers in WCDMA downlink receivers," in *Proc. IEEE GLOBECOM*, Rio de Janeiro, Brazil, Dec. 5-9, 1999.

[43] S. Housr, A. H. Tewfik and V. Ghazi-Moghadam, "Adaptive multiuser receiver schemes for antenna arrays," in *Proc. IEEE PIMRC*, 1995.

[44] B. L. Hughes, "Differential space-time modulation," *IEEE Trans. Info. Theory*, vol. 46, no. 7, pp. 2567-2578, Nov. 2000.

[45] A. L. C. Hui and K. B. Letaief, "Multiuser asynchronous DS/CDMA detectors in multipath fading links," *IEEE Trans. Commun.*, vol. 46, no. 3, pp. 384-391, Mar. 1998.

[46] Ronald A. Iltis, "Demodulation and code acquisition using decorrelator detectors for QS-CDMA," *IEEE Trans. Commun.*, vol. 44, no. 11, pp. 1553-1560, Nov. 1996.

[47] R. A. Iltis, "A DS-CDMA tracking mode receiver with joint channel/delay estimation and MMSE detection," *IEEE Trans. Commun.*, vol. 49, no. 10, pp. 1770-1779, Oct. 2001.

[48] J. Joutsensalo, J. Lilleberg, A. Hottinen and J. Karhunen, "A hierarchic maximum likelihood method for delay estimation in CDMA," in *Proc. VTC'96*, pp. 182-192.

[49] M. J. Juntti and B. Aazhang, "Finite memory-length linear multiuser detection for asynchronous CDMA communications," *IEEE Trans. Commun.*, vol. 45, no. 5, pp. 611-622, May 1997.

[50] M. J. Juntti, B. Aazhang and J. O. Lilleberg, "Iterative implementation of linear multiuser detection for dynamic asynchronous CDMA systems," *IEEE Trans. Commun.*, vol. 46, no. 4, pp. 503-508, Apr. 1998.

[51] M. J. Juntti, M. Latva-aho, K. Kansanen and O-P. Kaurahalme, "Performance of parallel interference cancellation for CDMA with delay estimation and channel coding," in *FRAMES Workshop*, pp. 196-204, Delft, The Netherlands, Jan. 18-19, 1999.

[52] M. J. Juntti and M. Latva-aho, "Bit-error probability analysis of linear receivers for CDMA systems in frequency-selective fading channels," *IEEE Trans. Commun.*, vol. 47, no. 12, pp. 1788-1791, Dec. 1999.

[53] K. Kansanen, M. Juntti and M. Latva-aho, "Performance of parallel interference cancellation receiver with delay errors," in *Proc. URSI/Remote Sensing Club of Finland/IEEE XXXIII Convention on Radio Science and Remote Sensing Symposium*, Epsoo, Finland, pp. 61-62, Aug. 24-25, 1998.

[54] D. Koulakiotis and A. H. Aghvami, "Data detection techniques for DS/CDMA mobile systems: a review," *IEEE Personal Commun.*, pp. 24-34, Jun. 2000.

[55] M. Latva-aho and J. Lilleberg, "Parallel interference cancellation based delay tracker for CDMA receivers," in *Proc. 30th Confer. on Information Science and Systems (CISS'96)*, Princeton, pp. 852-857, Mar. 20-22, 1996.

[56] M. Latva-aho and J. Lilleberg, "Delay trackers for multiuser receivers," in *Proc. Int. Conf. Universal Personal Communications*, pp. 326-330, 1996.

[57] M. Latva-aho and J. Lilleberg, "Parallel interference cancellation in multiuser CDMA channel estimation," *Wireless Personal Communications, Kluwer Academic Publishers, Special Issue on CDMA for Universal Communications Systems*, vol. 7, no. 2/3, pp. 171-195, Aug. 1998.

[58] M. Latva-aho and M. J. Juntti, "LMMSE detection for DS-CDMA systems in fading channels," *IEEE Trans. Commun.*, vol. 48, no. 2, pp. 194-199, Feb. 2000.

[59] K. Li and H. Liu, "A new blind receiver for downlink DS-CDMA communications," *IEEE Commun. Let.*, vol. 3, no. 7, pp. 193-195, Jul. 1999.

[60] Q. Li, C. N. Georghiades and X. Wang, "An iterative receiver for turbo-coded pilot-assisted modulation in fading channels," *IEEE Commun. Let.*, vol. 5, no. 4, pp. 145-147, Apr. 2001.

[61] J. Lilleberg, E. Nieminen and M. Latva-aho, "Blind iterative multiuser delay estimation for CDMA," in *Proc. PIMRC'96*, pp. 565-568.

[62] T. J. Lim and L. K. Rasmussen, "Adaptive symbol and parameter estimation in asynchronous multiuser CDMA detectors," *IEEE Trans. Commun.*, vol. 45, no. 2, pp. 213-220, Feb. 1997.

[63] J. Liu and J. Li, "Differential space-time modulation shcemes for DS-CDMA systems," in *Proc. IEEE Inter. Confer. ASSP*, Salt Lake City, May 2001.

[64] Y. Liu and S. Blostein, "Identification of frequency non-selective fading channels using decision feedback and adaptive linear prediction," *IEEE Trans. Commun.*, vol. 43, no. 2/3/4, pp. 1484-'492, Feb./Mar./Apr. 1995.

[65] Z. Liu, G. B. Giannakis and S. Zhou, "Space-time coding for broadband wireless communications," *Wireless Communications and Mobile Computing*, pp. 35-53, 2001.

[66] B. Lu and X. Wang, "Space-time code design in OFDM systems," in *Proc. IEEE Globecom*, San Francisco, Nov. 2000.

[67] R. Lupas and S. Verdú, "Near-far resistance of multi-user detectors in asynchronous channels," *IEEE Trans. Commun.*, vol. 38, no. 4, pp. 496-508, Apr. 1990.

[68] U. Madhow and M. L. Honig, "MMSE interference suppression for direct-sequence spread-spectrum CDMA," *IEEE Trans. Commun.*, vol. 42, no. 17, pp. 3178-3188, Dec. 1994.

[69] U. Madhow, "Blind adaptive interference supression for the near-far resistent acquisition and demodulation of direct-sequence CDMA signals," *IEEE Trans. Signal Process.*, vol. 45, no. 1, pp. 124-136, Jan. 1997.

[70] U. Madhow, "Blind adaptive interference suppression for direct-sequence CDMA," *Proc. IEEE*, pp. 2049-2069, Oct. 1998.

[71] U. Madhow, "MMSE interference suppression for timing acquision and demodulation in direct-sequence CDMA systems," *IEEE Trans. Commun.*, vol. 46, no. 8, pp. 1065-1075, Aug. 1998.

[72] T. L. Marzetta, "Blast training: estimating channel characteristics for high capacity space-time wireless," in *Proc. 1999 Allerton Conference*, Monticello, IL., 1999. Ailable on line: http://mars.bell-labs.com.

[73] S. Y. Miller and S. C. Schwartz, "Integrated spatial-temporal detectors for asynchronous Gaussian multiple-access channels," in *IEEE Trans. Commun.*, vol. 43, no. 2/3/4, pp. 396-411, Feb/Mar/Apr 1995.

[74] T. K. Moon, Z. Xie, C. K. Rushforth and R. T. Short, "Parameter estimation in a multi-user communication system," *IEEE Trans. Commun.*, vol. 42, no. 8, pp. 2553-2559, Aug. 1994.

[75] S. Moshavi, "Multi-user detection for DS-CDMA communications," *IEEE Commun. Mag.*, vol. 34, no. 10, pp. 124-136, Oct. 1996.

[76] R. R. Müller, P. Schramm and J. B. Huber, "Spectral efficiency of CDMA systems with linear interference suppression," in *Workshop Kommunikationstechnik'97*, Ulm, Germany, pp. 93-97, Jan. 1997.

[77] A. F. Naguib, N. Seshadri and A. R. Calderbank, "Space-time coding and signal processing for high data rate wireless communications" *IEEE Signal Processing Mag.*, vol. 17, no. 3, pp. 76-92, May 2000.

[78] L. B. Nelson and H. V. Poor, "Iterative multiuser receivers for CDMA channels: an EM-based approach," *IEEE Trans. Commun.*, vol. 44, no. 12, pp. 1700-1710, Dec. 1996.

[79] B. K. Ng and E. Sousa, "Space-time spreading multilayered CDMA systems," in *Proc. IEEE Inter. Confer. GLOBECOM*, San Franscisco, Nov. 2000.

[80] T. Ojanperä and R. Prasad, "An overview of air interface multiple accesss for IMT-2000/UMTS," *IEEE Commun. Mag.*, pp. 82-95, Sept. 1998.

[81] P. Orten and T. Ottosson, "Robustness of DS-CDMA multiuser detectors," in *Proc. GLOBECOM'97 Mini-Conference*, pp. 144-148.

[82] T. Östman, M. Kristensson and B. Ottersten, "Asynchronous DS-CDMA detectors robust to timing errors," in *Proc. VTC'97*, vol. 3, pp. 1704-1708, Phonex, AZ, Jan. 1997.

[83] T. Östman and B. Ottersten, "Near far robust time delay estimator for asynchronous DS-CDMA systems with vandlimited pulse shapes," in *Proc. VTC'98*, Ottawa, Canada, May 1998.

[84] P. Patel and J. M. Holtzman, "Analysis of a simple successive interference cancellation scheme in a DS-CDMA system," *IEEE J. Select. Areas Commun.*, vol. 12, no. 5, pp. 796-807, June 1994.

[85] S. Parkvall, E. Ström and B. Ottersten, "The impact of timing errors on the performance of linear DS-CDMA receivers," *IEEE J. Select. Areas Commun.*, vol. 14, no. 8, pp. 1660-1668, Oct. 1996.

[86] R. L. Peterson, R. E. Ziemer and D. E. Borth, " *Introduction to Spread Spectrum Communications*," Prentice-Hall, Englewood Cliffs, NJ, 1995.

[87] R. L. Pickholtz, D. L. Schilling and L. B. Milstein, "Theory of spread-spectrum communications - a tutorial," *IEEE Trans. Commun.*, vol. 30, no. 5, pp. 855-884, May 1982.

[88] H. V. Poor, "*An Introduction to Signal Detection and Estimation*," New York, NY:Springer-Verlag, 1994.

[89] J. G. Proakis, "*Digital Communications*," WCB/McGraw-Hill, 1995.

[90] A. Radović and B. Aazhang, "Iterative algorithms for joint data detection and delay estimation for code division multiple access communication systems," in *Proc. Allerton'93*, pp. 1-10.

[91] P. B. Rapajic and B. S. Vucetic, "Adaptive receiver structures for asynchronous CDMA systems," *IEEE J. Select. Areas Commun.*, vol. 12, no. 4, pp. 685-697, May 1994.

[92] P. B. Rapajic and D. K. Borah, "Adaptive MMSE maximum likelihood CDMA multiuser detection," *IEEE J. Select. Areas Commun.*, vol. 17, no. 12, pp. 2110-2122, Dec. 1999.

[93] L. K. Rasmussen, T. J. Lim and A. Johansson, "A matrix-algebraic approach to successive interference cancellation in CDMA," *IEEE Trans. Communications*, vol. 48, no. 1, pp. 145-151, Jan. 2000.

[94] T. Ristaniemi and J. Joutsensalo, "Code timing acquisition for DS-CDMA in fading channels by differential correlations," *IEEE Trans. Commun.*, vol. 49, no. 5, pp. 899-910, May 2001.

[95] A. M. Sayeed and B. Aazhang, "Multiuser timing acquisition overmultipath fading channels," in *Proc. CISS*, Princeton, NJ, Mar. 1998.

[96] A. M. Sayeed, A. Sendonaris and B. Aazhang, "Multiuser detection in fast fading multipath environments," *IEEE J. Select. Areas Commun. (special issure on Signal Processing for Wireelss Communications)*, vol. 16, no. , pp. 1691-1701, Dec. 1998.

[97] A. M. Sayeed and B. Aazhang, "Joint multipath-doppler diversity in mobile wireless communications," *IEEE Trans. Commun.*, vol. 47, no. 1, pp. 123-132, Jan. 1999.

[98] T. M. Schmidl, A. Gatherer, X. Wang and R. Chen, " Interference cancellation using the Gibbs sampler," in *Proc. VTC'2000-Fall*, Section 2.5.3.2, Boston, Oct. 2000.

[99] R. O. Schmidt, " *A Signal Subspace Approach to Multiple Emitter Location and Spectral Estimation*," Ph.D. thesis, Stanford University, Stanford, California, Nov. 1981.

[100] I. Seskar and N. B. Mandayam, "Software-defined radio architectures for interference cancellation in DS-CDMA systems," *IEEE Personal. Commun.*, pp. 26-34, Aug. 1999.

[101] J. Shen and Z. Ding, "Edge decision assisted decorrelators for asynchronous CDMA channels," *IEEE Trans. Commun.*, vol. 47, no. 3, pp. 438-445, Mar. 1999.

[102] R. Singh and L. B. Milstein, "Interference supression for DS/CDMA," *IEEE Trans. Commun.*, vol. 47 no. 3, pp. 446-453, Mar. 1999.

[103] J. E. Smee and S. C. Schwartz, "Adaptive feedforward/feedback architectures for multiuser detection in high data rate wireless CDMA networks," *IEEE Trans. Commun.*, vol. 48, no. 6, pp. 996-1011, Jun. 2000.

[104] J. E. Smee and S. C. Schwartz, "Adaptive space-time feedforward/feedback detection for high data rate CDMA in frequency-selective fading," *IEEE Trans. Commun.*, vol. 49, no. 2, pp. 317-328, Feb. 2001.

[105] R. F. Smith and S. L. Miller, "Code timing estimation in near-far environment for direct-sequence code-division multiple-access," in *Proc. Milcom'94*, pp. 47-51.

[106] R. F. Smith and S. L. Miller, "Acquision performance of an adaptive receiver for DS-CDMA," *IEEE Trans. Commun.*, vol. 47, no. 9, pp. 1416-1424, Sept. 1999.

[107] A. C. K. Soong and W. A. Krzymien, "A novel CDMA multiuser interference cancellation receiver with reference symbol aided estimation of channel parameters," *IEEE J. Select. Areas Commun.*, vol. 14, no. 8, pp. 1536-1547, oct. 1996.

[108] M. Stojanovic and Z. Zvonar, "Performance of multiuser diversity reception in Rayleigh fading CDMA channels," *IEEE Trans. Commun.*, vol. 47, no. 3, pp. 356-359, Mar. 1999.

[109] M. Stojanovic and Z. Zvonar, "Performance of multiuser detection with adaptive channel estimation," *IEEE Trans. Commun.*, vol. 47, no. 8, pp. 1129-1132, Aug. 1999.

[110] E. G. Ström, S. Parkvall, S. L. Miller and B. E. Ottersten, "Propagation delay estimation in asynchronous direct-sequence code-division multiple access systems," *IEEE Trans. Commun.*, vol. 44, no. 1, pp. 84-93, Jan. 1996.

[111] H. Sugimoto, L. K. Rasmussen, T. J. Lim and T. Oyama, "Mapping functions for successive interference cancellation in CDMA," in *Proc. IEEE VTC*, Ottawa, 1998.

[112] F. Swarts, P. van Rooyen, I. Oppermann and M. P. Lötter, "*CDMA Techniques for Third Generation Mobile Systems*," Kluwer academic publisher, Norwell, Massachusetts, 1999.

[113] P. H. Tan, L. K. Rasmussen and and T. J. Lim, "Constrained maximum-likelihood detection in CDMA," *IEEE Trans. Commun.*, vol. 49, no. 1, pp. 142-153, Jan. 2001.

[114] V. Tarokh, N. Seshadri and A. R. Calderband, "Space-time codes for high data rate wireless communication: performance criteron and code construction," *IEEE Trans. Info. Theory*, vol. 44, no. 2, pp. 744-765, Mar. 1998.

[115] V. Tarokh, A. Naguib, N. Seshadri and A. R. Calderband, "Space-time codes for high data rate wireless communication: performance criteron in the presence of channel estimation errors, mobility, and multiple paths," *IEEE Trans. Commun.*, vol. 47, no. 2, pp. 199-207, Feb. 1999.

[116] V. Tarokh, H. Jafarkhani and A. R. Calderband, "Space-time block coding for wireless communications: performance results," *IEEE J. Select. Areas Commun.*, vol. 17, no. 3, pp. 451-460, Mar. 1999.

[117] V. Tarokh, H. Jafarkhani and A. R. Calderband, "Space-time block codes from orthogonal designs," *IEEE Trans. Info. Theory*, vol. 45, no. 5, pp. 1456-1467, Jul. 1999.

[118] D. N. C. Tse and S. V. Hanly, "Linear multiuser receivers: effective interference, effective bandwidth and user capacity," *IEEE Trans. Info. Theory*, vol. 45, no. 2, pp. 641-657, Mar. 1999.

[119] M. K. Varanasi and B. Aazhang, "Multistage detection in asynchronous code-division multiple-access communications," *IEEE Trans. Commun.*, vol. 38, no. 4, pp. 509-519, Apr. 1990.

[120] S. Verdú, "Minimum probability of error for asynchronous Gaussian multiple-access channels," *IEEE Trans. Info. Theory*, vol. 32, no. 1, pp. 85-96, Jan. 1986.

[121] S. Verdú and S. Shamai(Shitz), "Spectral efficiency of CDMA with random spreading," *IEEE Trans. Info. Theory*, vol. 45, no. 2, pp. 622-640, Mar. 1999.

[122] R. Wang and S. D. Blostein, "Spatial-temporal CDMA receiver structures for Rayleigh fading channels," in *Proc. IEEE Inter. Conf. on Commun. (ICC'99)*, Vancouver, Jun. 1999.

[123] R. Wang, "*Spatial-Temporal Signal Processing for Multi-user CDMA Communication Systems*," Ph.D. Thesis, Queen's University, 1999.

[124] R. Wang and S. D. Blostein, "A spatial-temporal decorrelating receiver for CDMA systems with base-station antenna arrays," *IEEE Trans. Commun.*, vol. 49, no. 2, pp. 329-340, Feb. 2001.

[125] X. Wang and H. V. Poor, "Space-time multiuser detection in multipath CDMA channels," *IEEE Trans. Signal Process.*, vol. 47, no. 9, pp. 2356-2374, Sept. 1999.

[126] J. F. Weng, T. Le-Ngoc, G. Q. Xue and S. Tahar, "Performance of various multistage interference cancellation schemes for asynchronous QPSK/DS/CDMA over multipath Rayleigh fading channels," *IEEE Trans. Commun.*, vol. 49, no. 5, pp. 774-778, may 2001.

[127] P. H. Wu and A. Duel-Hallen, "Multiuser detectors with disjoint Kalman channel estimators for synchronous CDMA mobile radio channels," *IEEE Trans. Commun.*, vol. 48, no. 5, pp. 752-756, May 2000.

[128] Y. Xin, Z. Wang and G. B. Giannakis, "Space-time diversity systems based on unitary constellation-rotation precoders," in *Proc. IEEE Inter. Conf. ASSP*, Salt Lake City, May 2001.

[129] P. Xiao and E. Ström, "Synchronization algorithms for iterative demodulated M-ary DS-CDMA systems," in *Proc. IEEE GLOBECOM 2001 Conference*, San Antonio, Nov. 2001.

[130] G. Xue, J. Weng, T. Le-Ngoc and S. Tahar, " Adaptive multistage parallel interference cancellation for CDMA," *IEEE J. Select. Areas Commun.*, vol. 17, no. 10, pp. 1815-1827, Oct. 1999.

[131] W. Ye and P. K. Varshney, " A two-stage decorrelating detector for DS/CDMA systems," *IEEE Trans. Vehicular Tech.*, vol. 50, no. 2, pp. 465-479, Mar. 2001.

[132] D. J. Young and N. C. Beaulieu, "The generation of correlated Rayleigh random variates by inverse discrete Fourier transform," *IEEE Trans. Commun.*, vol. 48, no. 7, pp. 1114-1127, Jul. 2000.

[133] X. Zhang and D. Brady, " Asymptotic multiuser efficiencies for decision-directed multiuser detectors," *IEEE Trans. Infor. Theory*, vol. 44, no. 2, pp. 502-515, Mar. 1998.

[134] D. Zheng, J. Li, S. L. Miller and E. G. Ström, "An efficient code-timing estimator for DS-CDMA signals," *IEEE Trans. Signal Process.*, vol. 45, no. 1, pp. 82-89, Jan. 1997.

[135] F. Zheng and S. K. Barton, "Near-far resistant detection of CDMA signals via isolation bit insertion," *IEEE Trans. Commun.*, vol. 43, no. 4, pp. 1313-1317, Apr. 1995.

[136] F. Zheng and S. K. Barton, "On the performance of near-far resistant CDMA detectors in the presence of synchronization errors," *IEEE Trans. Commun.*, vol. 43, no. 12, pp. 3037-3045, Dec. 1995.

Vita

Wei Zha

EDUCATION

Ph.D.	Electrical and Computer Engineering, Queen's University	1998–2002
M.Sc.	Electronics Engineering, Shanghai Jiao Tong University	1992–1995
B.Sc	Electronics Engineering, Shanghai Jiao Tong University	1988–1992

AWARD

Ontario Graduate Scholarship in Science & Technology	2001-2002
Queen's Graduate Awards	2000–2002
Queen's Graduate Fellowship	1998–2001
Queen's University Tuition Bursary	1998–2001

EXPERIENCE

Research Assistant (1998–2002), Electrical & Computer Engineering, Queen's University

Teaching Assistant (1999–2001), Electrical & Computer Engineering, Queen's University

Research Engineer, Lecturer (1995–1998), Electronics Engineering, Shanghai Jiao Tong University, Shanghai, China

Research Assistant (1992–1995), Electronics Engineering, Shanghai Jiao Tong University, Shanghai, China

PUBLICATIONS

Journal

Wei Zha and Steven D. Blostein, "Multiuser Delay-Tracking CDMA Receiver", Accepted by *EURASIP Journal on Applied Signal Processing, Special Issue on Multiuser Detection and Blind Estimation*, July 2002, in press.

Wei Zha and Steven D. Blostein, "Soft-Decision Multistage Multiuser Interference Cancellation", Accepted by *IEEE Transactions on Vehicular Technology*, July 2002, in press.

Wei Zha and Steven D. Blostein, "Multiuser Receivers that are Robust to Delay Mismatch", Accepted by *IEEE Transactions on Communications*, June 2002, in press.

Conference

Wei Zha and Steven D. Blostein, "CDMA Multiuser Delay-Tracking and Detection", *Proc. 21st Biennial Symposium on Communications*, Kingston, Ontario, pp. 159-163, June 2002.

Wei Zha and Steven D. Blostein, "Improved Decorrelating Decision-Feedback Detection of BLAST Space-Time Systems", *Proc. IEEE International Conference on Communications (ICC 2002)*, New York, pp. 335-339, Apr.-May 2002.

Wei Zha and Steven D. Blostein, "Soft-Decision Successive Interference Cancellation CDMA Receiver with Amplitude Averaging and Robust to Timing Errors", *Proc. IEEE GLOBECOM 2001 Conference*, San Antonio, pp. CTS01-5, Nov. 2001.

Wei Zha and Steven D. Blostein, "Improved CDMA Multiuser Receivers Robust to Timing Errors", *Proc. IEEE International Conference on Acoustics, Speech, and Signal Processing (ICASSP 2001)*, Salt Lake City, pp. SPCOM-P8.3 1-4, May 2001.